MASTERARBEIT / MASTER'S THESIS

Titel der Masterarbeit / Title of the Master's Thesis

„Impact on the terrestrial water cycle through ENSO in the Antarctica past-current situation-prediction"

verfasst von / submitted by

Christina Jenner, BEd

angestrebter akademischer Grad / in partial fulfilment of the requirements for the degree of

Master of Education (MEd)

Wien, 2021 / Vienna 2021

Studienkennzahl lt. Studienblatt / degree programme code as it appears on the student record sheet:	A 199 506 510 02
Studienrichtung lt. Studienblatt / degree programme as it appears on the student record sheet:	Masterstudium Lehramt Sek (AB) UF Deutsch UF Geographie und Wirtschaft
Betreut von / Supervisor:	Univ.-Prof. Dipl.-Geogr. Dr. Thomas Glade

Eidesstattliche Erklärung

Hiermit versichere ich,

- dass ich die vorliegende Masterarbeit selbstständig verfasst, andere als die angegebenen Quellen und Hilfsmittel nicht benutzt und mich auch sonst keiner unerlaubter Hilfe bedient habe,
- dass ich dieses Masterarbeitsthema bisher weder im In- noch im Ausland in irgendeiner Form als Prüfungsarbeit vorgelegt habe
- und dass diese Arbeit mit der vom Begutachter beurteilten Arbeit vollständig übereinstimmt.

Wien, am 09.08.2021

Christina Jenner

Vorwort

An dieser Stelle möchte ich mich bei allen Personen bedanken, die zum Gelingen der vorliegenden Arbeit beigetragen haben.

Zuerst gebührt mein Dank Herrn Univ.-Prof. Dipl.-Geogr. Dr. Thomas Glade für die Möglichkeit, die vorliegende Masterarbeit im Fachbereich Physische Geographie zu verfassen.

Außerdem danken möchte ich meinem Freund Dipl.-Ing. Martin Hammerschmid für die Korrektur meiner Masterarbeit und die damit verbundene konstruktive Kritik, die meine Arbeit bereichert hat.

Abschließend möchte ich an dieser Stelle meiner gesamten Familie, allen voran meinen Eltern ein herzliches Dankeschön aussprechen, die mich während der gesamten Studienzeit moralisch und finanziell unterstützt haben. Nur mit deren Hilfe gelang es alle meine Ziele zu erreichen.

Abstract

In this master thesis an investigation about the connection between ENSO events and the water cycle in the Antarctica will be done. First, effects on the total water cycle of the Antarctica will be investigated, followed by regional differences in sub-regions of the Antarctica. Furthermore, historical data will be used to describe a possible intensification of ENSO events and consequently the involved impacts. The basis for the investigation is based on the following analysis and research work:

- explanation of the data acquisition and analysis methodology,
- current state of knowledge about ENSO events and their impacts,
- current state of knowledge about the Antarctic water cycle.

Based on the analysis and literature work, the Pearson correlation method was used to show a connection between ENSO events and the Antarctic water cycle. Additionally, a correlation with the essential wind parameters of the Antarctica was done. Following correlations regarding ENSO events were carried out:

- ice-mass change of the total, supra-regional parts and sub-regions of the Antarctica,
- water cycle variables covering the total and supra-regional parts of the Antarctica,
- wind parameters covering the total and supra-regional parts of the Antarctica,

These implemented correlations could confirm a connection between changes in the Antarctic ice-mass sheet and ENSO events. Over the West Antarctica a strong indirect proportional correlation between the ice-mass and the SST in the Niño 3.4 region could be observed. In the East and Central Antarctica, an average direct proportional correlation was noticed. Therefore, it can be confirmed that due to ENSO events the ice melting in the West Antarctica becomes boosted. Contrarily, the ice-mass gains in the East and Central Antarctica. This is the consequence of increased snowfall. The impacts from La Niña events are not that significant. Merely, average correlations for the evaporation and the water balance in the Antarctica could be visualized. A weak average correlation resulted for increasing easterly blowing winds.

Various centers and characteristics of ENSO events could be the reason for missing correlations and connections within the investigation of the water cycle and the wind parameters. Furthermore, the hypotheses of this master thesis are based on immediate impacts on the Antarctica. The partially missing correlations could therefore be explained by delayed impacts, which may show a correlation much later.

Kurzfassung

Die vorliegende Masterarbeit umfasst die Untersuchung des Zusammenhangs zwischen ENSO Ereignissen und dem Wasserkreislauf der Antarktis. Neben dem Einfluss auf den gesamten Wasserkreislauf der Antarktis, werden auch regionale Unterschiede in den Teilregionen der Antarktis untersucht. Historische Daten von ENSO Ereignissen und Wasserkreislaufdaten für eine mögliche Intensivierung von ENSO Ereignissen und die damit verbundenen Auswirkungen werden verwendet. Als Grundlage für die Untersuchung des Zusammenhangs zwischen ENSO Ereignissen und dem Wasserkreislauf der Antarktis wurden folgende Analyse- und Recherchearbeiten durchgeführt:

- Erklärung der Methodik zur Datenbeschaffung und Datenanalyse,
- aktueller Wissensstand zum Thema ENSO Ereignisse und dessen Auswirkungen,
- aktueller Wissensstand zum Thema Wasserkreislauf in der Antarktis.

Aufbauend auf den Analyse- und Recherchearbeiten wurde die Pearsons Korrelationsmethode angewandt, um den Zusammenhang zwischen ENSO Ereignissen und den antarktischen Wasserkreislauf darzustellen. Weiters wurden die wichtigsten Windparameter der Antarktis einer Analyse betreffend Korrelation mit ENSO Ereignissen unterzogen. Folgende Korrelationsuntersuchungen wurden bezüglich ENSO Ereignissen im Zuge der Arbeit durchgeführt:

- Eismassenänderung in der gesamten, in überregionalen und regionalen Gebieten der Antarktis,
- Wasserkreislaufvariablen in der gesamten und in überregionalen Gebieten der Antarktis,
- Windparameter in der gesamten und in überregionalen Gebieten der Antarktis.

Die durchgeführten Korrelationen konnten den Zusammenhang zwischen der Änderung der Eismasse in der Antarktis und El Niño Ereignissen bestätigen. In der Westantarktis besteht ein stark indirekt proportionaler Zusammenhang zwischen der Eismasse und der Meeresoberflächentemperatur in der Niño 3.4 Region. In der Ost- und Zentralantarktis konnten mittlere und stark direkt proportionale Zusammenhänge berechnet werden. Somit kann bestätigt werden, dass in der Westantarktis die Eisschmelze durch El Niño Ereignisse vorangetrieben wird. In der Ost- und Zentralantarktis überwiegt der zunehmende Schneefall gegenüber der Eisschmelze, wodurch eine Zunahme der Eismasse in diesen Gebieten erfolgt. Für La Niña Ereignisse konnte lediglich für die Verdunstung und die Wasserbilanz ein mittlerer Zusammenhang in der Gesamtantarktis nachgewiesen werden. Zunehmende Ostwinde konnten nur in der Westantarktis mit einem mittleren Zusammenhang bestätigt werden. Fehlende

Zusammenhänge in den Untersuchungen zum Wasserkreislauf und den Windparametern könnten in den sehr unterschiedlichen Ausprägungen und Entstehungsherden von ENSO Ereignissen liegen. Teilweise fehlende Korrelationen könnten auch aufgrund verzögerter Auswirkungen auf die Antarktis erklärt werden.

Table of contents

List of figures

List of tables

1 Introduction

The Antarctica represents the largest storage of freshwater, which is locked up in glaciers and ice sheets. Therefore, massive discharges of the ice-mass are one the most important drivers of global mean sea level rise. Between 1992 and 2017 the Antarctic Ice Sheet discharged 109 ± 56 Gt/year, which led to a mean sea level rise of 7.06 ± 3.9 mm (cf. SHEPERD et al., 2018). Furthermore, it was observed that the ice-mass change within the Antarctica is not uniform distributed. There are strong anomalies in the ice-mass sheet change over the Antarctica, which reach from much greater mass loss in the West Antarctica (94 ± 27 Gt/year) to mass gain in the East Antarctica (5 ± 46 Gt/year) in the period of 1992-2017 (cf. SHEPERD et al., 2018). Such regional ice-mass sheet variations in the Antarctica (25 different regions) are observed by the Gravity Recovery and Climate Experiment (GRACE) (cf. GFZ, 2020). Ice-mass sheet changes in the Antarctica are affected by climate change.

It is well known that ENSO is one of the most dominant climate phenomena and has widespread effects on seasonal weather and climate in many regions over the globe, which underlie alternation in the water cycle. The warming or cooling down of the sea surface temperature (SST) has a direct effect on the water cycle (cf. ZHANG et al., 2020). For the Antarctica this means that potentially the ice-mass sheet on water and land are affected by the warming of the SST, caused through ENSO.

Therefore, the hypotheses and research questions, explained in chapter 2, will be investigated in the master thesis. In Figure 1, the overview of the master thesis is visualized. Therein, the explanation of the hypotheses and research questions, the used methods regarding literature research, data acquisition and data processing will be explained. Then, a literature research of the basic mechanism of ENSO will be given. Furthermore, the recorded ENSO events and their impacts as well as the possible intensification of ENSO events due to climate change will be explained. Thereafter, the terrestrial water cycle with a focus on the key variables in the Antarctica will be considered. Additionally, the influences on the water cycle through climate change are investigated. Finally, the correlation results will be visualized and discussed.

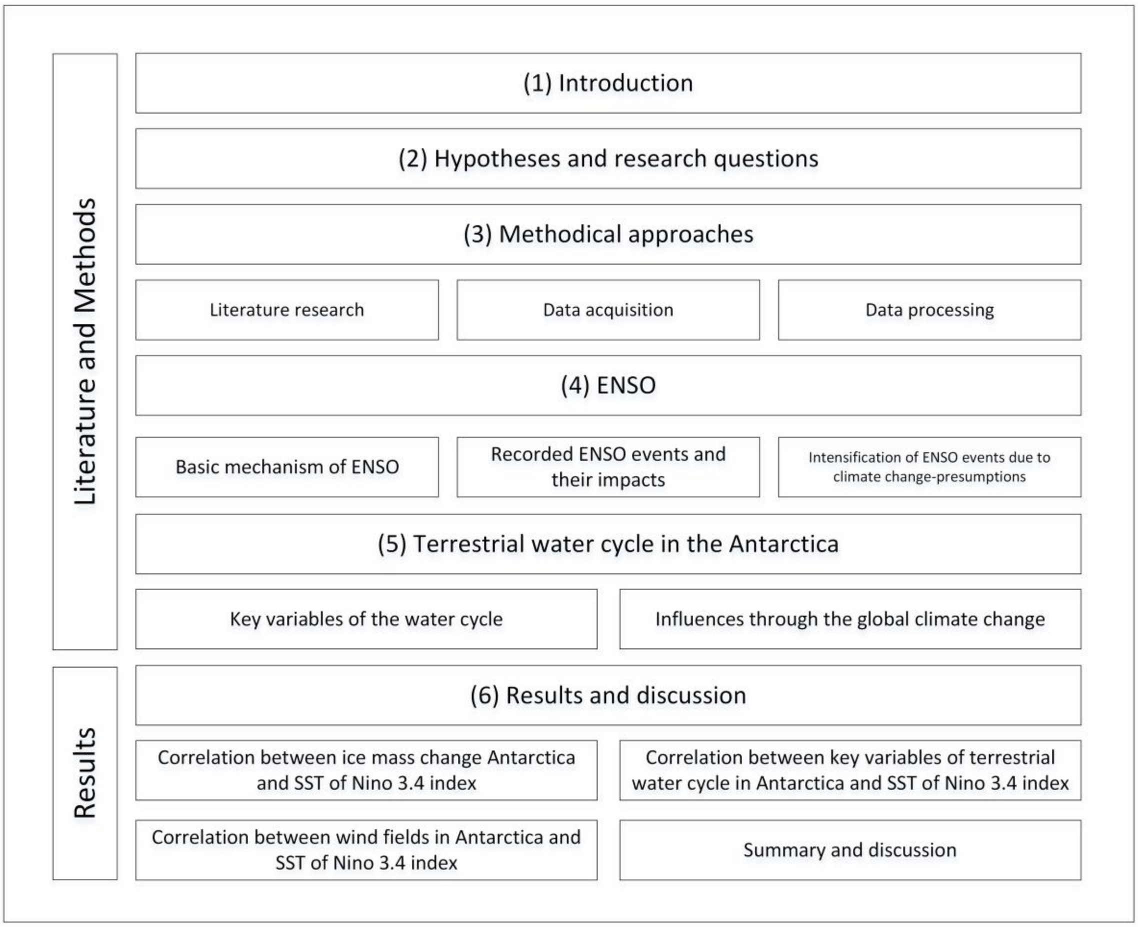

Figure 1: Overview of the master thesis

2 Hypotheses and research questions

The purpose of this master thesis is to find a possible connection between ENSO and changes in the Antarctic Ice Sheet. Therefore, the following hypothesis serves as a reference:

H1: Anomalies in the water cycle of the Antarctica are connected to ENSO.

This assumption suggests the following two research questions:

RQ1: Does ENSO have a crucial impact on the key variables of the Antarctic water cycle?

RQ2: Are there disparities of the anomalies in different regions in the Antarctica?

The second hypothesis is in some ways connected to the first one. Due to the assumption that ENSO events may occur stronger and more often, further impacts on the Antarctica could be the consequence. Therefore, the following hypothesis is given:

H2: Due to the intensification of ENSO events owing to climate change, anomalies in the Antarctic water cycle occur more often.

Hence, the following third and fourth research questions arise:

RQ3: Which impacts on the Antarctic water cycle does the intensification of ENSO events have?

RQ4: What does this mean for the average climate in the Antarctica?

For the discussion of these research questions a literature research about the basic mechanism of ENSO, recorded ENSO events and the intensification due to climate change presumption is fundamental. Furthermore, a literature research about the ice-mass sheet change and the key impacts on the terrestrial water cycle in the Antarctica, like precipitation will be elucidated. Based on the literature research a short data analysis about the impact of ENSO on the ice-mass sheet change and the terrestrial water cycle in the Antarctica will be done. Therefore, monthly provided data (period 2002-2017) about the ice-mass sheet change in different regions of the Antarctica (GFZ, 2020) will be correlated with monthly data from the Niño 3.4 index (NOAA, 2020). The provided datasets will be correlated with the Pearson method. The Niño 3.4 index represents the SST anomalies in the 3.4 region within the Pacific, which is favored for defining ENSO events (cf. NOAA, 2020). With the Pearson correlation method, linear relations between ENSO events (SST anomalies) and mass anomalies in the Antarctica (ice-mass sheet change) can be determined. In case of correlations further key variables of the water cycle, which influence the ice-mass sheet change will be consulted (cf. ECMWF, 2019). Finally, a prediction of water cycle anomalies in the Antarctica due to intensified ENSO events based on literature will be given (CAI et al. 2018).

3 Methodical approaches

For answering of the raised research questions, a well-structured methodical approach is necessary. Therefore, chapter 3 gives an overview about the literature research methodology, the data acquisition and the data processing steps.

3.1 Literature research

The master thesis is based on literature work. Therefore, a short overview of the used literature is given in Table 1.

Table 1: Methodology on screening literature

Searching index	Specific content
Database	Scopus, Google Scholar, Nature, Geophysical Research Letter, NASA, NOAA, ECWMF
Article type	Scientific articles published in peer-reviewed journals and conference papers, reports from institutions, reference book chapters
Search strings	“ENSO”, “Antarctica”, “El Niño”, “Niño 3.4 index”, “La Niña”, “ENSO impacts”, “water cycle”, “key variables”, “Pearson correlation”, “climate change”, “global warming”, “RCP8.5 scenario”, “intensification of ENSO events”
Search period	From 1966 to 2021
Screening procedure	Article relevance according to research focus has been checked by contents of abstract, introduction and conclusion of every article
Literature language	German and English

To find suitable scientifically literature in English and German, the search machines Scopus and Google Scholar were used. Most texts were published in Nature, Geophysical Research Letters or on the NASA, NOAA, BOM and ECWMF websites. For the literature research different search strings, like “ENSO”, “Antarctica” or the “Pearson correlation” method were used. Texts were selected based on their relevance according to the research focus and the issue of the chapter. First, the abstracts were consulted, skim read and later the introduction and the conclusion of the articles were checked. Based on this approach, texts were selected and used. To clarify general methods, statements or discoveries, like the function of the Walker

Circulation (1966), earlier texts were used. For the discussion of datasets and the used indices, the topicality of texts is crucial. For the comparison of past and current ENSO events and the impacts due to climate change, earlier and actual literature were used.

3.2 Data acquisition

For the correlation between the ice-mass change in the Antarctica and ENSO events, data need to be gathered. The Niño 3.4 index serves as an indicator for ENSO events due to the Sea Surface Temperature (SST) anomalies (NOAA, 2021b). Data products derived from GRACE (cf. GFZ, 2021) are used for the correlation of the ice-mass change in the Antarctica with the SST anomaly of the Niño 3.4 index. Data products from ECMWF provide records about parameters of the terrestrial water cycle of the Antarctica (cf. ECWMF, 2021a).

3.2.1 Niño 3.4 index

Nowadays, the Niño 3.4 index is one of the most used indices for measuring ENSO events. SST anomalies in the defined Niño 3.4 region are used to monitor the occurrence, duration and magnitude of an ENSO event (cf. VAN OLDENBORGH 2021: 2). The SST anomaly is defined as the standard deviation compared to the average SST within the defined area Niño 3.4 (cf. BOM, 2021). The index has a high reliability, especially because it is directly linked with changes in the SST (cf. BUNGE and CLARKE, 2009: 3979).
A registration of an El Niño event will be done with an SST anomaly of at least +0,8°C and a La Niña event with an SST anomaly of at least -0,8°C (cf. BOM, 2021). Additionally, these anomalies need to be sustained over at least three months with an SST anomaly threshold of +/-0,5°C. Values, which are inbetween, show no event and are registered as the neutral phase (cf. BOM, 2021).
As shown in Figure 2, there are four defined Niño regions over the Equatorial Pacific. The Niño regions 1+2 are used to describe SST anomalies over the South American coast, which can be relevant for changes in the local weather. These regions are though not relevant for the observation of teleconnections and consequently not for the Niño 3.4 index. The Niño 3 region (90-150° W) covers the Eastern Equatorial Pacific and the Cold Tongue. The Niño 4 region (160° E-150°W) is located in the Central Equatorial Pacific and covers parts of the Warm Pool (cf. VAN OLDENBORGH, 2021: 3). Data for the SST anomalies in these regions are available since 1982 (cf. BARNSTON 1997: 368). For observations and data acquisitions, parts of the Niño 3 and Niño 4 regions are especially relevant. Consequently, the Niño 3.4 region, which overlaps these two regions, was defined. This area may be the most meaningful to show the direct interaction with the atmosphere. Mainly because the region covers an area where the SST is relative warm

and an area where the SST anomalies can be relatively high (cf. LATIF 2006: 197). The Niño 3.4 region is also the place where an ENSO event typically originates (cf. BOM, 2021).

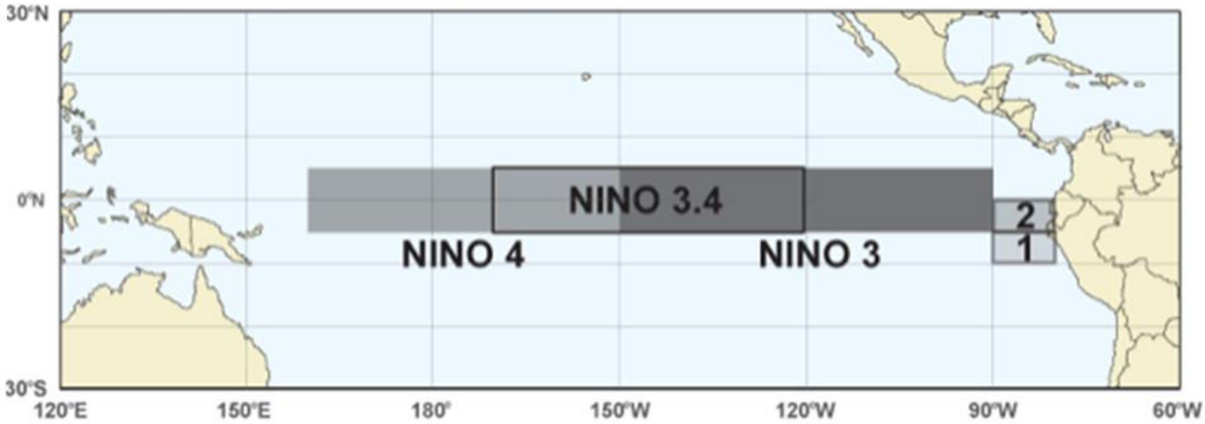

Figure 2: Defined Niño regions 1, 2, 3 and 3.4 over the Pacific Ocean (BOM 2021)

Data products for the SST anomaly and the absolute SST values are derived from the National Oceanic and Atmospheric Administration (NOAA). Datasets are available since 1950. For the visualization and correlation, the monthly ERSSTv5 – Niño 3.4 index will be used (NOAA, 2021b).

3.2.2 GRACE: Ice- mass change Antarctica

The Gravimetric Earth Observation Satellite Missions GRACE and GRACE-FO, launched in 2002, deliver data products regarding the ice-mass change within the Antarctica. Beside the ice-mass change within the Antarctica, also data products according to the ice-mass change in Greenland, the ocean bottom pressure variability and terrestrial water storage anomalies around the world have been gathered (GFZ, 2021). Time-resolved gravity observations and measurements of global mass redistribution enable the understanding of the complex interactions and phenomena within the climate change (cf. TAPLEY et al., 2021: 358).

The measurement principle, which is shown in Figure 3, could be explained by two identical satellites (GRACE A/B) orbiting one behind the other in a near-polar orbit plane. Varying mass distribution below the satellites effect positive and negative along-track accelerations, which are gravitationally induced (cf. TAPLEY et al., 2021: 358). The monthly aggregated measurements of GRACE and GRACE-FO enable to track mass changes in the hydrosphere, cryosphere and oceans. The results of the measurements are gathered in user-friendly Level-3 products (.csv data) which are available for download at GFZ´s Information System and Data Center (ISDC). For the visualization and correlation, the GFZ dataset will be used (cf. TAPLEY et al., 2021: 358; GFZ, 2021).

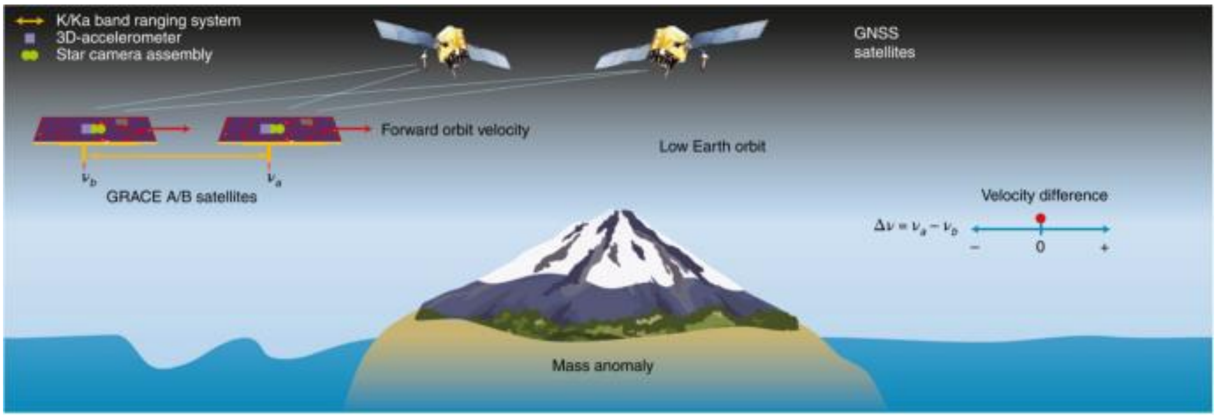

Figure 3: Measurement principle of the GRACE mission (cf. TAPLEY et al., 2021: 359)

In Figure 4, the ice-mass change in the Antarctica within the years 2002 to 2020 based on GRACE data is shown. Therein, it can be seen, that within the last two decades the ice-mass sheet in the total Antarctica decreased by approximately 166 gigatons of ice per year. Furthermore, ice-mass change data are available within this period for 25 different regions in the Antarctica. (GFZ, 2021) Within the period between June 2017 and June 2018, no data was recorded. Therefore, a time gap is given.

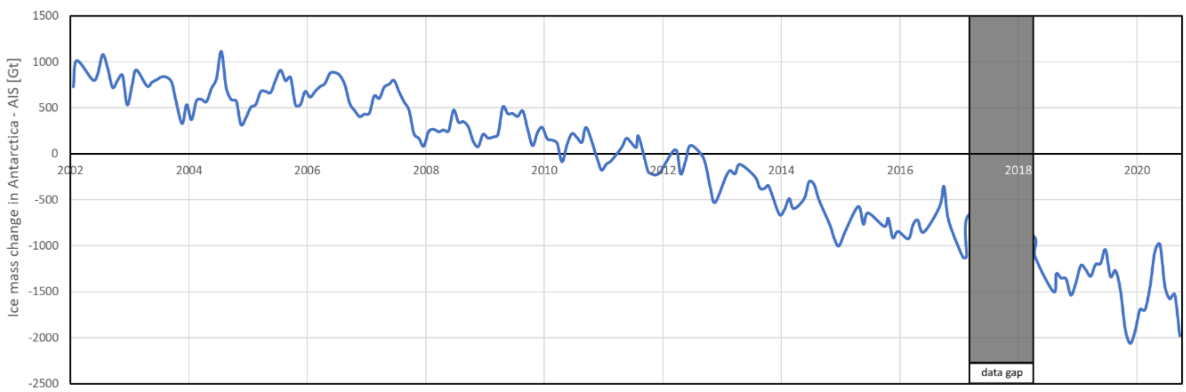

Figure 4: Ice-mass change Antarctica within the years 2002 to 2020 (own representation, data from GFZ, 2021)

3.2.3 ECMWF – Terrestrial water cycle parameters of Antarctica

The European Center for Medium-Range Weather Forecasts (ECMWF) gathers time-resolved climate data about the ocean, atmosphere and land (cf. ECMWF, 2021b). There, many public datasets are available (cf. ECMWF, 2021a). Within this master thesis, the ERA5 dataset, which is the fifth generation of ECMWF reanalysis for the global climate and weather, will be used (cf. ECMWF, 2021c). The combination of model data with observations from across the world is named reanalysis, which enables the generation of a globally complete dataset by using the laws of physics. ERA5 consists of hourly estimates for a large number of atmospheric, ocean-wave and land-surface parameters (cf. ECMWF, 2021c). In Figure 5, exemplary the globally monthly mean horizontal wind component at 100m above surface in January 2019 is shown to visualize the possibilities of the ERA5 dataset.

ERA5 delivers hourly, daily or monthly global gridded datasets from 1979 to present with a horizontal resolution from 0.25 degrees for the reanalysis of the atmosphere. The dataset is available on NetCDF format, which will be exported in CSV by defining specific regions (latitude and longitude) within common applications (cf. ECMWF, 2021c).

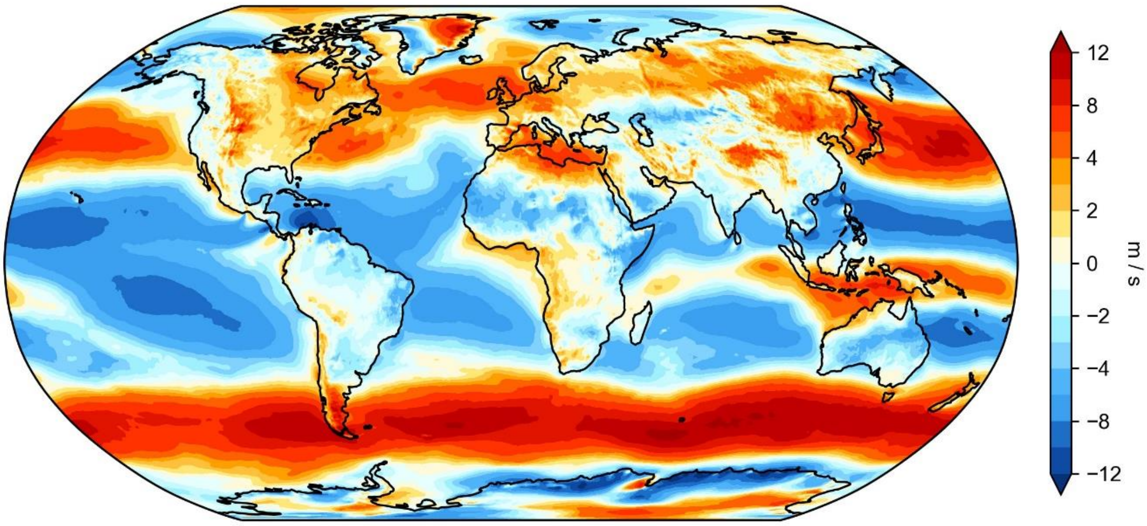

Figure 5: ERA 5 monthly mean horizontal wind component at 100m above surface in January 2019 (ECMWF, 2021c)

By using the ERA5 dataset, the terrestrial water cycle of the Antarctica can be described. Therefore, the parameters of evaporation, total precipitation and runoff will be used. The evaporation, which is given in meters of water equivalent, represents according to ECMWF "*the accumulated amount of water that has evaporated from the Earth´s surface, including a simplified representation of transpiration (from vegetation), into vapour in the air above*" (ECMWF, 2021c). The total precipitation is defined according to ECMWF as "*the accumulated liquid and frozen water, comprising rain and snow, that falls to the Earth´s surface*" (ECMWF, 2021c). This parameter does not include fog or dew and is also given in meters of water equivalent (cf. ECMWF, 2021c). Besides the precipitation and evaporation, the water balance can also be influenced by runoff, which means the sum of surface runoff and sub-surface runoff (under the ground) (cf. ECMWF, 2021c). Within ECMWF data, the runoff values are very low compared to evaporation and precipitation. Therefore, the runoff values were only considered as parameter within the water cycle but not separately. The runoff parameter is also given in meters of water equivalent (cf. ECMWF, 2021c). Therefore, the water cycle, which is explained in detail in chapter 5, can be described by summing up the total precipitation (positive), the evaporation (negative) and the runoff (negative).

For the total precipitation, evaporation and runoff parameters, it must be considered that observations are often dependent on time and space. The data from ECMWF are describing average water equivalents over a model grid box. Therefore, comparison with other literature data and observation data are not always meaningful (cf. ECMWF, 2021c).
Changes in the Antarctic water cycle are also driven by ocean circulation changes, which are influenced by surface near wind fields (cf. RAPHAEL, 2016: 1). Therefore, three different surfaces near wind parameters will be considered. The eastward and northward surface near (10m height), neutral wind speed, as well as the horizontal surface near neutral wind speed (10m height) (cf. ECMWF, 2021c). Neutral wind is defined as the mean wind speed by taking into account a neutrally stratified atmosphere (cf. ECMWF, 2021c). The wind parameters are given in meters per second (cf. ECMWF, 2021c).
The ECMWF data export is based on the definition of grid boxes. Therefore, longitude and latitude values must be defined, which cover the searched area. In Table 2, the used ECMWF data export values are shown for the supra-regional parts of the Antarctica as well as for the total Antarctica. Within the period between June 2017 and June 2018, no data was recorded within the GRACE mission (GFZ, 2021). Therefore, within the ECMWF data investigation, this time period was also not considered.

Table 2: ECMWF data export values for supra-regional parts of Antarctica

ECMWF data export	Longitude*	Latitude*
Total Antarctica	180W to 180E (-180W to 180E)**	60S to 90S (-60N to -90S)**
East Antarctica	40W to 175E (-40W to 175E)**	66.5S to 75S (-66.5N to -75S)**
Central Antarctica	60W to 175E (-60W to 175E)**	75S to 90S (-75N to -90S)**
West Antarctica and Antarctic Peninsula	160W to 60W (-160W to -60E)**	72.5S to 90S (-72.5N to -90S)**
* N…North / S…South / W…West / E…East		
** classification export data according to ECMWF		

In Figure 6, the visualization of the used ECMWF data export values is shown. Therein, it can be seen, that the West Antarctic Ice Sheet and Antarctic Peninsula Ice Sheet, which is colored red, fits mostly the regions defined by GRACE (GFZ, 2021). Only region AIS_025 is not covered by the used ECMWF export data. The separation of the East Antarctic Ice Sheet (green) and the Central Antarctic Ice Sheet (blue) was assumed to be on the 75°S latitude. Both supra-regional parts are covered well. Within the predefined values, some parts of the Southern Ocean as well as some parts of the Ross and Ronne Ice Shelf were also taken into consideration. The total Antarctica was defined by the sum of the green, blue, red and grey segments.

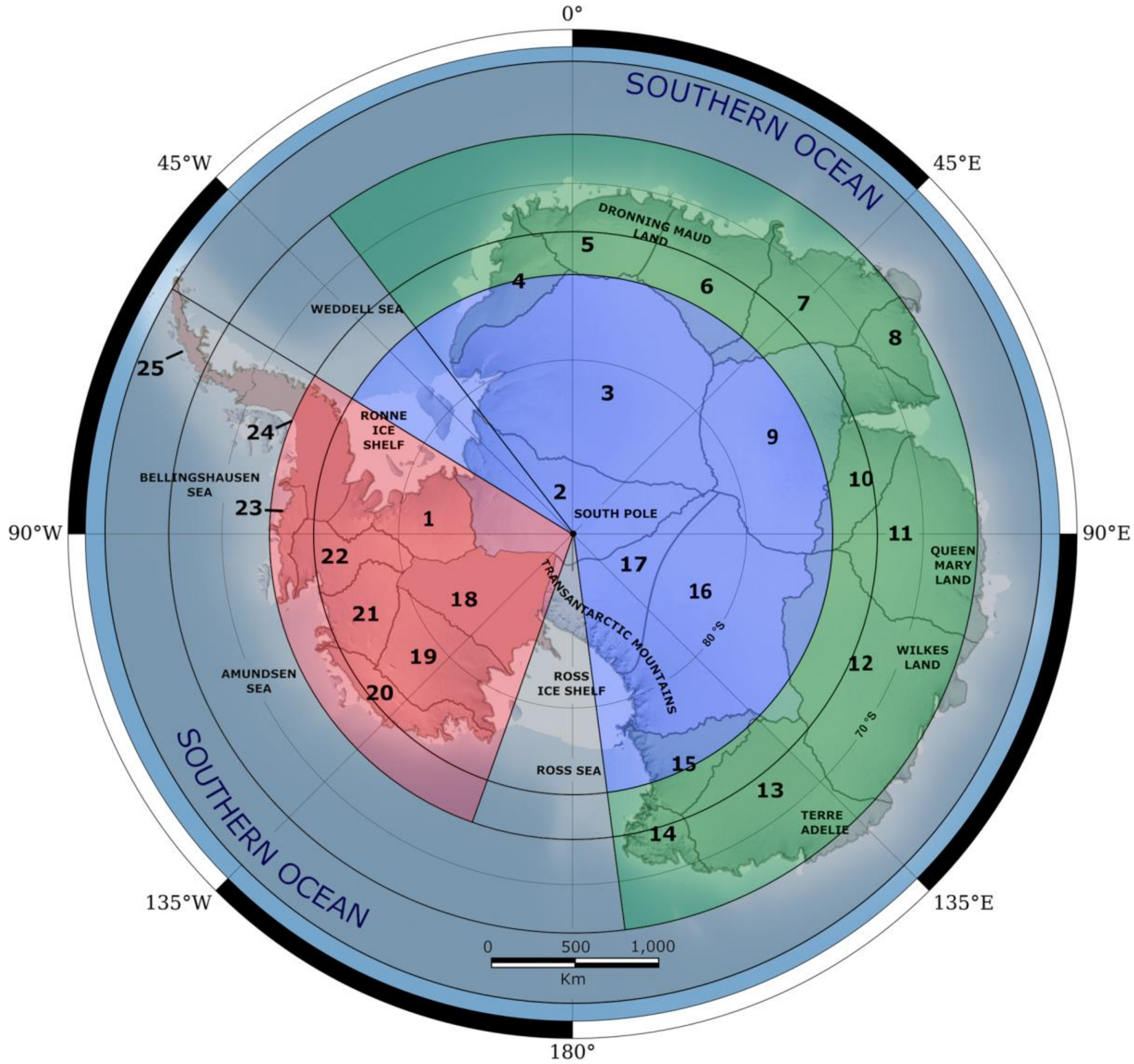

Figure 6: Supra-regional distribution of ECMWF data for West Antarctic Ice Sheet and Antarctic Peninsula Ice Sheet (red), the East Antarctic Ice Sheet (green) and the Central Antarctic Ice Sheet (blue) (adapted from (BODART, 2019: 4))

3.3 Data processing

Based on the datasets, which are explained in chapter 3.2, data processing steps will be applied. To find linear correlations between the ice-mass change, water cycle key variables and wind parameters in the Antarctica and the SST of the Nino 3.4 index, the Pearson´s product-moment correlation method will be used.

Therein, metric datasets from the ice-mass change and other parameters of the Antarctica and the SST / SST anomaly of the Nino 3.4 index within the same time-resolution will be used to quantify the degree of correlation. The metric datasets in this work are paired. For the quantification of the degree of correlation, the correlation coefficient has to be calculated. The value of the correlation coefficient could range from -1 to +1, which express the quantification of the correlation and the direction of the correlation. A correlation coefficient of +1 means a complete directly proportional connection between the two considered metric datasets. A value of -1 means a complete indirectly proportional connection. If two metric datasets have no correlation, the correlation coefficient will be near to 0. These correlations can be visualized by scatter diagrams, which are shown in Figure 7. Therein, typically graphs of positive (a), negative (b) and no correlation (c) can be seen (cf. HELLER et al, 1979: 122 ff).

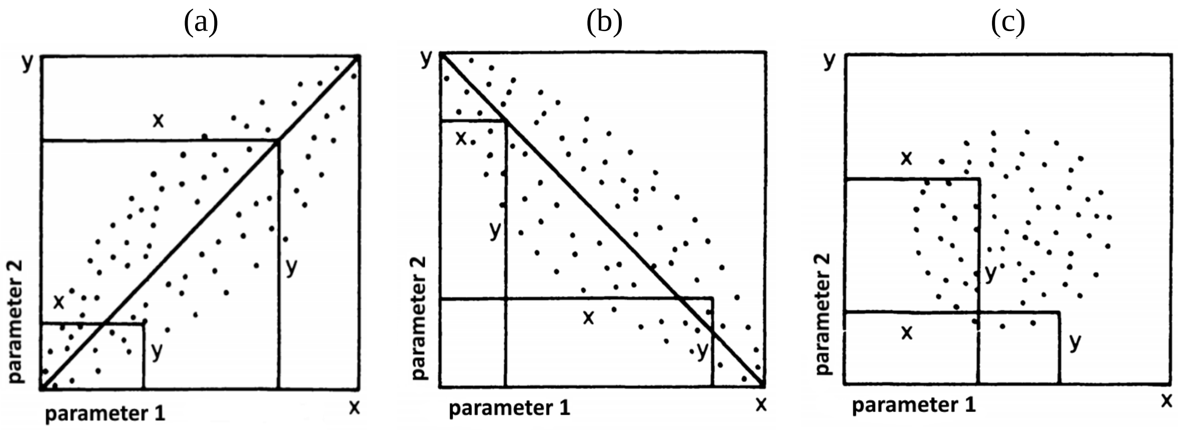

Figure 7: Scatter diagrams for positive (a), negative (b) and no correlation (c) (HELLER et al, 1979: 124)

The results of correlation coefficients could be quantified by the following classification (HELLER et al, 1979: 122):

negative correlation				**positive correlation**
0.00	=	**no correlation**	=	0.00
from 0.00 to > -0.40	=	**low correlation**	=	from 0.00 to < 0.40
from -0.40 to > -0.70	=	**average correlation**	=	from 0.40 to < 0.70
from 0.70 to > -1.00	=	**high correlation**	=	from 0.70 to < 1.00
-1.00	=	**complete correlation**	=	1.00

For the calculation of the Pearson´s product-moment correlation coefficient, two statements (null hypothesis and alternative hypothesis) have to be formulated in advance:

$\boldsymbol{H_0}$ **(null hypothesis)**: Between key variables in the Antarctica (parameter x) and ENSO events (parameter y) **no correlation** exists.

$\boldsymbol{H_1}$ **(alternative hypothesis)**: Between key variables in the Antarctica (parameter x) and ENSO events (parameter y) a **significant correlation** exists.

Following formula (HELLER et al, 1979: 126) has been used to quantify the alternative hypothesis:

$$r_{xy} = \frac{N * \sum xy - (\sum x) * (\sum y)}{\sqrt{[N * \sum x^2 - (\sum x)^2] * [N * \sum y^2 - (\sum y)^2]}}$$

r_{xy} … Pearson´s product-moment correlation coefficient dependent on metric datasets x and y
x … ice-mass change Antarctica
y … sea surface temperature (SST) Nino 3.4 index
N … sample size

For the examination of the Pearson´s product-moment correlation coefficient against the null hypothesis, the t-value will be considered (HELLER et al, 1979: 126). The t-value will be calculated by following formula (HELLER et al, 1979: 126):

$$t_{xy} = \frac{r_{xy} * \sqrt{N-2}}{\sqrt{1 - {r_{xy}}^2}}$$

After calculation of the t-value with the belonging correlation coefficient, a comparison with the critical values from Fisher & Yates (tables in (HELLER et al, 1979: 263)) by consideration of different significance levels and degrees of freedom (N-2) can be conducted. If the calculated t-value is equal or larger than the critical t-value, the null hypothesis may be rejected. Otherwise, the null hypothesis remains (HELLER et al, 1979: 126). Within this work, a significance level (one-sided test) of 0.01 will be used. Therefore, the following critical t-values after Fisher & Yates (HELLER et al, 1979: 263) are considered for the calculation:

data point classification	**sample size**	**critical t-value (Fisher & Yates)** (HELLER et al, 1979: 263)
Super El Niño (SST anomaly ≥ 1°C)	16	2.624
Large La Nina (SST anomaly ≤ -1°C)	20	2.552
Other data points (-1°C < SST anomaly > 1°C)	156	2.326

It must be noted that the Pearson´s product-moment correlation method only considers two metric datasets. Therefore, a correlation between two datasets does not mean a causal relationship, because the correlation coefficient does not allow predictions in terms of cause-effect relationship. Therefore, a third parameter (dataset) could be responsible for the correlation. Furthermore, only linear correlations could be analyzed. Summing up, a critical verification of the results should be conducted (cf. HELLER et al, 1979: 122 ff).

4 ENSO

The climate phenomenon El Niño Southern Oscillation (ENSO) is known as the most dominant fluctuation of the world´s climate system. ENSO includes the two complementary phases El Niño and La Niña, which both lead to anomalies of the sea surface temperature (SST) over the Tropical East and the Central Pacific Ocean (cf. CAPOTONDI et al. 2015: 921). The basic mechanism and the impacts of the strongest ENSO events will be explained in this chapter. Furthermore, a possible intensification due to global warming will be discussed.

4.1 Basic mechanism of ENSO

El Niño events are characterized by an unusual warming of the SST, which happens every two to eight years and lasts from 9-18 month (cf. GLANTZ and RAMIREZ 2020: 394). La Niña often occurs afterwards and is characterized by a cooling down of the SST (cf. VIKAS and DWARAKISH 2015: 131).

The normal weather and climate over the Pacific are controlled by the temperature differences in the Western and Eastern Pacific. Due to the differences, an atmospheric cell along the Equatorial Belt is generated (cf. LATIF 2018: 193). In the 1920s this was described by Sir Gilbert Walker as the Southern Oscillation. In 1996, Jacob Bjerkness expanded this concept. He described the Southern Oscillation as an atmospheric convective circle and introduced the term Walker Circulation (cf. BJERKNESS 1966, OLIVER 2004: 797). He also emphasized the coupling of the atmosphere and the temperature of the ocean (cf. YANG and LAU 2002: 1).

Under normal conditions, water surface temperatures and the sea level in the Pacific Ocean are determined by the position of the thermocline. The thermocline separates the cold ground water from the warm surface water. Due to westerly blowing trade winds, the thermocline is tilted and has a lower depth in the Equatorial Eastern Pacific. A strengthening factor is the Humboldt Current along the western coast of South America. It is driven by strong winds and provides the upwelling process, which is necessary for the local ecosystem (cf. LIPPELT and SCHRICKER 2016: 57). This area, also known as the Cold Tongue, extends to the Central Equatorial Pacific. From there the SST rises continuously and reaches a temperature around 28 °C. That´s why this region is known as the Warm Pool (cf. LATIF 2018: 193).

As shown in Figure 8, surface near winds are blowing westerly, where the warm aerial masses ascend. Consequently, heavy precipitations occur over the western part of the Pacific. In the upper part of the atmosphere, the air shifts eastwards and drops. Due to the descending air mass, a sufficient convection is not possible. Therefore, the Eastern Pacific regions are characterized by a severe drought. A common example is the Atacama Desert, which is the driest desert on Earth (cf. LATIF 2018: 195).

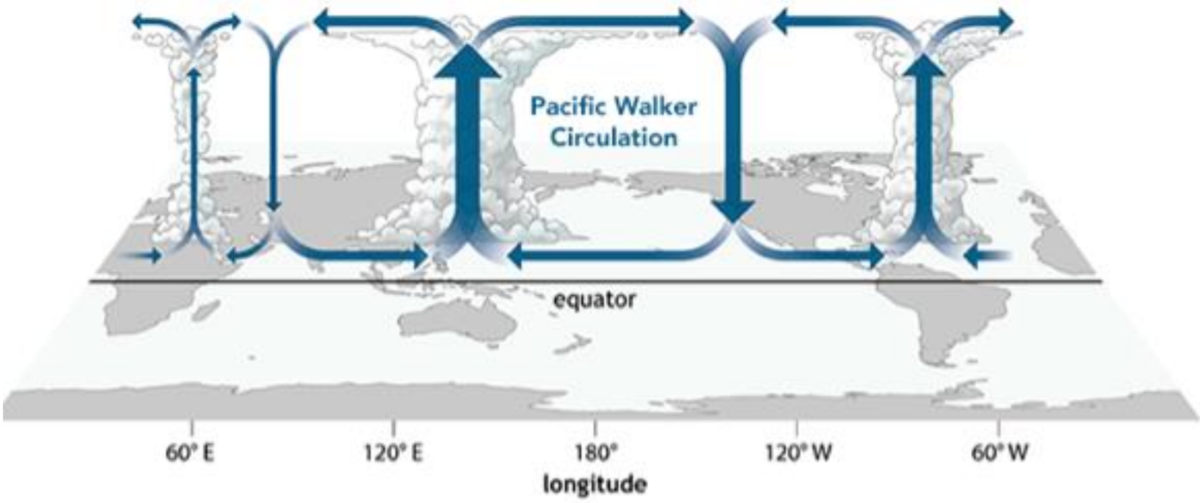

Figure 8: Neutral Conditions in the Pacific Ocean (NOAA 2016: 3)

El Niño, Spanish for the Christ Child, was originally observed and named by fishermen in Peru. They described a warm, southwards flowing current around Christmas time. During this event, the warm current displaces the cold water from the Humboldt Current. Consequently, the important upwelling process is not possible and the regional ecosystem changes. Fish species, which are normally located in Warm Pool areas, occur at the western coast of South America and were a pleasant surprise for the fishermen (cf. LATIF 2006: 123). Nowadays, the understanding of El Niño extends the idea of the occurrence of new fish species and the alternation around Christmas Time. Until the 1960s, the climate anomaly was just combined with the coasts of Ecuador and Peru (BARNSTON 1997: 368). Since the 1960s, El Niño is considered as a global phenomenon, which is linked to oceanic and atmospheric processes (cf. CAI et al. 2020: 215).

The situation during an El Niño event is shown in Figure 9. The SST warms up (orange) and equally the Cold Tongue. The tilt of the thermocline decreases, zonal differences vanish and a weakening of the Walker Circulation is generated (cf. CAPOTONDI et al. 2015: 921).

Furthermore, a strong weakening of the westerly blowing trade winds and a change in the atmospheric pressure leads to a lower water transport from the eastern to the western part of the Pacific Ocean (cf. L´HEUREUX and LEE 2013: 571). Thereby, a high-pressure area over Indonesia and North Australia arises and a low-pressure area over the Central and East Pacific, also covering parts of South America. This also leads to a weakening of the Humboldt Current and the warm surface water prevents the ascent of the cold nutritious water. The upwelling process cannot be implemented and fish species from warm water areas can be found (cf. LATIF 2006: 193).

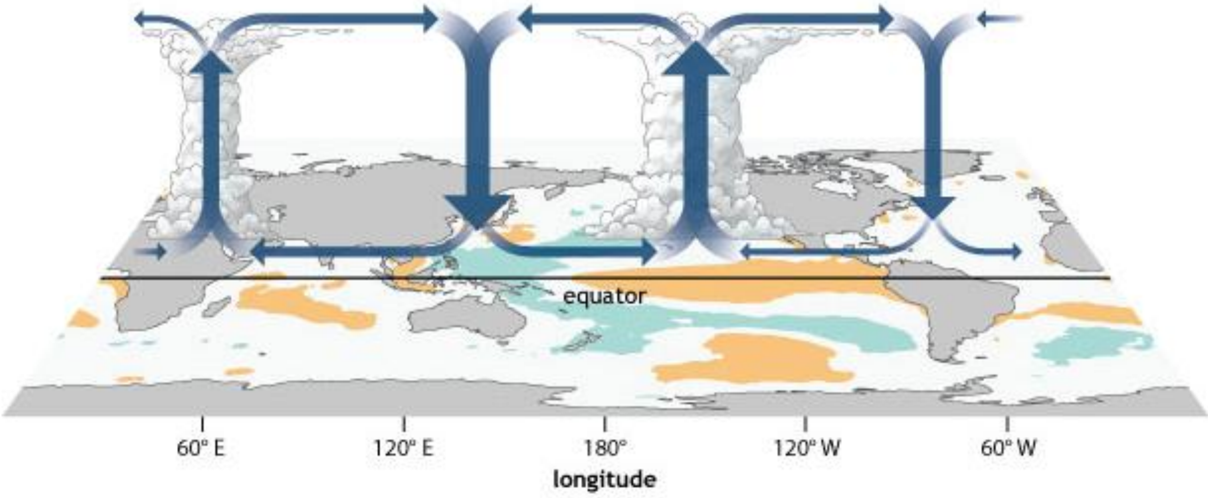

Figure 9: El Niño Conditions in the Pacific Ocean (NOAA 2016: 4)

La Niña events usually follow El Niño events. During La Niña events, the SST over large portions of tropical Pacific Ocean is cooler than average and the Cold Tongue continuous to cool. Figure 10 shows that strengthened easterly blowing trade winds push cooler water (blue-green) from the eastern part of the Pacific to the Central Pacific and to the western part. There, warmer water (orange) blends with the cooler water. The warmer water lead to a stronger evaporation and stronger precipitations follow (cf. NOAA 2016).

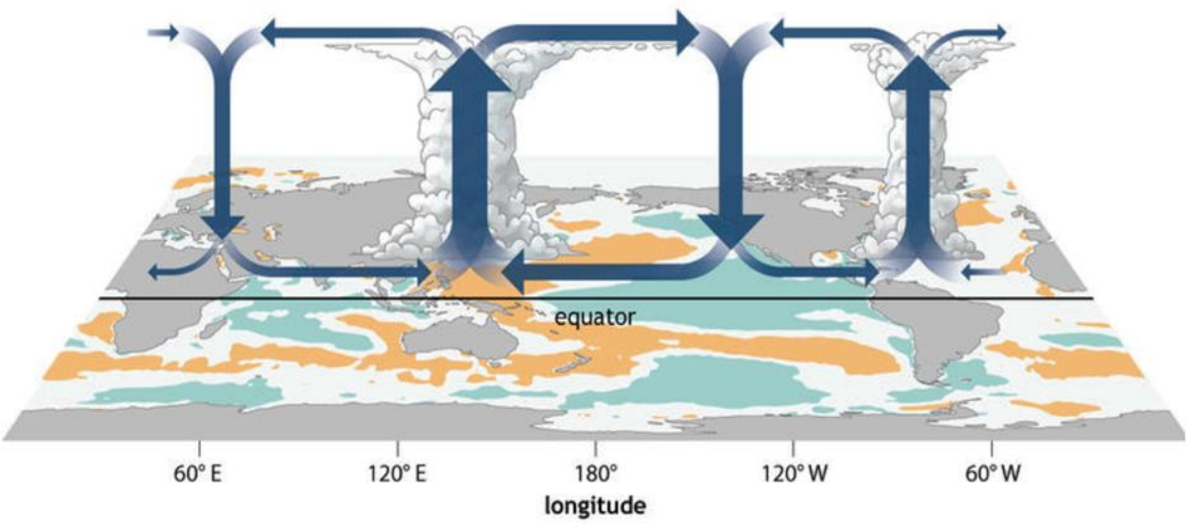

Figure 10: La Niña Conditions in the Pacific Ocean (NOAA 2016: 4)

4.2 Recorded ENSO events and their impacts

The observational knowledge of ENSO events it limited (cf. SANTOSO et al., 2017: 1079). Solid recordings exist only since the 1950s. Though every event is characterized by a warming or cooling of the SST, recordings show that every event regarding their magnitude and consequently their range and power of impacts is different (cf. TRENBERTH and STEPANIAK 2001: 1697; cf. HAMEED et al. 2018: 1).

There are two types of ENSO events, one is located in the Central Equatorial Pacific (CP-ENSO) and the other one in the Eastern Equatorial Pacific (EP-ENSO). They are distinguished according to their center of the highest SST anomaly (cf. CAI et al. 2018: 20). The strongest ones are defined as Super El Niños or Large La Niñas (cf. HONG et al., 2014: 2141). Super El Niños tend to be EP-ENSOs. La Niña events are weaker in this area. The Central Equatorial Pacific (CP- ENSO) is the center for Large La Niña events but moderate El Niño events (cf. CAI et al. 2018: 21). Within the Niño 3.4 index these definitions are used with a SST anomaly threshold larger than 1°C or smaller than -1°C (cf. YU et al., 2009: 7-8).

As shown in Figure 11 and Figure 12, 15 Super El Niños and 19 Large La Niña events were registered since the 1950s. These Super El Niño and Large La Niña events starting from 2002, will be used for data processing.

Since the 2000s, especially the Super El Niño 2015/2016 is conspicuous. After a long interruption from 1997/1998 it was the most powerful one. This event had many impacts on climate patterns across the Pacific Ocean (direct impacts). Also, global impacts (indirect impacts) could be observed (cf. NASA 2017). These disrupting impacts, which occur worldwide, are known as teleconnections (cf. GLANTZ and RAMIREZ 2020: 394). Because they also influence the stratosphere, weather- related anomalies are subsequently (cf. MCPHADEN et al. 2006: 1740).

A strong warming of the SST, which can be partly reduced to El Niño, has major impacts on the marine life. Direct impacts over the Equatorial Pacific are fatal. Due to the missing of the important upwelling process, the phytoplankton occur less. Therefore, dependent animals move to new feeding grounds. Consequently, the distribution of the marine life changes (cf. NASA 2017).

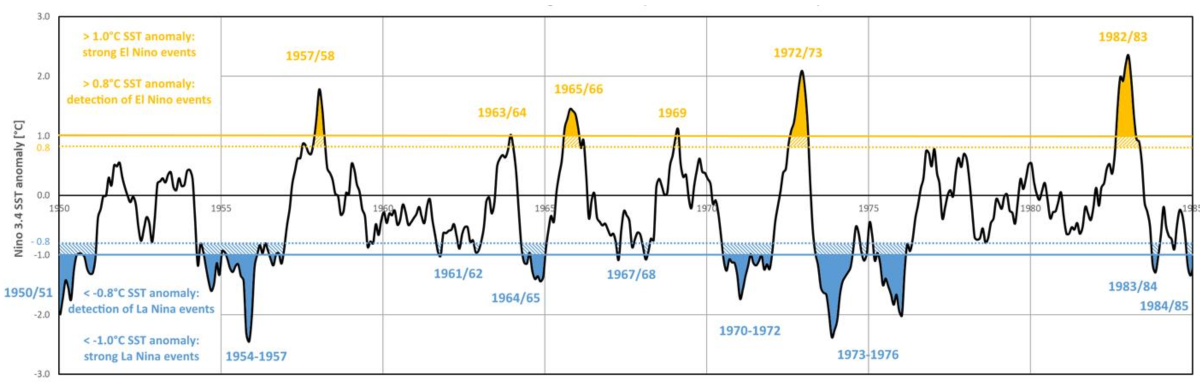

Figure 11: ENSO events during 1950-1985 (own representation, data from NOAA 2021)

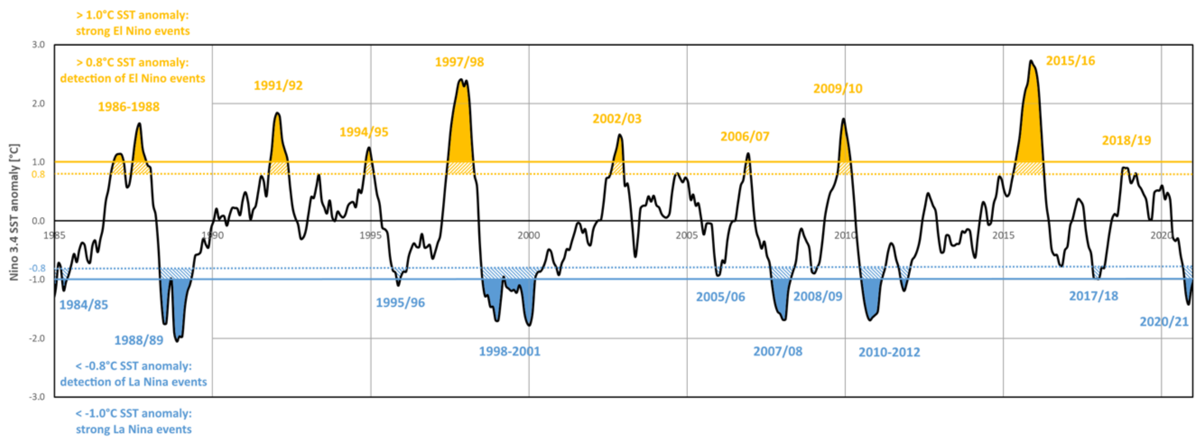

Figure 12: ENSO events during 1985-2020 (own representation, data from NOAA 2021)

Furthermore, the changes in the Walker Circulation due to ENSO lead to rainfall over the eastern part of the Pacific and to heavy flooding in the surrounding regions. Figure 13 shows a consequence of the Super El Niño 2015/2016. Heavy precipitations over parts of Argentina and Paraguay led to a flooding of the Rio Paraguay. On the left image the Rio Paraguay is shown under normal conditions in December 2013 and on the right side during the Super El Niño in January 2016 (cf. NASA 2017). It shows the strongest flood since 1983. Hence, more than 100.000 people had to be evacuated (cf. RUTH 2016).

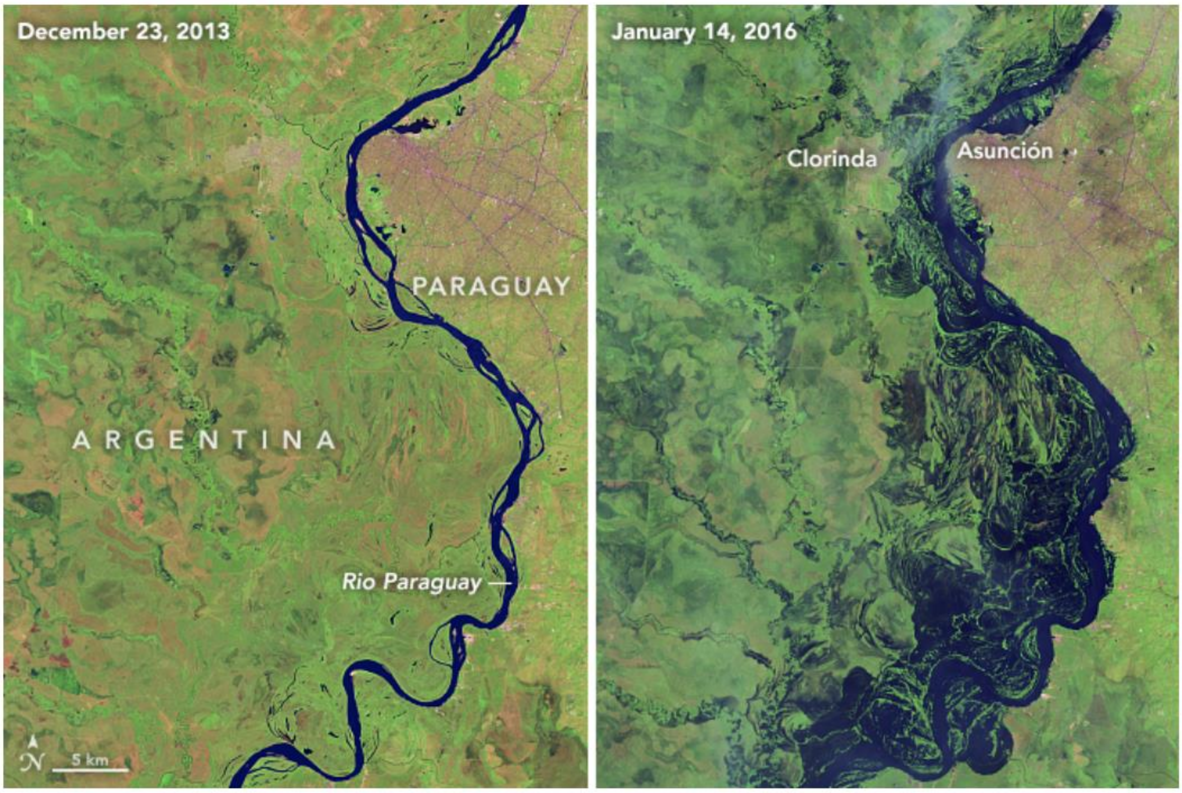

Figure 13: Rio Paraguay flooding due to the Super El Niño 2015/2016 (NASA 2017)

Though these regions had strong precipitation, other regions in South America, such as Brazil and Peru underwent less precipitation and drought. This shows that climate and weather patterns are disturbed during El Niño events. Further regions, such as Indonesia, Southeast Asia and Northern Australia, which experienced extreme drought and wildfires, are shown in Figure 14. Subsequently to large uncontrolled fires, air pollution occurs. Furthermore, extra carbon dioxide gets into the atmosphere. The vegetation, which suffers from heat and fire are not able to absorb this carbon as usual (cf. NASA 2017). The southern part of Africa had the most severe drought since 37 years. Crop failures and famines are just some of the severe consequences (cf. HOVE and KAMBANJE 2019: 33).

Floods and droughts due to El Niño events can be observed around the globe. The central part of America for instance experienced warmer and drier winter months (cf. NASA 2017). Additionally, temperature records could be measured. For instance, the winter 2016 in Alaska was the warmest one since the 92 years of records. In Australia the summer 2015 and the autumn 2016 were the warmest ones since 1910. A consequence of this Super El Niño event was also the strengthening of extreme droughts in Central America, in the northeastern and southern part of Africa, and in the Southeast of Asia (cf. HAESELER and ZIESE 2016: 3).

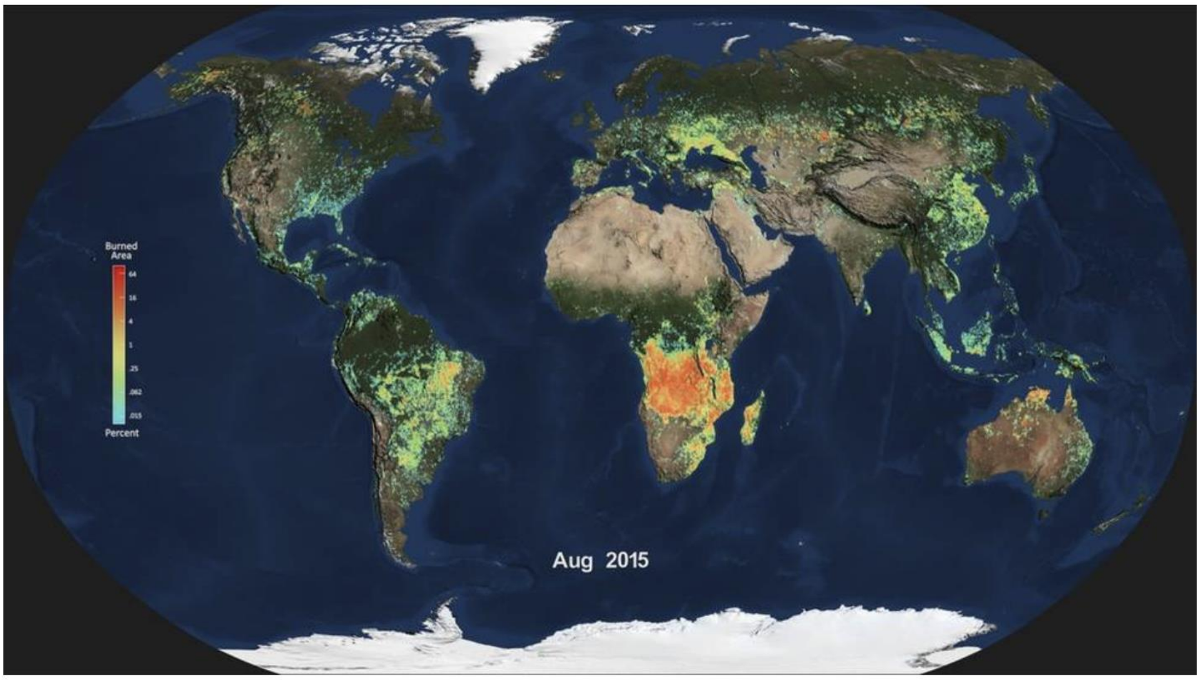

Figure 14: Global burned areas for in August 2015 - during the Super El Niño 2015/2016. Areas marked as light blue demonstrates a low percentage of burned areas. Orange and red marked areas have a high percentage of burned areas (cf. NASA 2015)

Compared to the impacts of El Niño events, those from La Niña are not that much studied, though they can be equally severe. In 1998/1999 for example, extreme flooding events in Bangladesh or Venezuela could be observed. Furthermore, La Niña events tend to bring drought to the southern part of the USA and more precipitation led to flooding in Canada (cf. DELNINNO and DOROSH, 2001: 337). The Large La Niña event 2010/2011 is considered to be responsible for extreme floods in Pakistan. From year to year the Asian Monsoon brings rain, but under the Large La Niña event the Monsoon was enhanced. Even month later, regions of Pakistan were flood (cf. NASA 2010).

The influence of ENSO on the Antarctica is less studied. It is not certain which concrete impacts these events have. The main reason for that are other climate and weather disruptions, which can have impacts on the Antarctica (DOMEISEN et al. 2019: 1)

It should be taken into consideration that the pattern of ENSO events are not laws of nature. Every event is different and it depends mainly on the characteristics of these events. Though impacts can occur global, the occurrence is different in every region. The described impacts cannot clearly be reduced only to ENSO events, because there are many other factors, such as the Indian Ocean Dipole, which influence the climate patterns around the world. An explicit statement about the impacts is therefore not possible (cf. BALDENHOFER 2017: 30).

4.3 Intensification of ENSO events due to climate change-presumptions

Climate change can be defined as *"the state of the climate that can be identified statistically by changes in the mean and/or the variability of its properties and that persists for an extended period, typically decades or longer" (*DAGBEGNON et al. 2015: 36).

Climate change can be seen as a geophysical phenomenon with no clear quantification. A common parameter is though the temperature fluctuation. The most considered one is nevertheless its effects, such as glacier recession, rise of the sea level or the increased incidences of natural hazard *(*DAGBEGNON et al. 2015: 38).

ENSO events can have major impacts on the ecology and economy of the human life. Therefore, the future behavior of ENSO events, especially their intensity and frequency under greenhouse warming is a major issue. The mechanism of ENSO is a very complicated process with various variables. It is not certain how the variables act under different climate conditions. Each of these can be influenced through climate change patterns (cf. DI LIBERTO 2018). Furthermore, there is no evidence of how the SSTs of the Pacific reacts to the future global warming (cf. CAI et al. 2018: 20). Therefore, the prediction of ENSO events remains a highly uncertain field (cf. DI LIBERTO 2018).

A factor for consideration is the combination of ENSO events with the global warming. Both lead to a warming of the SST, which may be higher in combination. An example which illustrates these impacts are the corrals. The Great Barrier Riff withstood all former ENSO events before 1970. Since then, impacts from the global warming became noticeable. The Riff suffered with corral bleaching, which can be observed regularly. From a temperature starting mostly with 29 °C, corrals react sensitive. They lose their symbiotic micro algae, which are responsible for their color (cf. BALDENHOFER 2017: 34).

Generally, in literature there are different opinions and studies about how ENSO will act in the future. Studies mostly refer to climate models. Some studies, like BAYR et al. 2014 predict weaker but constant future ENSO events. Others, like COBB et al. 2013 predict a higher intensity of ENSO events. A study from CAI et al. 2018 focused on the unreliability and contradictions from earlier studies. Therefore, they distinguished the two types (CP- ENSO, EP ENSO) of ENSO and considered their precise origin. They adduced wind and sea conditions from 17 CMIP 5 climate models. They simulated the conditions under the RCP 8.5 scenario, within the period 1900-2099. *"This scenario combines assumptions about high population a relatively slow income growth with modest rates of technological change and energy intensity improvements, leading in the long term to high energy demand and GHG emissions in absence of climate change policies" (*RIAHI et al. 2011: 33).

The RCP 8.5 scenario assumes therefore the highest greenhouse gas emission. In the study, they first observed that the various distribution of ENSO events regarding location and magnitude are the most important factors, to get reliable results. So, the CP ENSO includes stronger La Niña events and the EP ENSO stronger El Niño events. Under consideration of these anomalies, 88% (15 of the 17 models) showed an increased SST anomaly under the future global warming, especially in the Eastern Equatorial Pacific. The consequent would be, that Super El Niño and Large La Niña events will occur more often. This also implies an increase of these events. However, these prediction goes along with a high uncertainty. It is uncertain how the climate change continues. Furthermore, it is not clear, how individual features of ENSO, such as the onset and termination react to global warming (CAI et al. 2015: 857).

5 Terrestrial water cycle in the Antarctica

The water cycle visualizes the constant movement of water within the atmosphere and Earth. It combines water in all its physical states (cf. NOAA 2019).

Beside the temperature, water in combination with air and soil is the fundamental factor for the global climate. Though the water cycle constitutes a complex process, it will be simplified in this chapter. The main function will be clarified and the key variables will be described (cf. NOAA 2019).

5.1 Key variables of the water cycle

The basis for the water cycle is the connection of the salty seawater (96.5%) and freshwater (3.5%) to the atmosphere. Half of the freshwater is groundwater and the other half is stored in ice or snow. 89.8% of this storage can be found in the Antarctica and 9.7% in Greenland (cf. SIEGERT 2006: 2; SCHÖNWIESE 2020, 152).

Briefly, as shown in Figure 15, the seawater and the water from land surface evaporates through the sun and gets into the atmosphere. The following condensation and freezing result in the formations of clouds. Through the process of precipitation, the water comes back to ground surface. This whole process is called the terrestrial global water cycle.

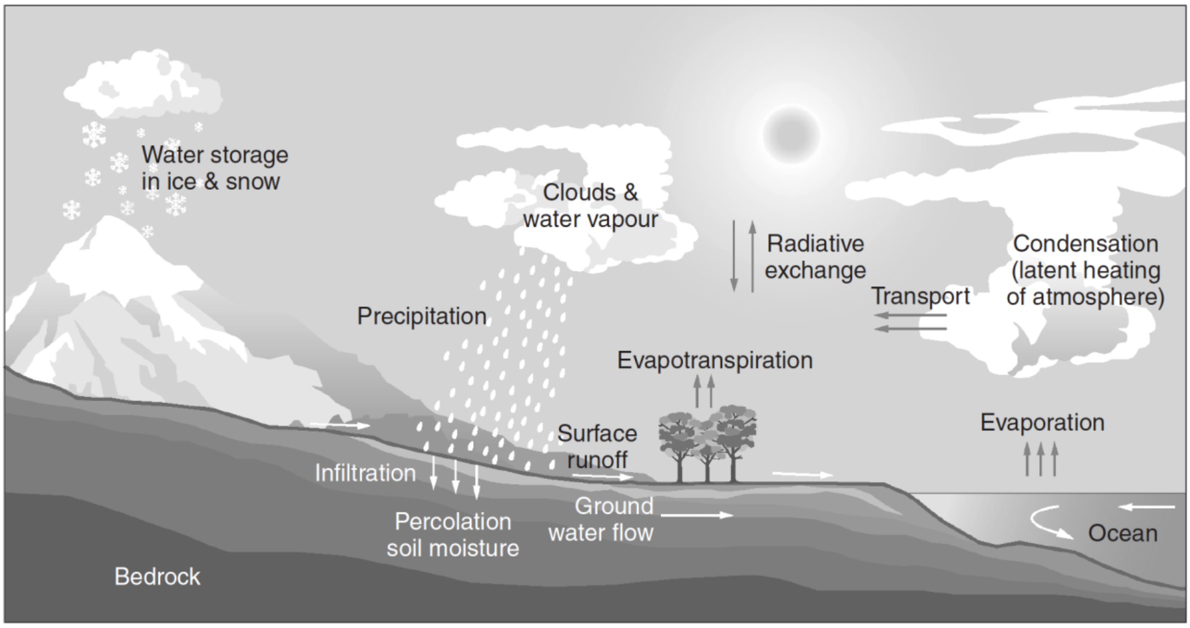

Figure 15: Flowchart of the global water cycle (SIEGERT 2006: 2)

The water cycle is though not only influenced by the precipitation and evaporation. Additionally, there is an atmospheric transport of oceanic water in the continental area, which will be balanced through surface and subsurface runoff. Therefore, the global terrestrial water balance integrated over many years can be written as following: (cf. SCHÖNWIESE 2020, 152 f)

$$P + E + R = 0$$

P…Total precipitation (positive)
R…Runoff (negative)
E…Evaporation (negative)

For calculation with a temporary regional water balance, a more detailed approach need to be considered. Therefore, the evaporation parameter (inanimate nature) has to be extended by the transpiration, which is the evaporation of animate nature. Summing up, both parts of evaporation could be written in a sum as evapotranspiration. Furthermore, the introduction of a balanced storage variable for soil and vegetation as well as deep groundwater must be considered. Additionally, the runoff has to be written as balanced variable, which consider the inflow as well. In this case, the regional water balance can be written as following: (cf. SCHÖNWIESE 2020, 153 f)

$$P + ET + \Delta R + \Delta S + \Delta IG = 0$$

P…Total precipitation (positive)
ΔR…Runoff (balanced with inflow, negative)
E…Evaporation (negative)
T…Transpiration (negative)
$ET = E + T$…Evapotranspiration (negative)
ΔIG…Deep groundwater
ΔS…Change in soil and vegetation

For the calculation of the regional water cycle in the Antarctica, the transpiration will be neglected. To sum up all storage variables ($\Delta IG + \Delta S$), the water balance as a new variable will be introduced:

$$water\ balance = P + E + \Delta R$$

Though the Antarctica is the driest and coldest continent on Earth, the process of the water cycle does not differ from other continents. Liquid water can be found in lakes and in melting ice. Besides water in liquid and gaseous form, snow crystals and ice particles are also integrated in the water cycle. Snow is blown up by the wind and gets into the atmosphere (cf. SCHÖNWIESE 2020, 153 f). During the winter month, where the sun is not visible, the wind causes the process of evaporation. Wind is therefore an important factor to maintain the cycle. For the Antarctic continent, the part of the ice-mass balance is the most interesting one (cf. VAN LIPZIG 2016).

The climate of the Antarctica reacts sensitive to changes. In the West Antarctica, the climatological low-pressure center, the Amundsen Sea Low, mainly influences the key variables from the water cycle. There, anomalies arise through ocean circulation changes, which are driven by surface near winds (cf. RAPHAEL et al. 2016:1). ENSO events may have impacts on the water cycle over the Antarctic continent. During an El Niño event an upward wave propagation in the polar vortex, in the Southern Hemisphere (SH) occurs. Consequently, the weather and global climate become disrupted. In the polar stratosphere, strong easterly blowing winds within the polar stratosphere arise (cf. DOMEISEN et al. 2019:1 ff). Upwelling processes, which are suppressed during El Niño, result in warmer water layers, which can be a reason for increased ice melting in the western part of the Antarctica (cf. PAOLO et al. 2018:1).

5.2 Influences through climate change

The global climate change has major impacts on the process of the water cycle. The global climate and the water reservoir are closely linked. Alterations in climate patterns lead to alternations in the water cycle and vice versa (cf. KUNDZEWICZ 2008: 195).

The consequences of the global warming are mostly extreme weather events. Mainly affected are the temperature, precipitation and the sea level (cf. NOAA 2019). Changes in precipitation patterns are one of the most dominant factors worldwide, but it is not uniformly distributed. Due to a warming of the lower atmosphere and the SST, the evaporation rate grows and consequently the atmospheric moisture increases. A stronger cloud formation and further, more precipitation are the consequences (cf. NASA 2010).

Though some regions are not affected, others undergo strong precipitations or even extreme floods. Therefore, the water balance in the cycle is affected. Anomalies in the precipitation patterns can occur through the increasing heat (cf. DAGBEGNON et al. 2015: 40).

On the other hand, some regions undergo less precipitation or even extreme drought. Furthermore, natural water storages, such as ice or snow are concerned. The retreatment of glaciers and the decrease of ice storages, minimize the space for water deposits. For the Antarctica this means, that some regions would get more precipitation and an increase of the ice-mass. In other regions, less precipitation could be the consequence (cf. KERRES et al. 2020: 25).

How ENSO will act in the future and especially under global warming, is an unknown issue. Also, the impacts which ENSO may have on the Antarctica cannot be predicted. However, it can be said, that the Antarctic climate reacts sensitive to changes, such as ENSO events or the global warming. The reason for that are the tropical and Southern Hemispheric (SH) teleconnections. It can therefore be assumed, that a possible increasing of ENSO events due to global warming could have major impacts on the Antarctic climate (cf. RAHAMAN et al. 2019: 1).

6 Results and discussion

Based on the described methodology for data processing by Pearson's product moment correlation method, the results of the correlation between the ice-mass change in the Antarctica and the sea surface temperature (SST) of the Niño 3.4 index are summarized and discussed in this chapter. Furthermore, the correlation results between key variables of the terrestrial water cycle and the SST of the Niño 3.4 index are shown. Finally, three different parameters of the Antarctic wind fields will be correlated with the Niño 3.4 index. For the ice-mass change correlations, the total Antarctic Ice Sheet, supra-regional parts of the Antarctic Ice Sheet as well as sub-regions of the Antarctica will be considered. Within the water cycle and wind field correlations, only supra-regional parts of the Antarctic Ice Sheet and the total Antarctica will be investigated.

As mentioned in chapter 4.3, the prediction of future ENSO events is a huge research field, with contrary statements and studies. Therefore, a quantitative investigation of the water cycle anomalies due to the intensification of ENSO events is not conclusive.

6.1 Correlation between ice-mass change Antarctica and SST of Nino 3.4 index

For the answering of the research question regarding the correlation between ENSO events and the ice-mass sheet change in the Antarctica, the Pearson's product moment correlation method has been used. Therefore, the Antarctica has been split into 25 regions according to GRACE data from GFZ (GFZ 2021). As shown in Figure 16, the Antarctic Ice Sheet is divided into the West Antarctic Ice Sheet and Antarctic Peninsula Ice Sheet (red), the East Antarctic Ice Sheet (green) and the Central Antarctic Ice Sheet (blue) (cf. BODART 2019: 4). Floating ice shelfs like the Ronne or Ross Ice Shelf are not considered in the correlation calculations.

Subsequent, the correlation results for the comparison of the SST from the Niño 3.4 index with the ice-mass change of the total Antarctic Ice Sheet, supra-regional parts of the Antarctica as well as different sub-regions from the Antarctica will be listed. The regional distribution of the Antarctic Ice Sheet allows the assessment of the regionally different impacts through climate phenomena like ENSO on the Antarctica.

For every region in the Antarctica as well as for supra-regional parts of the Antarctica, the correlation between Super El Niño events (SST anomaly ≥ 1°C) and the regional ice-mass change in the Antarctic region will be shown. Furthermore, the correlation between Large La Niña events (SST anomaly ≤ -1°C) and the regional ice-mass change in the Antarctic region will be investigated. For cross checking, all other data pairs (SST anomaly between -1°C and

+1°C), which are not dated within a Super El Niño or Large La Nina events, will also be correlated with the regional ice-mass change in the Antarctic region.

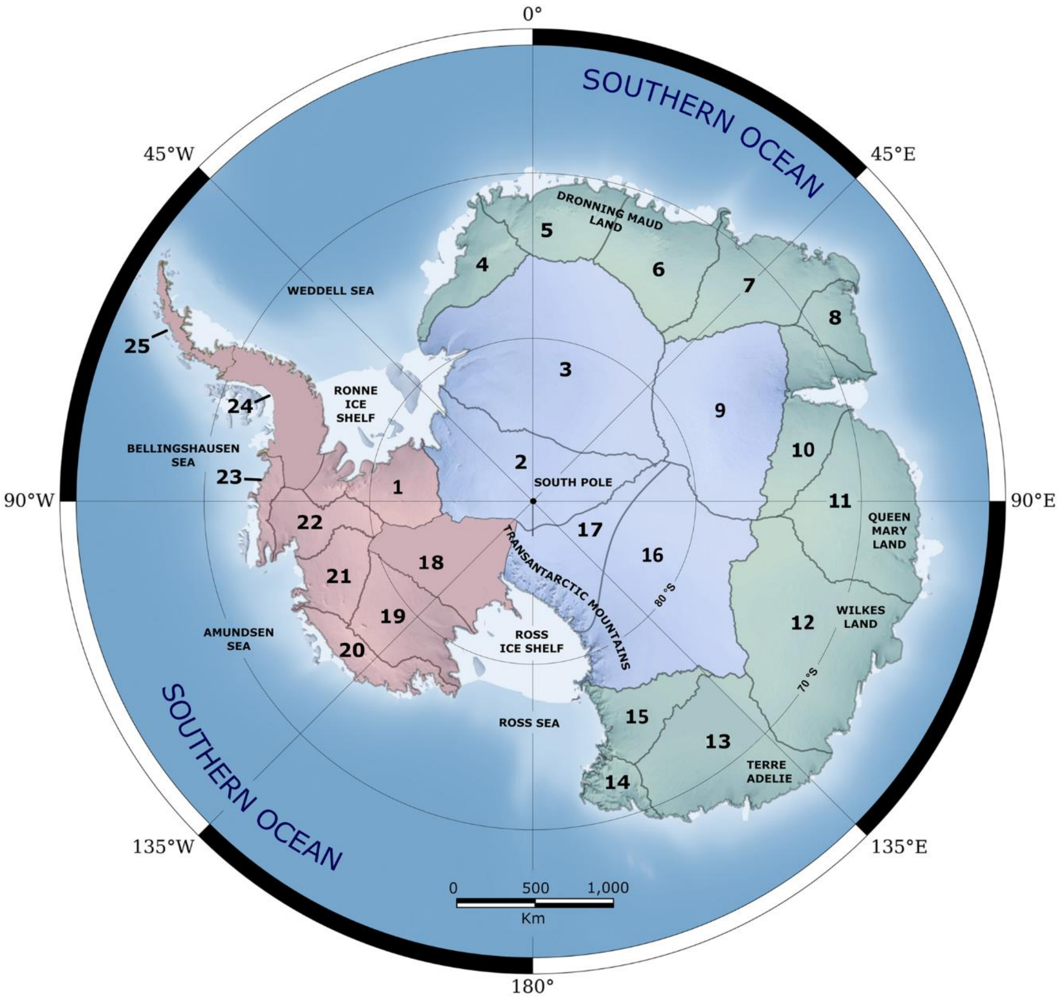

Figure 16: Regional distribution of the Antarctica with the sub-regions West Antarctic Ice Sheet and Antarctic Peninsula Ice Sheet (red), the East Antarctic Ice Sheet (green) and the Central Antarctic Ice Sheet (blue) (adapted from (BODART 2019:4))

The following statements will be used for the correlation:

H_0 **(null hypothesis)**: Between ice-mass change in the Antarctic region – AIS_0XX and ENSO events **no correlation** exists.

H_1 **(alternative hypothesis)**: Between ice-mass change in the Antarctic region – AIS_0XX and ENSO events a **significant correlation** exists.

The Pearson's product moment correlation coefficient (r_{XXX}) quantifies the stated correlation within the alternative hypothesis. The t-value (t_{XXX}) helps for examination against the null hypothesis.

6.1.1 Correlation total Antarctic Ice Sheet with Nino 3.4 index

First, the correlation between the SST from the Niño 3.4 index and the ice-mass change of the total Antarctic Ice Sheet are investigated. In Figure 17, the ice-mass change in the total Antarctica as well as the results of the correlation with the total Antarctica are shown. Therein, it could be observed that between the years 2002 and 2020 the ice-mass in the Antarctica decreased by 2750 Gt (Figure 17a). The correlation between the data points from Super El Niño events (chapter 4.2) with the SST from the Niño 3.4 index results in a high negative correlation ($r_{AIS/El} = -0.77$, Figure 17b) with a high t-value ($t_{AIS/El} = 4.50$, Figure 17b). This means that during Super El Niño events with increasing SST from the Niño 3.4 index, the ice-mass of the total Antarctica decreases. Furthermore, the calculated t-value is higher than the critical t-value ($t_{krit,El} = 2.624$). Therefore, the null hypothesis (no correlation) could be declined. The correlation results within Large La Niña events ($r_{AIS/La} = -0.26$, Figure 17c) and all other data points ($r_{AIS/other} = -0.12$, Figure 17d) show only very low correlations.

The investigation of the ice-mass change in the total Antarctica results in a correlation between the SST of the Niño 3.4 index and the ice-mass change during Super El Niño events, which could be effected due to warm ocean currents and changes in the weather patterns.

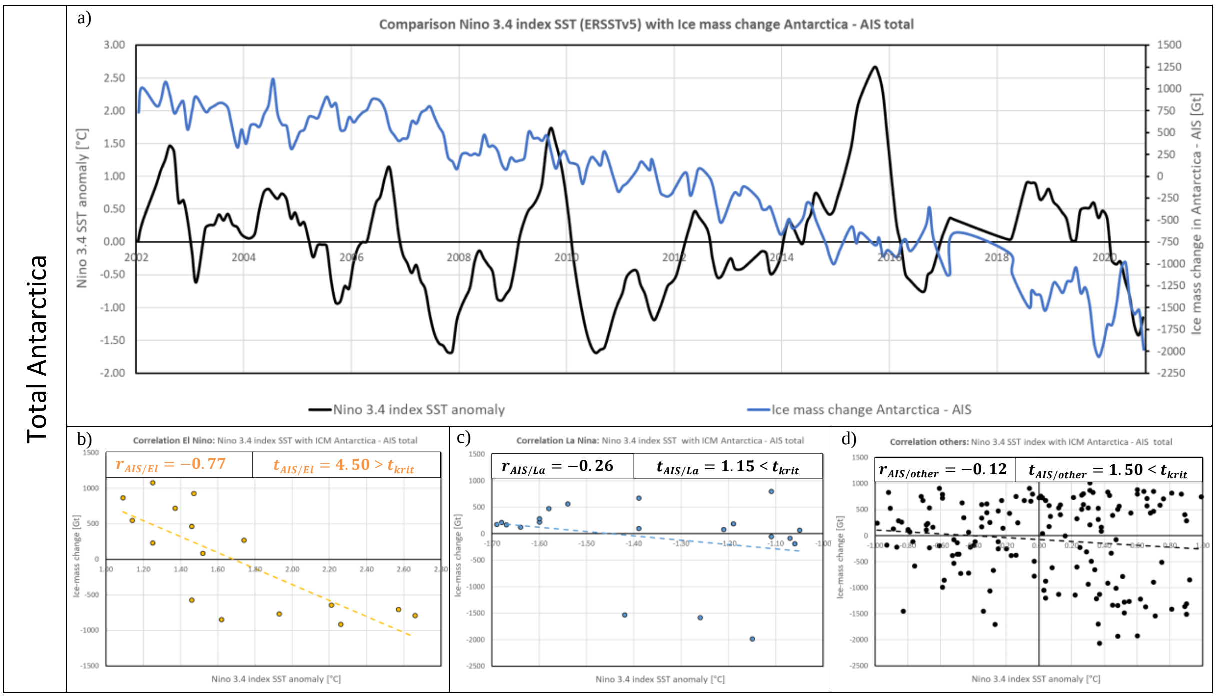

Figure 17: Results of the correlation from the ice-mass change of the total Antarctic Ice Sheet with the SST anomaly from the Niño 3.4 index [a) Ice-mass change and Niño 3.4 index within the selected region between the years 2002 and 2020, b) Correlation of ice-mass change with SST anomaly of Niño 3.4 index during Super El Niño events, c) Correlation of ice-mass change with SST anomaly of Niño 3.4 index during Large La Niña events, d) Correlation of ice-mass change with SST anomaly of Niño 3.4 index between Large La Niña and Super El Niño events]

6.1.2 Correlation supra-regional parts of the Antarctic Ice Sheet with Niño 3.4 index

After the correlation of the total Antarctic Ice Sheet, supra-regional parts of the Antarctic Ice Sheet will be investigated. In Figure 18, the ice-mass change in the supra-regional parts of the Antarctica as well as the correlation results between the Niño 3.4 index and the ice-mass change within supra-regional parts of the Antarctic Ice Sheet are shown. Therein, it is illustrated that the ice-mass within the West Antarctic Ice Sheet and Antarctic Peninsula Ice Sheet decreased continuously by around 3000 Gt of ice-mass within the last 18 years (Figure 18a$_W$). In the same period, the East Antarctic Ice Sheet increased by around 325 Gt of ice-mass (Figure 18a$_E$). Furthermore, the East Antarctic ice-mass was very fluctuating in this period. The biggest increase of ice-mass was between the years 2008 and 2013. The Central Antarctic Ice Sheet was more or less constant between the years 2002 and 2020. Between the years 2008 and 2015 small increases within the Central Antarctic Ice Sheet could be observed (Figure 18a$_C$). The results of the correlation between the ice-mass change of the supra-regional ice sheets and the Niño 3.4 index for the West Antarctic and Antarctic Peninsula Ice Sheet during Super El Niño events show a high negative correlation ($r_{W\&AP/El} = -0.76$, Figure 18b$_W$). The Central Antarctic Ice Sheet showed a high positive correlation ($r_{Central/El} = 0.82$, Figure 18b$_C$) during Super El Niño events and the East Antarctic Ice Sheet showed an average positive correlation ($r_{East/El} = 0.62$, Figure 18b$_E$). During Large La Niña events as well as during all other periods only low correlations ($|r| < 0.4$) could be observed.

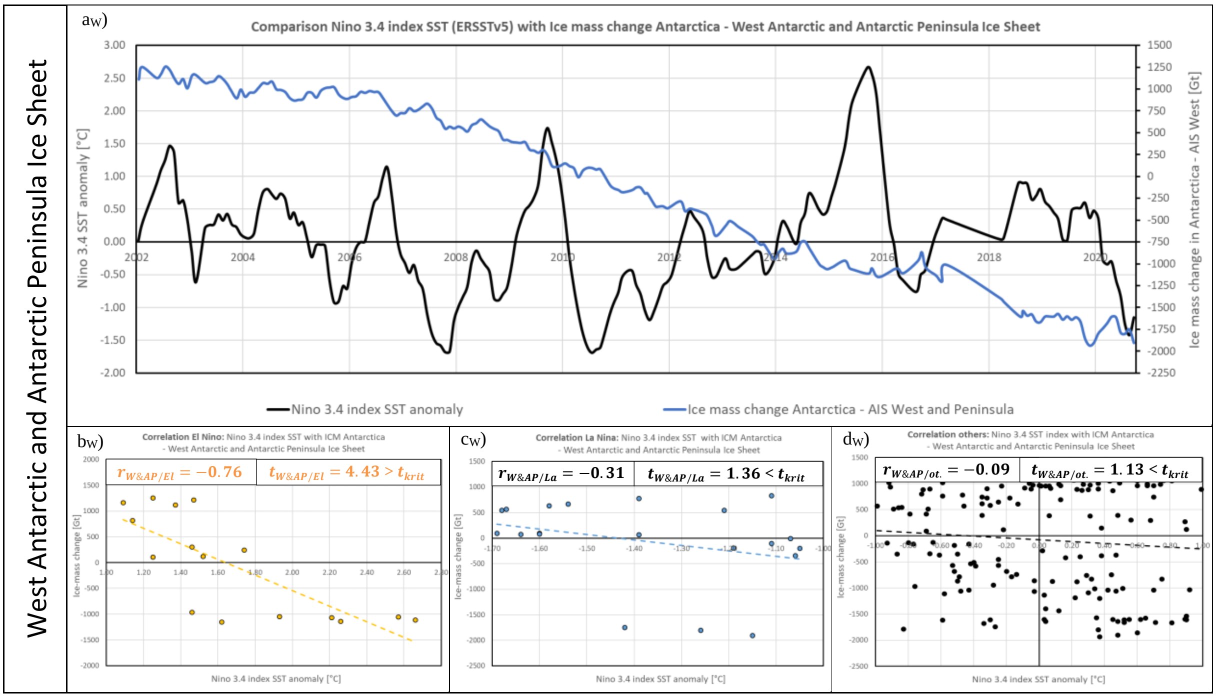

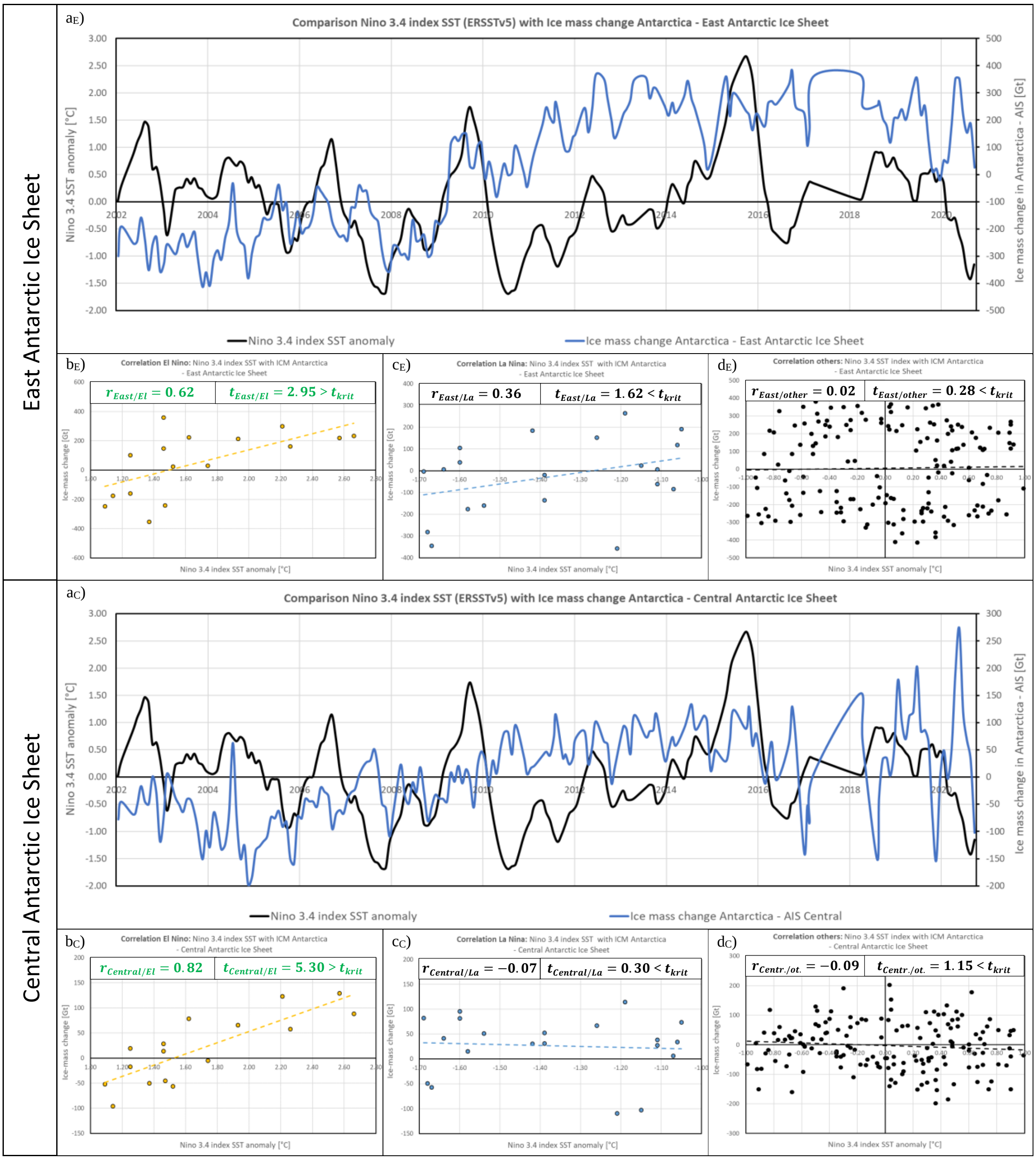

Figure 18: Results of the correlation from the ice-mass change of supra-regional parts of the Antarctica with the SST anomaly from the Niño 3.4 index [a) Ice-mass change and Niño 3.4 index within the selected region between the years 2002 and 2020, b) Correlation of ice-mass change with SST anomaly of Niño 3.4 index during Super El Niño events, c) Correlation of ice-mass change with SST anomaly of Niño 3.4 index during Large La Niña events, d) Correlation of ice-mass change with SST anomaly of Niño 3.4 index between Large La Niña and Super El Niño events]

The high negative correlation during Super El Niño events in the West Antarctic and Antarctic Peninsula Ice Sheet could be explained by the geographical location near to the Equatorial Pacific, where the Niño 3.4 index is located. The positive correlations during Super El Niño events in the Central and East Antarctic could be explained by the geological differences in comparison to the West Antarctica. The East and Central Antarctica mostly consists of a stable shield of rocks above sea level (cf. LUIS 2013: 2).

6.1.3 Correlation sub-regions of Antarctic Ice Sheet with Nino 3.4 index

To find regional correlations the Antarctic Ice Sheet is divided into 25 regions. In Figure 19, the ice-mass change in the main sub-regions of the Antarctica as well as the results of the correlation from the ice-mass change with the SST anomaly from the Niño 3.4 index can be seen. Therein, the correlation results for the main regions of the Antarctica regarding the distribution in Figure 16 is shown. Results for sub-regions, which are not shown in Figure 19 could be found in the appendix. In the period 2002 to 2020, the ice-mass in the sub-regions AIS_001 (Figure $19a_1$), AIS_018 and AIS_019 (Figure $19a_{19}$), which are located in the West Antarctic and Antarctic Peninsula Ice Sheet, increased between 200 and 400 Gt. In the sub-regions AIS_020 – AIS_025, also located in the West Antarctic and Antarctic Peninsula Ice Sheet, an ice-mass decrease of 200 (Figure $19a_{24}$) to 1300 Gt (Figure $19a_{21}$) occurred. In addition, high and average positive correlations between the SST anomaly and the ice-mass sheet of the West Antarctic and Antarctic Peninsula sub-regions AIS_001 (Figure $19b_1$), AIS_018 and AIS_019 (Figure $19b_{19}$) could be observed during Super El Niño events. High negative correlations during Super El Niño events could be seen within the other West Antarctic and Antarctic Peninsula sub-regions AIS_020 – AIS_025 (Figure $19b_{21}$ and Figure $19b_{24}$). In the East Antarctica, moderate ice-mass gains were observed in most sub-regions (exemplary Figure $19a_5$ and Figure $19a_7$). Only within the East Antarctic sub-region AIS_011 (Figure $19a_{11}$). a very fluctuating ice-mass change profile and in AIS_012 (Figure $19a_{12}$) an ice-mass decrease could be visualized. In line with the ice-mass change profiles, high positive correlations in the East Antarctic sub-regions AIS_005 (Figure $19b_5$) and AIS_007 (Figure $19b_7$) and a high negative correlation in AIS_012 (Figure $19b_{12}$) are noticeable. A very low positive correlation is visible in the sub-region AIS_011 (Figure $19b_{11}$). Within the Central Antarctic Ice Sheet, in the sub-regions AIS_009 (Figure $19a_9$), AIS_016 and AIS_017 (Figure $19a_{17}$), the ice-mass remained relative constant. Furthermore, an ice-mass increase in the sub-region AIS_003 (Figure $19a_3$) and a decrease in AIS_002 could be detected. Additionally, the regions AIS_003 (Figure $19b_3$) and AIS_009 (Figure $19b_9$) showed also high positive correlations within Super El Niño events. Very low negative correlation could be observed within the sub-region AIS_017 (Central Antarctica). All other sub-regions showed positive or negative average correlations during Super El Niño events. For the correlation with Large La Niña events, within the sub-region AIS_024 (Antarctic Peninsula) a negative average correlation and within AIS_007 (East Antarctic) a positive average correlation could be observed. For all other sub-regions, only low correlations are shown. For all other data points no correlation occurs.

El Niño events arise within the Niño 3.4 region, which is located over the Equatorial Pacific. Due to the fact, that the West Antarctic and Antarctic Peninsula regions are located closest to the El Niño origin, the high negative correlations, which means more ice melting within El Niño periods, in this area seems to be reasonable. Again, the geological differences could be the reason for ice-mass gains in the Central and East Antarctica and ice-mass loss in the West Antarctic and Antarctic Peninsula.

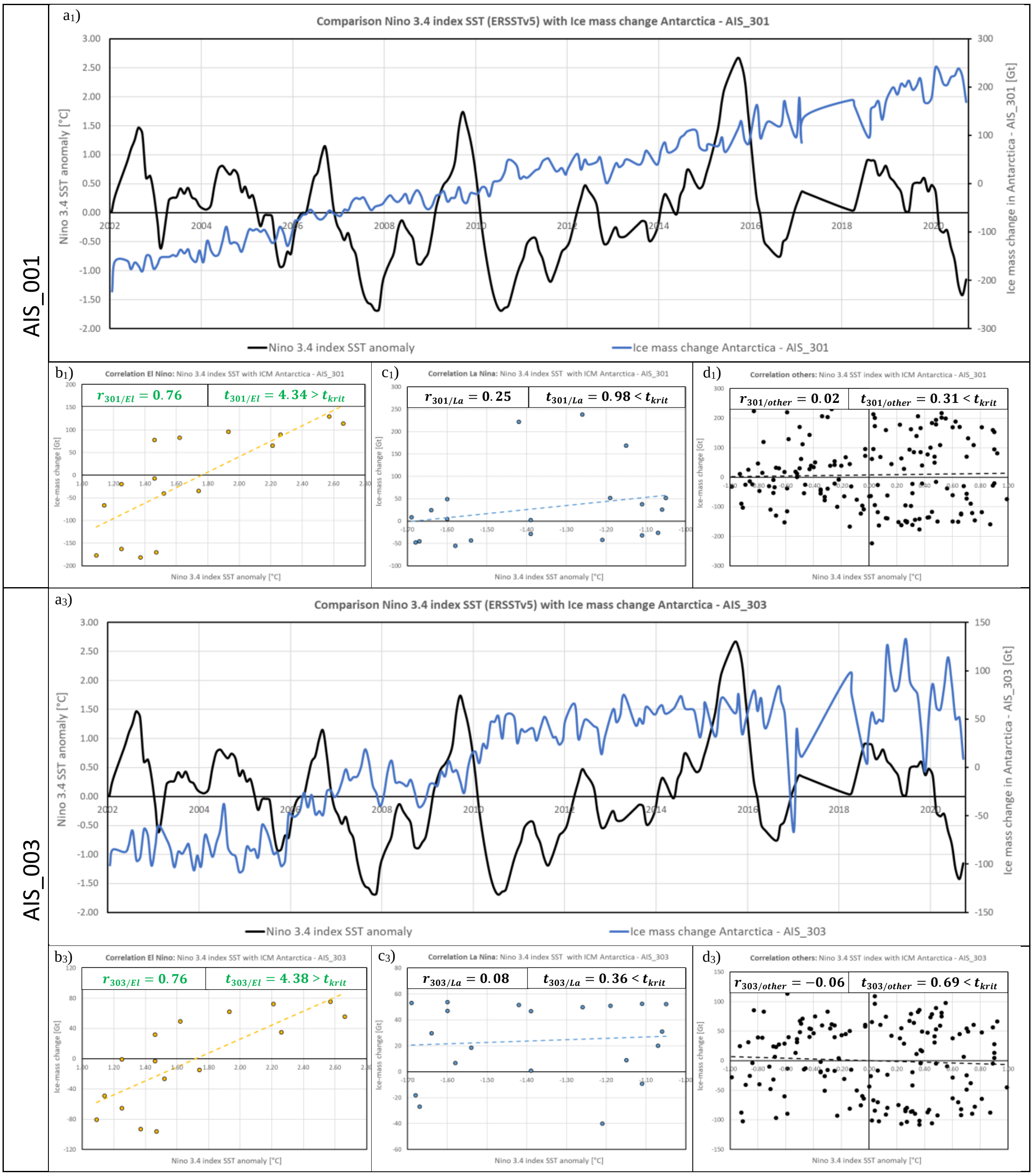

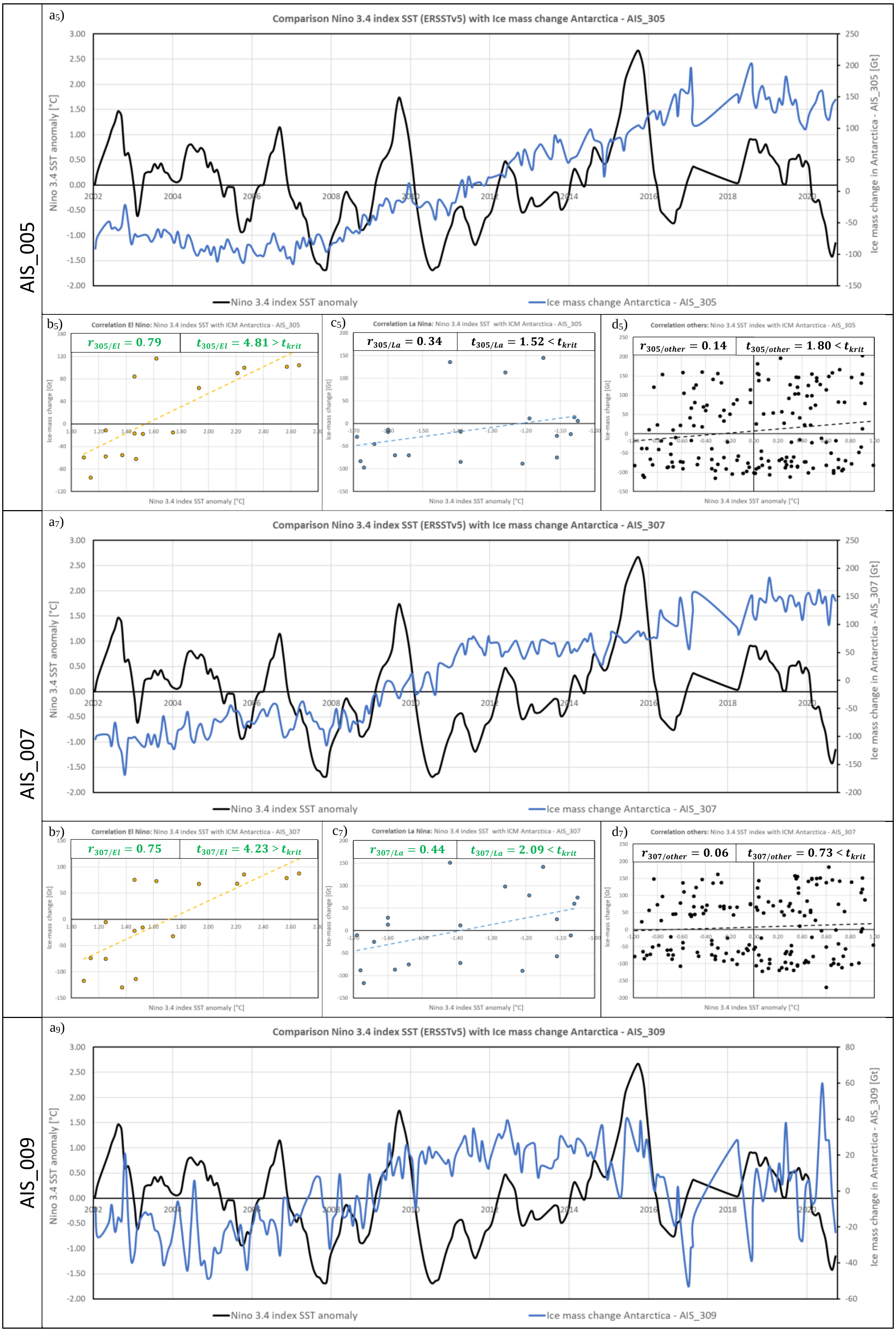
AIS_005
a5)
Comparison Nino 3.4 index SST (ERSSTv5) with Ice mass change Antarctica - AIS_305
Nino 3.4 SST anomaly [°C]
Ice mass change in Antarctica - AIS_305 [Gt]
Nino 3.4 index SST anomaly
Ice mass change Antarctica - AIS_305
b5)
Correlation El Nino: Nino 3.4 index SST with ICM Antarctica - AIS_305
$r_{305/El} = 0.79$
$t_{305/El} = 4.81 > t_{krit}$
Ice-mass change [Gt]
Nino 3.4 index SST anomaly [°C]
c5)
Correlation La Nina: Nino 3.4 index SST with ICM Antarctica - AIS_305
$r_{305/La} = 0.34$
$t_{305/La} = 1.52 < t_{krit}$
d5)
Correlation others: Nino 3.4 SST index with ICM Antarctica - AIS_305
$r_{305/other} = 0.14$
$t_{305/other} = 1.80 < t_{krit}$
AIS_007
a7)
Comparison Nino 3.4 index SST (ERSSTv5) with Ice mass change Antarctica - AIS_307
Ice mass change in Antarctica - AIS_307 [Gt]
Ice mass change Antarctica - AIS_307
b7)
Correlation El Nino: Nino 3.4 index SST with ICM Antarctica - AIS_307
$r_{307/El} = 0.75$
$t_{307/El} = 4.23 > t_{krit}$
c7)
Correlation La Nina: Nino 3.4 index SST with ICM Antarctica - AIS_307
$r_{307/La} = 0.44$
$t_{307/La} = 2.09 < t_{krit}$
d7)
Correlation others: Nino 3.4 SST index with ICM Antarctica - AIS_307
$r_{307/other} = 0.06$
$t_{307/other} = 0.73 < t_{krit}$
AIS_009
a9)
Comparison Nino 3.4 index SST (ERSSTv5) with Ice mass change Antarctica - AIS_309
Ice mass change in Antarctica - AIS_309 [Gt]
Ice mass change Antarctica - AIS_309

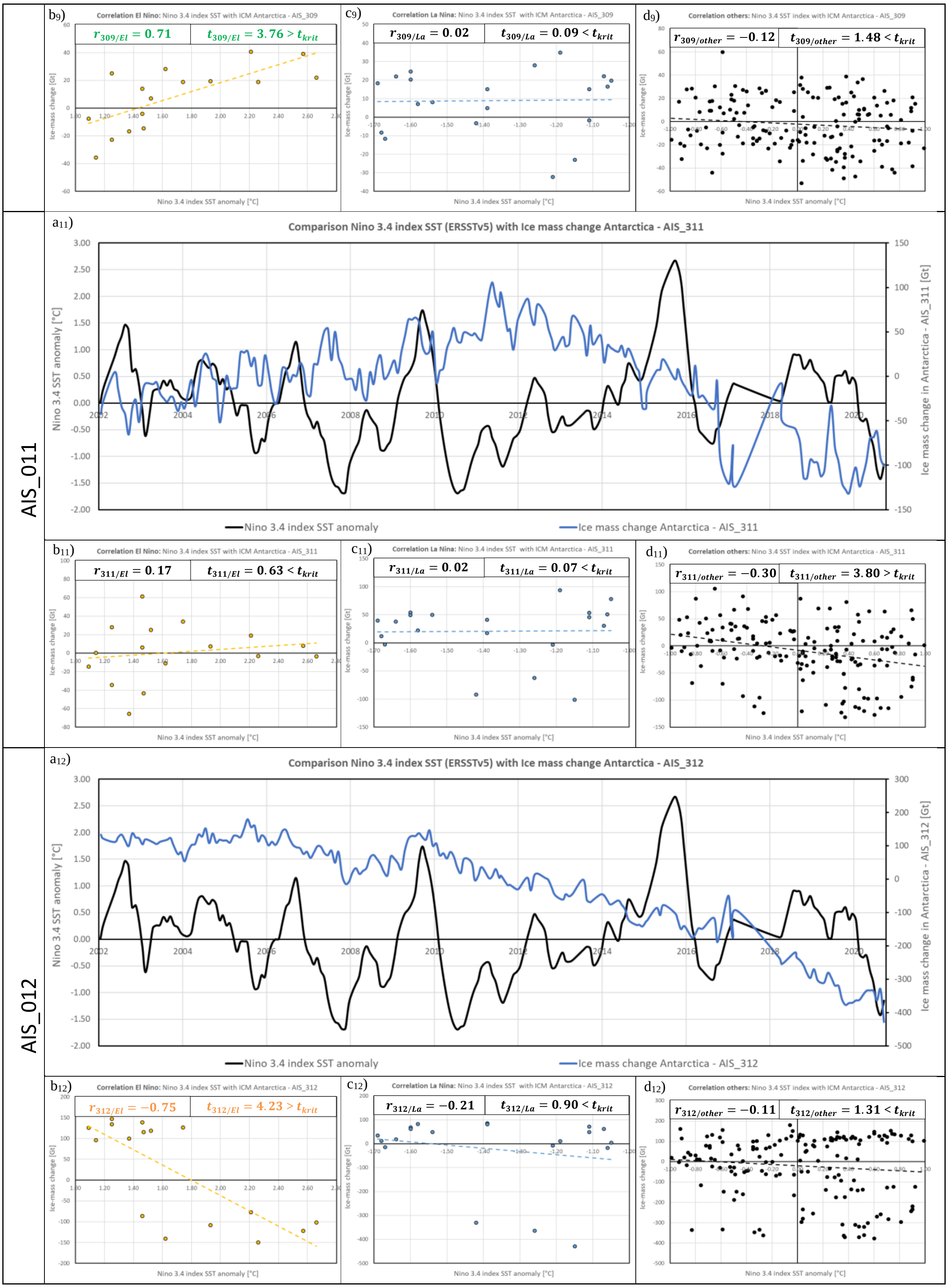
AIS_011
AIS_012
b9)
Correlation El Nino: Nino 3.4 index SST with ICM Antarctica - AIS_309
$r_{309/El} = 0.71$
$t_{309/El} = 3.76 > t_{krit}$
c9)
Correlation La Nina: Nino 3.4 index SST with ICM Antarctica - AIS_309
$r_{309/La} = 0.02$
$t_{309/La} = 0.09 < t_{krit}$
d9)
Correlation others: Nino 3.4 SST index with ICM Antarctica - AIS_309
$r_{309/other} = -0.12$
$t_{309/other} = 1.48 < t_{krit}$
Ice-mass change [Gt]
Nino 3.4 index SST anomaly [°C]
a11)
Comparison Nino 3.4 index SST (ERSSTv5) with Ice mass change Antarctica - AIS_311
Nino 3.4 SST anomaly [°C]
Ice mass change in Antarctica - AIS_311 [Gt]
Nino 3.4 index SST anomaly
Ice mass change Antarctica - AIS_311
b11)
Correlation El Nino: Nino 3.4 index SST with ICM Antarctica - AIS_311
$r_{311/El} = 0.17$
$t_{311/El} = 0.63 < t_{krit}$
c11)
Correlation La Nina: Nino 3.4 index SST with ICM Antarctica - AIS_311
$r_{311/La} = 0.02$
$t_{311/La} = 0.07 < t_{krit}$
d11)
Correlation others: Nino 3.4 SST index with ICM Antarctica - AIS_311
$r_{311/other} = -0.30$
$t_{311/other} = 3.80 > t_{krit}$
a12)
Comparison Nino 3.4 index SST (ERSSTv5) with Ice mass change Antarctica - AIS_312
Nino 3.4 SST anomaly [°C]
Ice mass change in Antarctica - AIS_312 [Gt]
Nino 3.4 index SST anomaly
Ice mass change Antarctica - AIS_312
b12)
Correlation El Nino: Nino 3.4 index SST with ICM Antarctica - AIS_312
$r_{312/El} = -0.75$
$t_{312/El} = 4.23 > t_{krit}$
c12)
Correlation La Nina: Nino 3.4 index SST with ICM Antarctica - AIS_312
$r_{312/La} = -0.21$
$t_{312/La} = 0.90 < t_{krit}$
d12)
Correlation others: Nino 3.4 SST index with ICM Antarctica - AIS_312
$r_{312/other} = -0.11$
$t_{312/other} = 1.31 < t_{krit}$

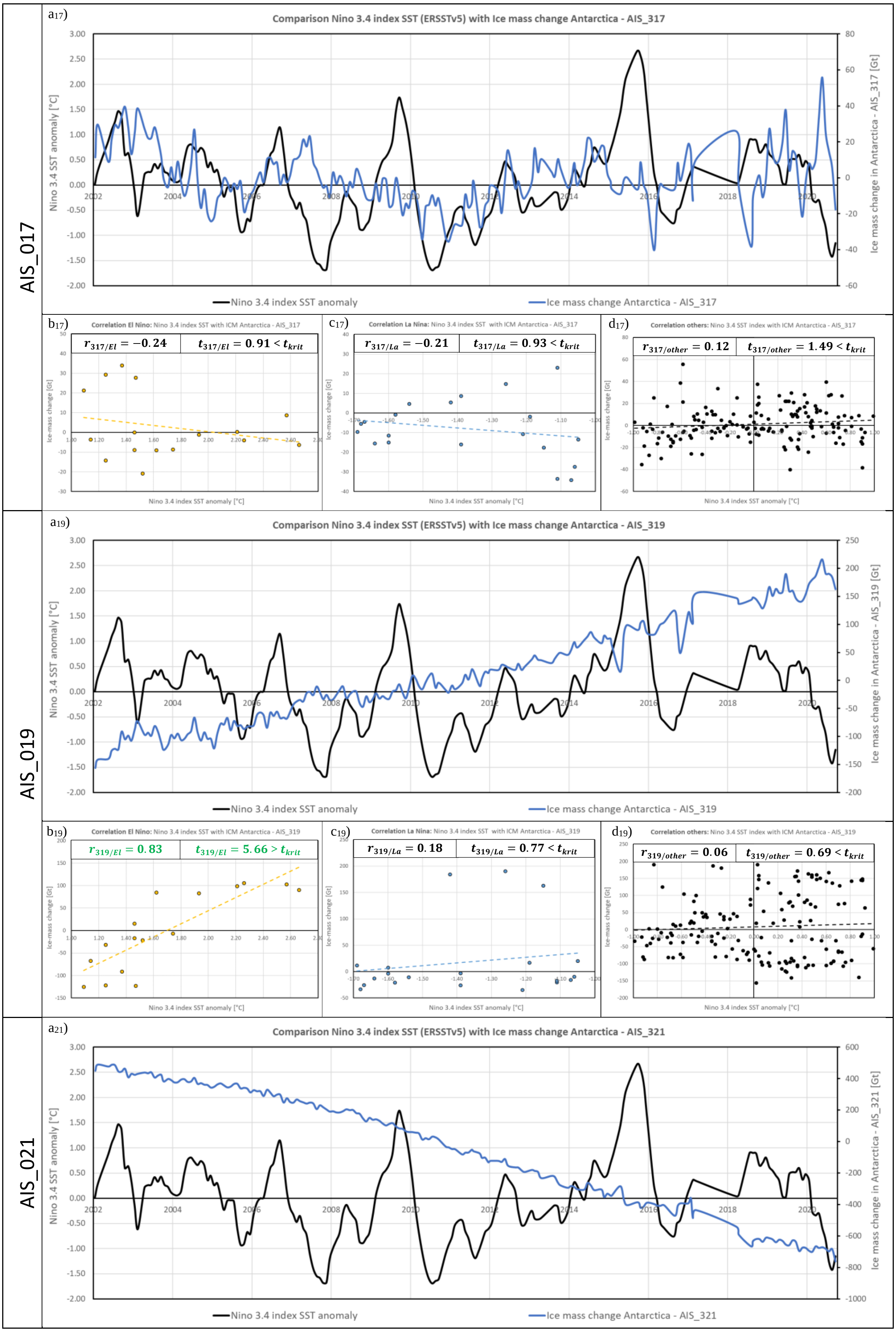
AIS_017
a17)
Comparison Nino 3.4 index SST (ERSSTv5) with Ice mass change Antarctica - AIS_317
Nino 3.4 SST anomaly [°C]
Ice mass change in Antarctica - AIS_317 [Gt]
Nino 3.4 index SST anomaly
Ice mass change Antarctica - AIS_317
b17)
Correlation El Nino: Nino 3.4 index SST with ICM Antarctica - AIS_317
$r_{317/El} = -0.24$
$t_{317/El} = 0.91 < t_{krit}$
c17)
Correlation La Nina: Nino 3.4 index SST with ICM Antarctica - AIS_317
$r_{317/La} = -0.21$
$t_{317/La} = 0.93 < t_{krit}$
d17)
Correlation others: Nino 3.4 SST index with ICM Antarctica - AIS_317
$r_{317/other} = 0.12$
$t_{317/other} = 1.49 < t_{krit}$
Nino 3.4 index SST anomaly [°C]
AIS_019
a19)
Comparison Nino 3.4 index SST (ERSSTv5) with Ice mass change Antarctica - AIS_319
Nino 3.4 SST anomaly [°C]
Ice mass change in Antarctica - AIS_319 [Gt]
Nino 3.4 index SST anomaly
Ice mass change Antarctica - AIS_319
b19)
Correlation El Nino: Nino 3.4 index SST with ICM Antarctica - AIS_319
$r_{319/El} = 0.83$
$t_{319/El} = 5.66 > t_{krit}$
c19)
Correlation La Nina: Nino 3.4 index SST with ICM Antarctica - AIS_319
$r_{319/La} = 0.18$
$t_{319/La} = 0.77 < t_{krit}$
d19)
Correlation others: Nino 3.4 SST index with ICM Antarctica - AIS_319
$r_{319/other} = 0.06$
$t_{319/other} = 0.69 < t_{krit}$
Nino 3.4 index SST anomaly [°C]
AIS_021
a21)
Comparison Nino 3.4 index SST (ERSSTv5) with Ice mass change Antarctica - AIS_321
Nino 3.4 SST anomaly [°C]
Ice mass change in Antarctica - AIS_321 [Gt]
Nino 3.4 index SST anomaly
Ice mass change Antarctica - AIS_321

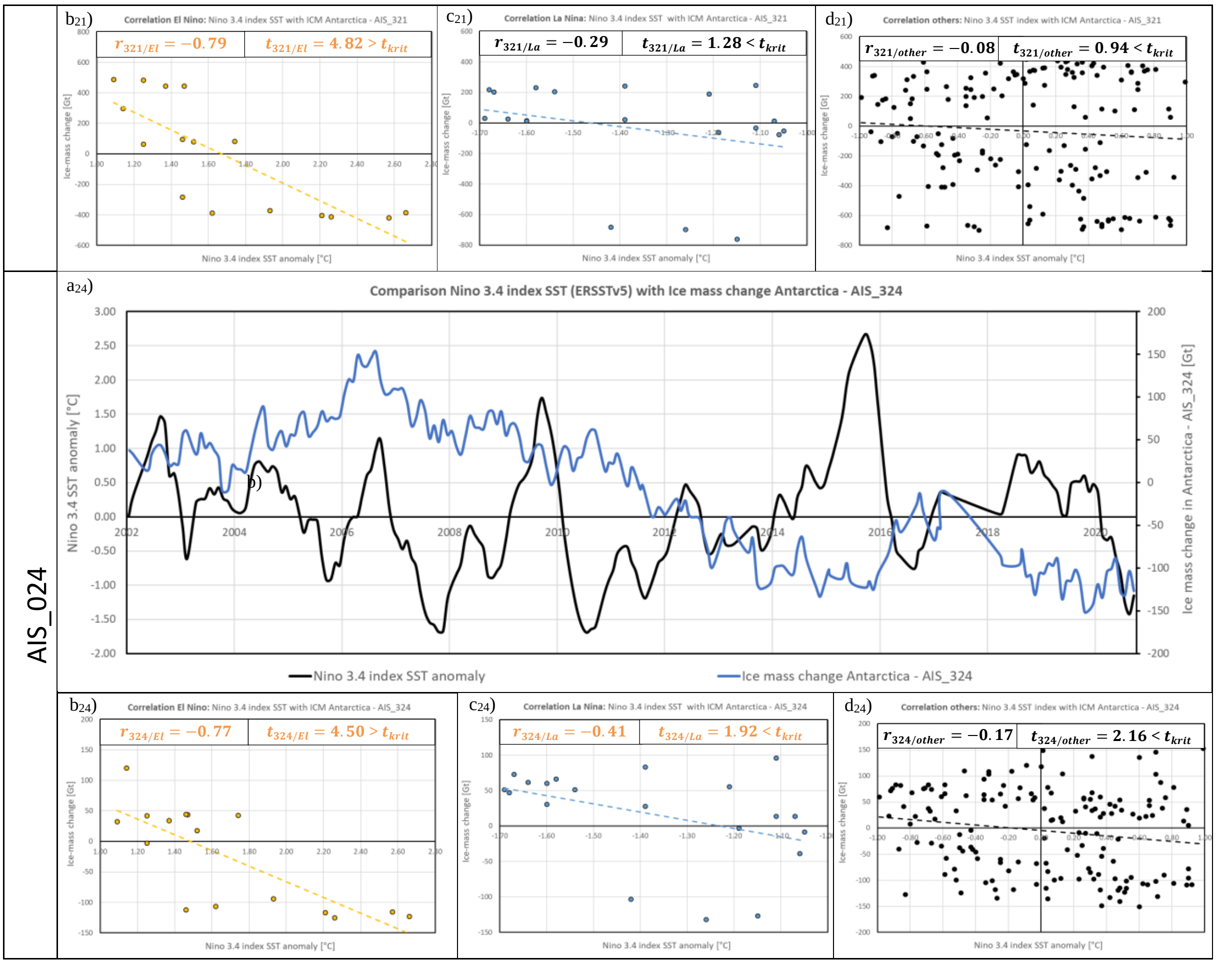

Figure 19: Main results of the correlation from the ice-mass change of the Antarctic sub-regions with the SST anomaly from the Niño 3.4 index [a) Ice-mass change and Niño 3.4 index within the selected region between the years 2002 and 2020, b) Correlation of ice-mass change with SST anomaly of Niño 3.4 index during Super El Niño events, c) Correlation of ice-mass change with SST anomaly of Niño 3.4 index during Large La Niña events, d) Correlation of ice-mass change with SST anomaly of Niño 3.4 index between Large La Niña and Super El Niño events]

6.2 Correlation between key variables of terrestrial water cycle in Antarctica and SST of Niño 3.4 index

After the investigation of the ice-mass change with the Niño 3.4 index, a deeper look within the terrestrial water cycle of the Antarctica and the correlation with the Niño 3.4 index will be done. In chapter 5, the key variables of the terrestrial water cycle are explained. In a nutshell, the ice-mass change, which is the most important value for the terrestrial water balance in the Antarctica, will be influenced by the evaporation, runoff and total precipitation. Instead of the runoff parameter, the total water balance, which is a function of the total precipitation, evaporation and runoff will be visualized. Therefore, the calculated correlation within chapter 6.1 should be argued by the investigation of sub-parameters of the terrestrial water cycle. In the following chapter, ECMWF data for the supra-regional parts of the Antarctica as well as data for total Antarctica will be correlated with the Niño 3.4 index. Floating ice shelfs like the Ronne or Ross Ice Shelf are not considered in the correlation calculations.

The following statements will be used for the correlation:

H_0 **(null hypothesis)**: Between key variables of the water cycle in the Antarctic region – AIS_0XX and ENSO events **no correlation** exists.

H_1 **(alternative hypothesis)**: Between key variables of the water cycle in the Antarctic region – AIS_0XX and ENSO events a **significant correlation** exists.

The Pearson's product moment correlation coefficient (r_{XXX}) quantifies the stated correlation within the alternative hypothesis. The t-value (t_{XXX}) helps for examination against the null hypothesis.

6.2.1 Correlation total Antarctic water cycle with Niño 3.4 index

As shown in Figure 20, within the years 2002 and 2020, the evaporation in the total Antarctica ranges from 0.3 - 3.6 mm water equivalent (Figure $20a_{ev}$). During the Large La Niña event 2007/08 the lowest evaporation value could be observed. The highest evaporation values could not be linked directly to El Niño or La Niña events. All the other fluctuations in evaporation could be explained through the seasonal differences over the year. The correlation of the monthly evaporation values with the Niño 3.4 index, shows only an average negative correlation during Large La Niña events ($r_{AIS/La} = -0.49$, Figure $20c_{ev}$) The total precipitation in the total Antarctica ranges within the same period from 1.4 - 4.9 mm water equivalent

(Figure 20a$_{tp}$). Anomalies due to La Niña or El Niño events couldn´t be recognized. The water balance, which is the sum of total precipitation, evaporation (negative) and runoff (negative), ranges for the years 2002 to 2020 from -0.5 – 3.5 mm water equivalent (Figure 20a$_{wb}$). By analogy with the evaporation, the highest water balance value could be detected within the Large La Niña event 2007/08. All the other fluctuations could not be linked with La Niña or El Niño events. The water balance correlation results in an average negative correlation during Large La Niña events ($r_{AIS/La} = -0.41$, Figure 20c$_{wb}$).

By the use of the ECMWF values, it can be said that evaporation and precipitation have much more impact on the water balance of the total Antarctica than runoff. The reason is that the runoff is influenced by the dynamic interaction between ice flow and ocean-driven melt below the floating ice shelves (cf. VAN DEN BROEKE 2018: 219). Warmer conditions lead to more instable ice shelves. Consequently, fracturing and subsequent disintegration of the ice shelves can be observed (cf. BANWELL 2013: 5872). These complex processes could only be estimated trough detailed physically based representations of the precipitation generation and surface melting process (cf. VAN DE BERG 2019: 3). Therefore, the influence through runoff is underestimated within the ECMWF model.

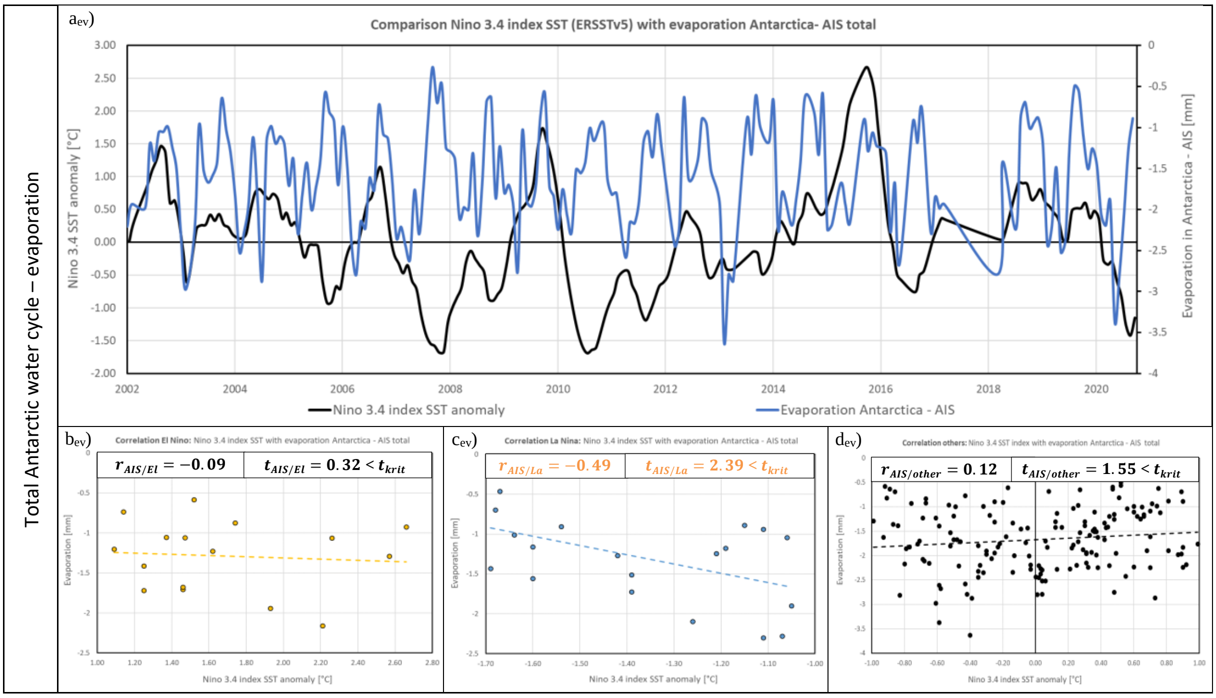

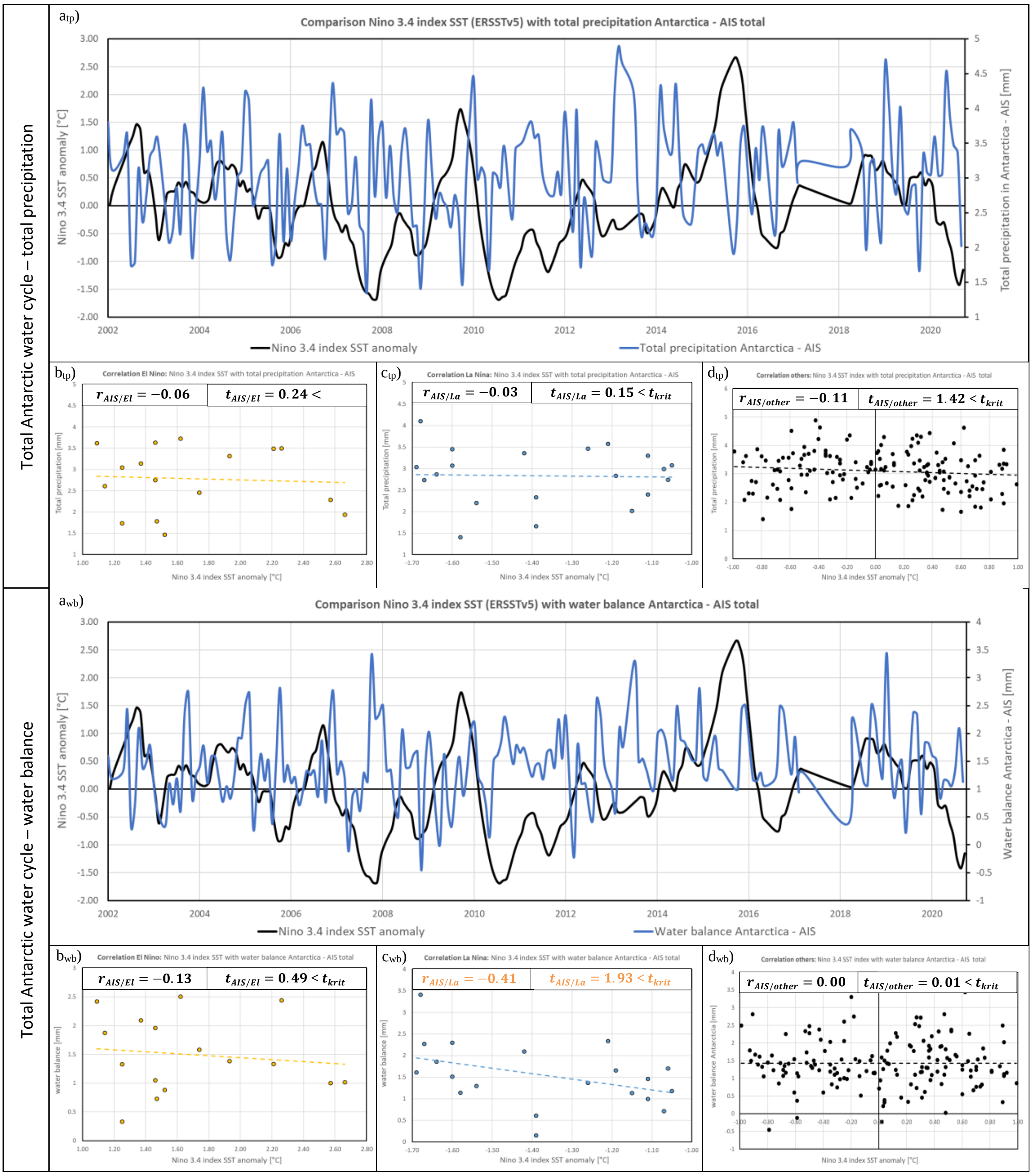

Figure 20: Results of the correlation from the water cycle of the total Antarctic Ice Sheet with the SST anomaly from the Niño 3.4 index [a) Water cycle key variable and Niño 3.4 index within the selected region between the years 2002 and 2020, b) Correlation of water cycle key variable with SST anomaly of Niño 3.4 index during Super El Niño events, c) Correlation of water cycle key variable with SST anomaly of Niño 3.4 index during Large La Niña events, d) Correlation of water cycle key variable with SST anomaly of Niño 3.4 index between Large La Niña and Super El Niño events]

6.2.2 Correlation supra-regional parts of Antarctic water cycle with Niño 3.4 index

After the representation of the correlation results for the total Antarctic water cycle parameters, the investigation will be extended to the supra-regional parts of the Antarctic water cycle. In Figure 21, the water cycle key variables within the years 2002 to 2020 as well as the correlation results from the water cycle of the supra-regional West and Central Antarctic Ice Sheets will be listed. For the results for the East Antarctica, a reference is made to the appendix. The evaporation ranges within the period 2002 to 2020 from 0 - 1.8 mm water equivalent for the supra-regional parts of the Antarctica. The maximum evaporation within the West Antarctic and Antarctic Peninsula water cycle was at the end of the year 2011, which could be a consequence of the Large La Niña events within the years 2010-2012 (Figure $21a_{ev,W}$). The evaporation peaks within the East Antarctic Ice Sheet in the years 2009 and 2010 could be caused by the Super El Niño event in the year 2009/10 as well the following Large La Niña event in the year 2010/11. Within the Central Antarctic Ice Sheet, the maximum evaporation could be detected within the year 2015, which could be related to the Super El Niño event 2015/16 (Figure $21a_{ev,C}$). The total precipitation within the supra-regional parts of the Antarctica ranges from 0 - 3.3 mm water equivalent. For the total precipitation within the West Antarctic and Antarctic Peninsula, the peak within the end of the year 2011, which could be in analogy to the evaporation a result of the Large La Niña event 2011 (Figure $21a_{tp,W}$). The minimum precipitation within the East Antarctica was recognized in the year 2016. In the same period, 2015 and 2016, a Super El Niño event was recorded. For the Central Antarctic Ice Sheet, no visual correlations within the total precipitation could be recognized (Figure $21a_{tp,C}$). The values for the water balance range within the supra-regional parts of the Antarctica between -1.5- and 2.5-mm water equivalent. The lowest values for the water balance within the West Antarctica and Antarctic Peninsula could be recorded in 2010 and 2015, which are periods for a Large La Niña (2010) event as well as a Super El Niño (2015/16) event (Figure $21a_{wb,W}$). Therefore, the evaporation exceeded the total precipitation within these periods. For the other supra-regional parts, no correlations could be visualized (Figure $21a_{wb,C}$). Nevertheless, within the correlation results only for the water balance within the Central Antarctica, a negative average correlation could be determined ($r_{AIS/El} = -0.41$) during Super El Niño events. All the other calculations within the water cycle of the supra-regional parts of the Antarctica results in low correlations ($|r| < 0.4$).

Due to the explanation of the terrestrial water cycle in chapter 5, the water balance should correlate with the ice-mass change. Therefore, correlations between the key variables of the water cycle with the Niño 3.4 index should be the result in analogy to the ice-mass change. The fluctuating seasonal profiles of the water cycle key variables and the time delay between the upcoming ENSO event and the impact on the Antarctica could be the reason for the missing correlations. Furthermore, the runoff variables within the ECMWF dataset are very low in the Antarctica compared to the total precipitation and evaporation. The reason could be the neglected basal melting and floating ice shelfs, which are responsible for the most runoff in the Antarctica.

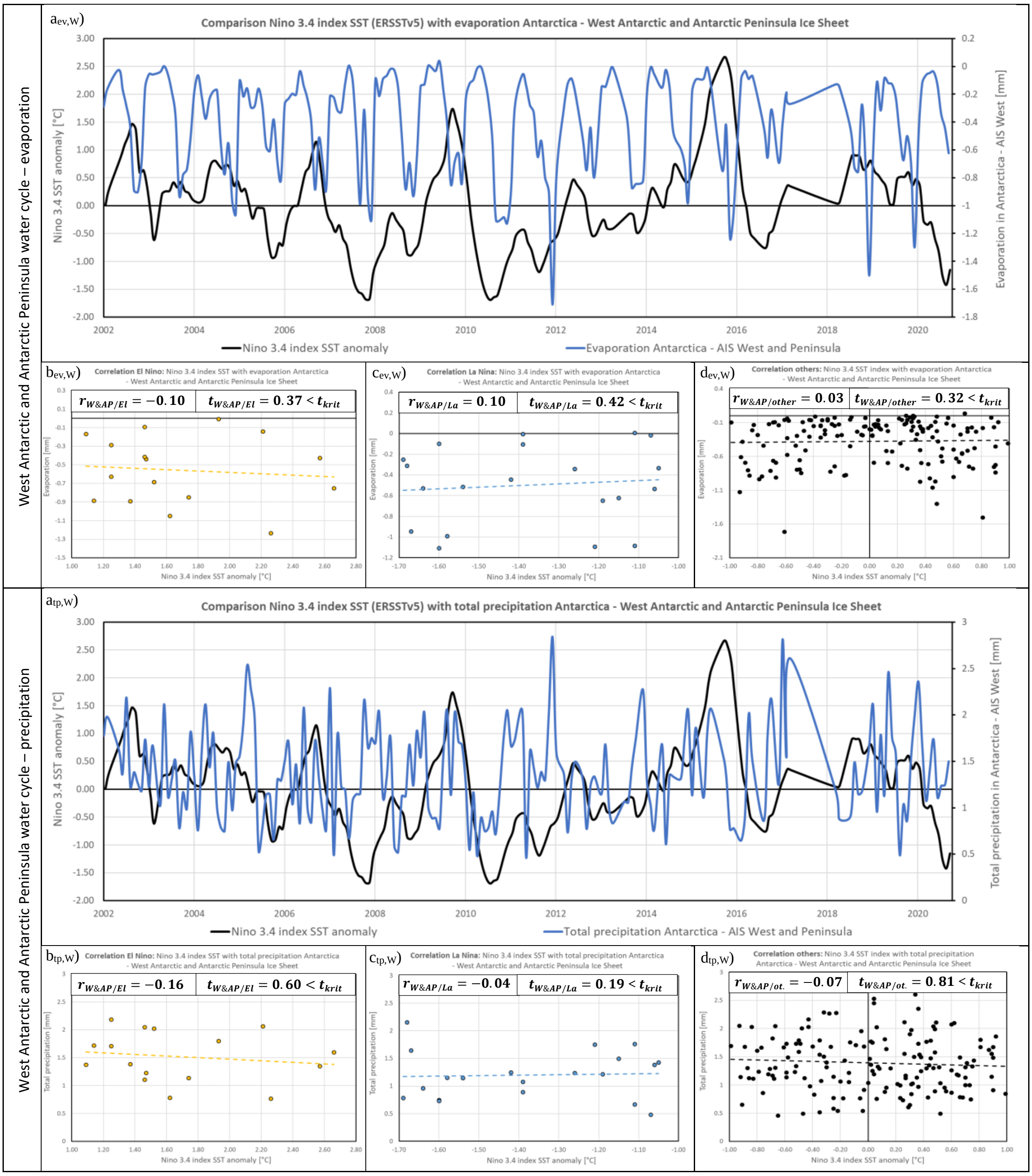

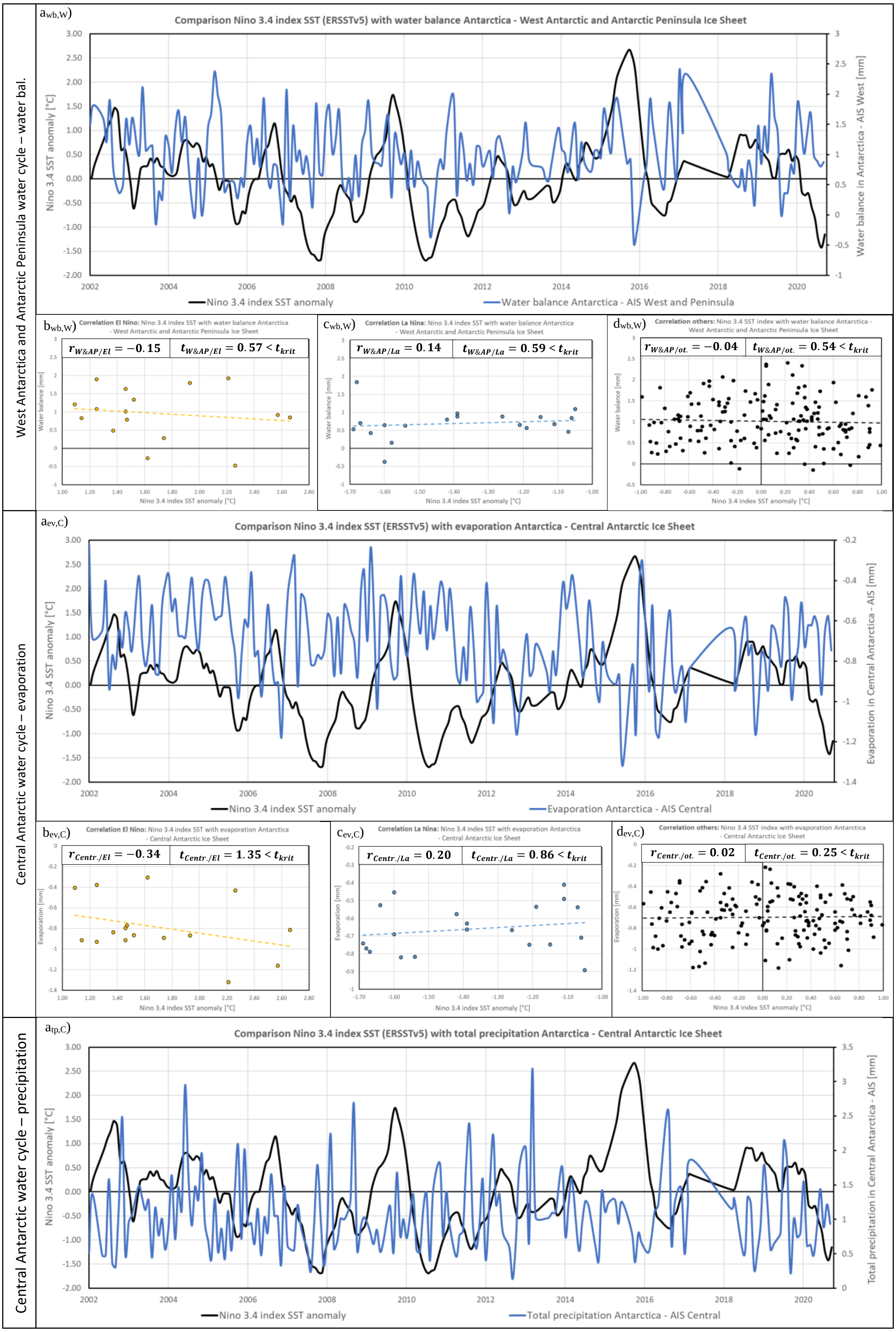
West Antarctica and Antarctic Peninsula water cycle – water bal.
a_wb,W)
Comparison Nino 3.4 index SST (ERSSTv5) with water balance Antarctica - West Antarctic and Antarctic Peninsula Ice Sheet
Nino 3.4 SST anomaly [°C]
Water balance in Antarctica - AIS West [mm]
Nino 3.4 index SST anomaly
Water balance Antarctica - AIS West and Peninsula
b_wb,W)
Correlation El Nino: Nino 3.4 index SST with water balance Antarctica - West Antarctic and Antarctic Peninsula Ice Sheet
$r_{W\&AP/El} = -0.15$
$t_{W\&AP/El} = 0.57 < t_{krit}$
c_wb,W)
Correlation La Nina: Nino 3.4 index SST with water balance Antarctica - West Antarctic and Antarctic Peninsula Ice Sheet
$r_{W\&AP/La} = 0.14$
$t_{W\&AP/La} = 0.59 < t_{krit}$
d_wb,W)
Correlation others: Nino 3.4 SST index with water balance Antarctica - West Antarctic and Antarctic Peninsula Ice Sheet
$r_{W\&AP/ot.} = -0.04$
$t_{W\&AP/ot.} = 0.54 < t_{krit}$
Water balance [mm]
Nino 3.4 index SST anomaly [°C]
Central Antarctic water cycle – evaporation
a_ev,C)
Comparison Nino 3.4 index SST (ERSSTv5) with evaporation Antarctica - Central Antarctic Ice Sheet
Evaporation in Central Antarctica - AIS [mm]
Evaporation Antarctica - AIS Central
b_ev,C)
Correlation El Nino: Nino 3.4 index SST with evaporation Antarctica - Central Antarctic Ice Sheet
$r_{Centr./El} = -0.34$
$t_{Centr./El} = 1.35 < t_{krit}$
c_ev,C)
Correlation La Nina: Nino 3.4 index SST with evaporation Antarctica - Central Antarctic Ice Sheet
$r_{Centr./La} = 0.20$
$t_{Centr./La} = 0.86 < t_{krit}$
d_ev,C)
Correlation others: Nino 3.4 SST index with evaporation Antarctica - Central Antarctic Ice Sheet
$r_{Centr./ot.} = 0.02$
$t_{Centr./ot.} = 0.25 < t_{krit}$
Evaporation [mm]
Central Antarctic water cycle – precipitation
a_tp,C)
Comparison Nino 3.4 index SST (ERSSTv5) with total precipitation Antarctica - Central Antarctic Ice Sheet
Total precipitation in Central Antarctica - AIS [mm]
Total precipitation Antarctica - AIS Central

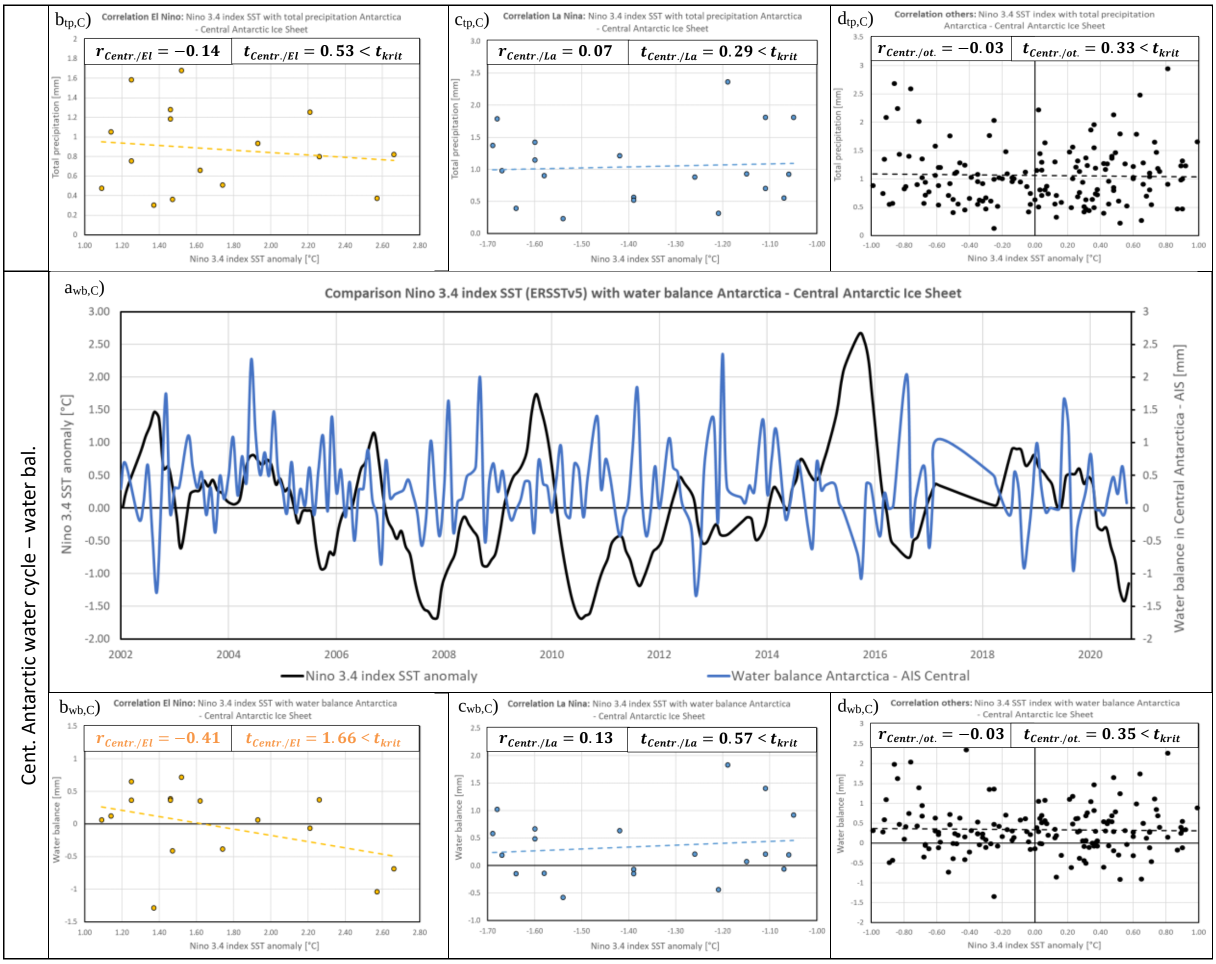

Figure 21: Main results of the correlation from the water cycle of the supra-regional Antarctic Ice Sheets with the SST anomaly from the Niño 3.4 index [a) Water cycle key variable and Niño 3.4 index within the selected region between the years 2002 and 2020, b) Correlation of water cycle key variable with SST anomaly of Niño 3.4 index during Super El Niño events, c) Correlation of water cycle key variable with SST anomaly of Niño 3.4 index during Large La Niña events, d) Correlation of water cycle key variable with SST anomaly of Niño 3.4 index between Large La Niña and Super El Niño events]

6.3 Correlation between wind fields in Antarctica and SST of Niño 3.4 index

In the following chapter, ECMWF data for the supra-regional regions of the Antarctica as well as data for total Antarctica will be correlated with the Niño 3.4 index. In addition to the water cycle parameters three different wind parameters will be considered within the correlation calculations. The wind parameters are the horizontal surface near wind speed as well as the eastward and northward surface near neutral wind speed. Floating ice shelfs like the Ronne or Ross Ice Shelf are not considered in the correlation calculations.

The following statements will be used for the correlation:

H_0 **(null hypothesis)**: Between wind fields in the Antarctic region – AIS_0XX and ENSO events **no correlation** exists.

H_1 **(alternative hypothesis)**: Between wind fields in the Antarctic region – AIS_0XX and ENSO events a **significant correlation** exists.

The Pearson's product moment correlation coefficient (r_{XXX}) quantifies the stated correlation within the alternative hypothesis. The t-value (t_{XXX}) helps for examination against the null hypothesis.

6.3.1 Correlation total Antarctic wind fields with Niño 3.4 index

First, the wind fields of the total Antarctica will be investigated. In Figure 22, the temporal progression from 2002 to 2020 and the correlation results of the total Antarctic wind fields are visualized. The eastward wind within the total Antarctica ranges from 0 - 11.2 m/s within the years 2002 to 2020 (Figure $22a_{ew}$). Large peaks for the eastward wind could be detected within the years 2009, 2010 and 2016, which could be related to the Super El Niño and Large La Niña events in these periods. The northward neutral wind peaks are in the range from -6 - 4 m/s for the total Antarctic Ice Sheet and could not be linked with ENSO events (Figure $22a_{nw}$). The horizontal wind speed was recorded for the years 2002 to 2020 within a range of 7 - 15 m/s and the lowest horizontal wind speed was determined in the year 2016, which could also be a consequence of the Super El Niño event in the years 2015/16 (Figure $22a_{hw}$). For the calculation results it could be summarized, that only low correlations between the wind parameters of the total Antarctica and the Niño 3.4 index were determined.

In analogy to the interpretation of the water key variable correlation results, the missing correlations could be linked with the time delay between the upcoming ENSO event and the impact on the Antarctic wind fields.

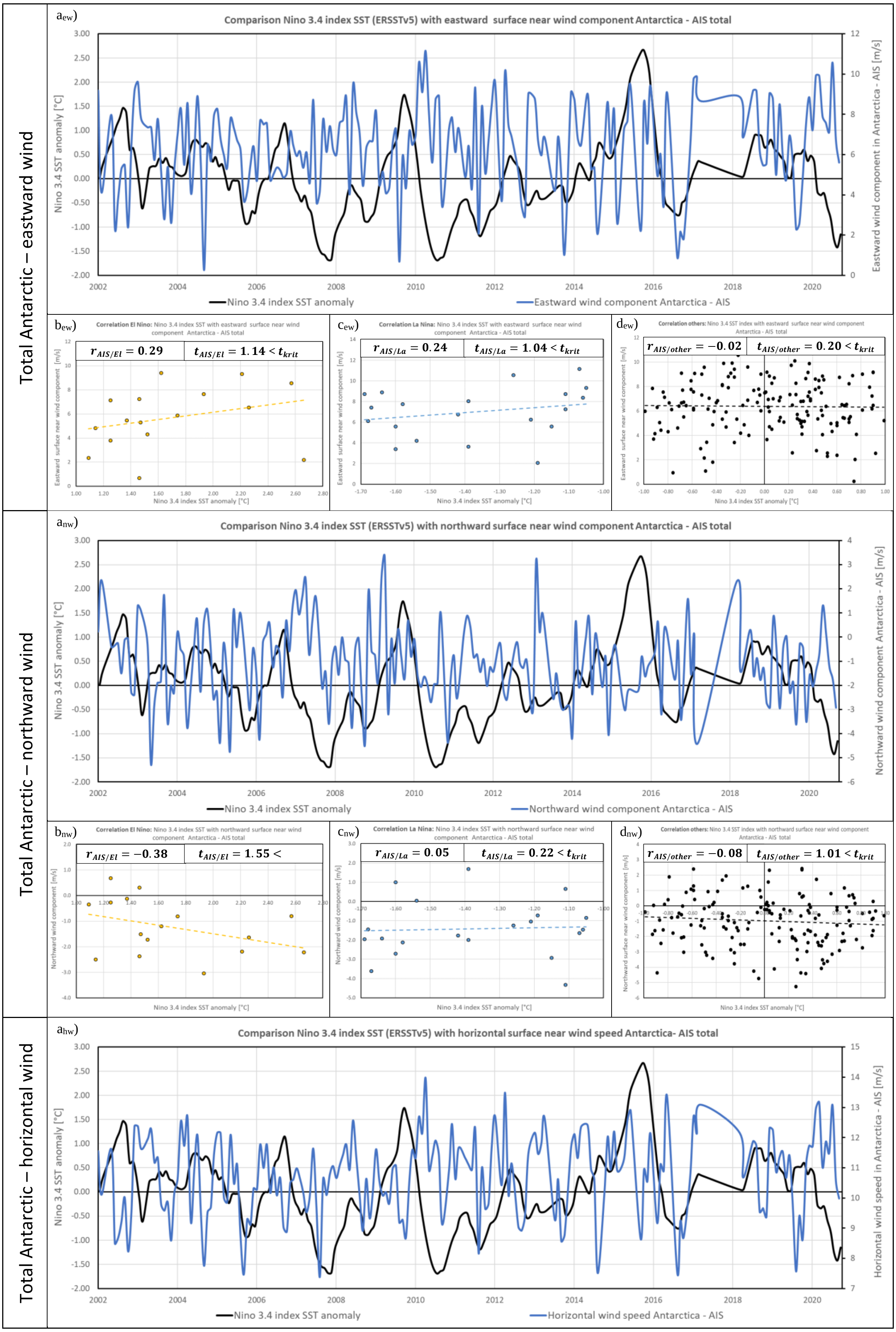
Total Antarctic – eastward wind
aew)
Comparison Nino 3.4 index SST (ERSSTv5) with eastward surface near wind component Antarctica - AIS total
Nino 3.4 SST anomaly [°C]
Eastward wind component in Antarctica - AIS [m/s]
Nino 3.4 index SST anomaly
Eastward wind component Antarctica - AIS
bew)
Correlation El Nino: Nino 3.4 index SST with eastward surface near wind component Antarctica - AIS total
$r_{AIS/El} = 0.29$
$t_{AIS/El} = 1.14 < t_{krit}$
cew)
Correlation La Nina: Nino 3.4 index SST with eastward surface near wind component Antarctica - AIS total
$r_{AIS/La} = 0.24$
$t_{AIS/La} = 1.04 < t_{krit}$
dew)
Correlation others: Nino 3.4 SST index with eastward surface near wind component Antarctica - AIS total
$r_{AIS/other} = -0.02$
$t_{AIS/other} = 0.20 < t_{krit}$
Eastward surface near wind component [m/s]
Nino 3.4 index SST anomaly [°C]
Total Antarctic – northward wind
anw)
Comparison Nino 3.4 index SST (ERSSTv5) with northward surface near wind component Antarctica - AIS total
Nino 3.4 SST anomaly [°C]
Northward wind component Antarctica - AIS [m/s]
Nino 3.4 index SST anomaly
Northward wind component Antarctica - AIS
bnw)
Correlation El Nino: Nino 3.4 index SST with northward surface near wind component Antarctica - AIS total
$r_{AIS/El} = -0.38$
$t_{AIS/El} = 1.55 <$
cnw)
Correlation La Nina: Nino 3.4 index SST with northward surface near wind component Antarctica - AIS total
$r_{AIS/La} = 0.05$
$t_{AIS/La} = 0.22 < t_{krit}$
dnw)
Correlation others: Nino 3.4 SST index with northward surface near wind component Antarctica - AIS total
$r_{AIS/other} = -0.08$
$t_{AIS/other} = 1.01 < t_{krit}$
Northward wind component [m/s]
Nino 3.4 index SST anomaly [°C]
Total Antarctic – horizontal wind
ahw)
Comparison Nino 3.4 index SST (ERSSTv5) with horizontal surface near wind speed Antarctica- AIS total
Nino 3.4 SST anomaly [°C]
Horizontal wind speed in Antarctica - AIS [m/s]
Nino 3.4 index SST anomaly
Horizontal wind speed Antarctica - AIS

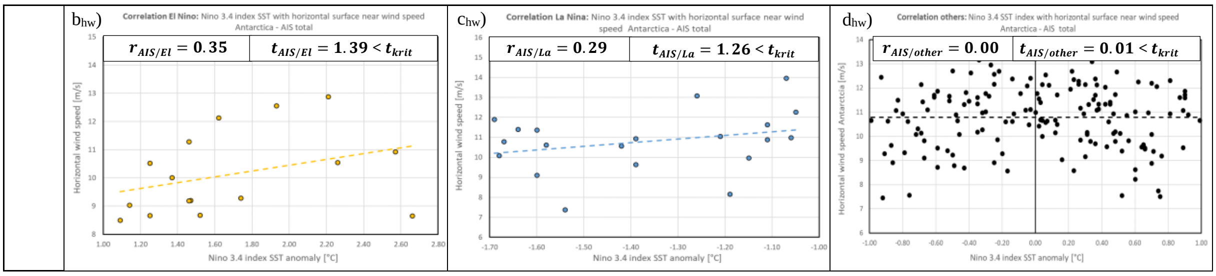

Figure 22: Results of the correlation from the wind parameters of the total Antarctic Ice Sheet with the SST anomaly from the Niño 3.4 index [a) Wind field variable and Niño 3.4 index within the selected region between the years 2002 and 2020, b) Correlation of wind field variable with SST anomaly of Niño 3.4 index during Super El Niño events, c) Correlation of wind field variable with SST anomaly of Niño 3.4 index during Large La Niña events, d) Correlation of wind field variable with SST anomaly of Niño 3.4 index between Large La Niña and Super El Niño events]

6.3.2 Correlation supra-regional parts of Antarctic wind fields with Niño 3.4 index

The correlation results of the supra-regional parts of the Antarctic wind fields reveals a similar picture. In Figure 23, the corresponding supra-regional temporal wind field propagations and correlation results are listed. For the supra-regional parts of the Antarctica regarding the eastward neutral surface near wind, a wind speed of -4 to 5 m/s within the years 2002 and 2020 was detected. Within the same period, the northward neutral wind speed was in the range from -5 to 7 m/s and the horizontal wind speed in the range from -4 to 9.5 m/s. The lowest eastward wind speed within the West Antarctica and Antarctic Peninsula was recorded within the year 2002, which could be a consequence to the Super El Niño event in 2002/03 (Figure 23$a_{ew,W}$). The northward wind peaks within the West Antarctic and Antarctic Peninsula could be recorded within the beginning of the year 2007 and the end of the year 2015, which could be related with the Super El Niño events in the year 2006/07 and 2015/16 (Figure 23$a_{nw,W}$). Within the year 2010, the highest eastward wind speed within the East Antarctica could be recognized (Figure 23$a_{ew,E}$). The highest northward wind speed in the East Antarctica in the year 2016, could be connected to the 2015/16 Super El Niño event. The highest horizontal wind speed in the year 2010, could be a consequence of the 2009/10 Super El Niño event. In the Central Antarctic wind fields, the lowest eastward wind was recorded within the years 2009 and 2015. Within the years 2009/10 and 2015/16 Super El Niño events took place. Therefore, a relation to the Niño 3.4 index could be assumed. The correlation results revealed a positive average correlation between the Niño 3.4 index and the eastward wind speed during Super El Niño events ($r_{AIS/El} = 0.40$) in the West Antarctica and Antarctic Peninsula. For all the other correlation investigations within the supra-regional wind fields, only low correlations could be obtained ($|r| < 0.4$).

During El Niño events, surface near winds are more northwest to southeast (cf. PAOLO et al. 2018: 1). Therefore, the determined correlation in the West Antarctic and Antarctic Peninsula during Super El Niño events agree with that. In the temporal propagations of the wind fields, several possible connections between ENSO events and wind field variables could be detected. Though, a time delay between the upcoming ENSO event and the impact on the Antarctic wind fields could be the reason.

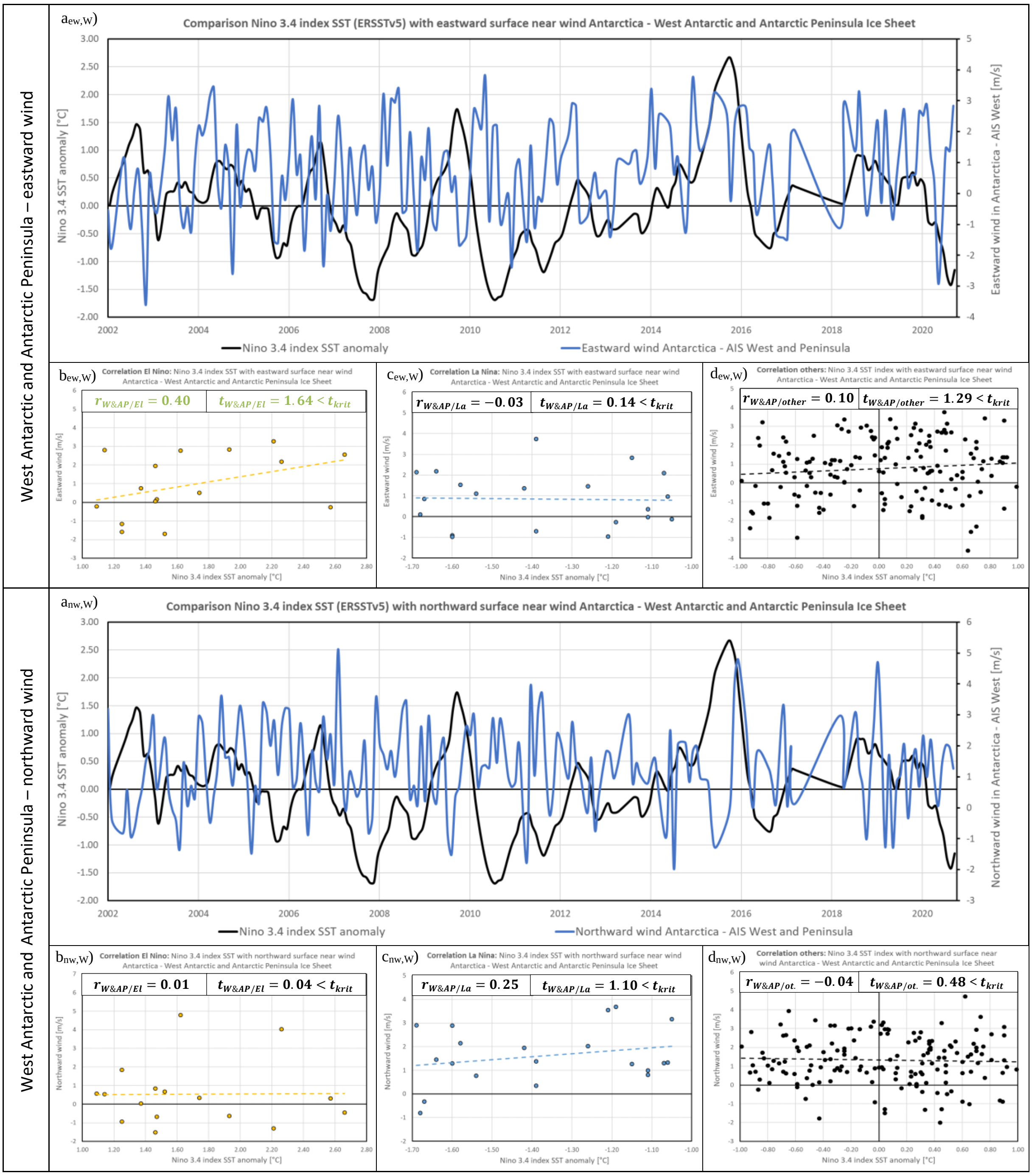

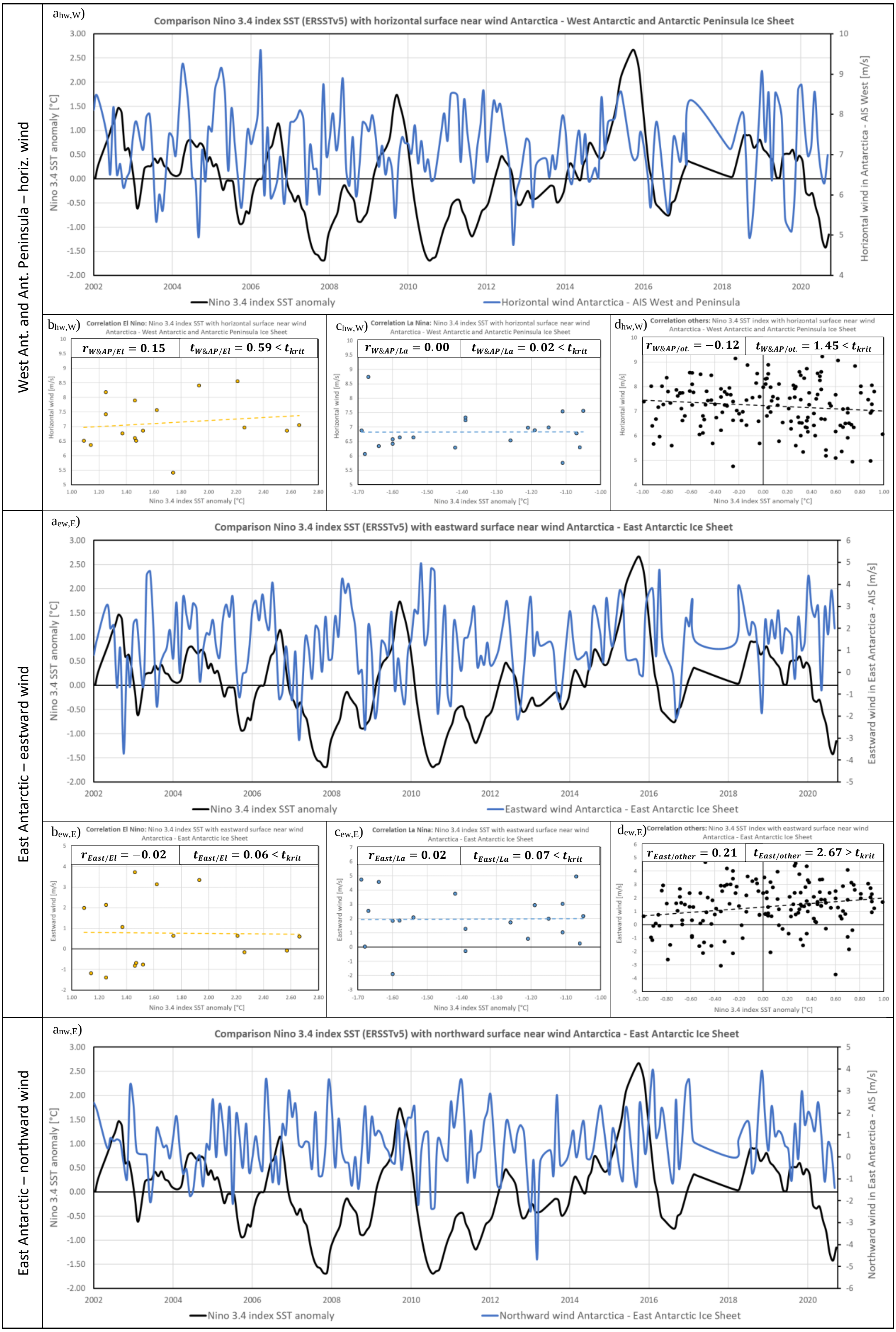
West Ant. and Ant. Peninsula – horiz. wind
ahw,W)
Comparison Nino 3.4 index SST (ERSSTv5) with horizontal surface near wind Antarctica - West Antarctic and Antarctic Peninsula Ice Sheet
Nino 3.4 SST anomaly [°C]
Horizontal wind in Antarctica - AIS West [m/s]
Nino 3.4 index SST anomaly
Horizontal wind Antarctica - AIS West and Peninsula
bhw,W) Correlation El Nino: Nino 3.4 index SST with horizontal surface near wind Antarctica - West Antarctic and Antarctic Peninsula Ice Sheet
$r_{W\&AP/El} = 0.15$
$t_{W\&AP/El} = 0.59 < t_{krit}$
chw,W) Correlation La Nina: Nino 3.4 index SST with horizontal surface near wind Antarctica - West Antarctic and Antarctic Peninsula Ice Sheet
$r_{W\&AP/La} = 0.00$
$t_{W\&AP/La} = 0.02 < t_{krit}$
dhw,W) Correlation others: Nino 3.4 index SST with horizontal surface near wind Antarctica - West Antarctic and Antarctic Peninsula Ice Sheet
$r_{W\&AP/ot.} = -0.12$
$t_{W\&AP/ot.} = 1.45 < t_{krit}$
Horizontal wind [m/s]
Nino 3.4 index SST anomaly [°C]
East Antarctic – eastward wind
aew,E)
Comparison Nino 3.4 index SST (ERSSTv5) with eastward surface near wind Antarctica - East Antarctic Ice Sheet
Eastward wind in East Antarctica - AIS [m/s]
Nino 3.4 index SST anomaly
Eastward wind Antarctica - East Antarctic Ice Sheet
bew,E) Correlation El Nino: Nino 3.4 index SST with eastward surface near wind Antarctica - East Antarctic Ice Sheet
$r_{East/El} = -0.02$
$t_{East/El} = 0.06 < t_{krit}$
cew,E) Correlation La Nina: Nino 3.4 index SST with eastward surface near wind Antarctica - East Antarctic Ice Sheet
$r_{East/La} = 0.02$
$t_{East/La} = 0.07 < t_{krit}$
dew,E) Correlation others: Nino 3.4 index SST with eastward surface near wind Antarctica - East Antarctic Ice Sheet
$r_{East/other} = 0.21$
$t_{East/other} = 2.67 > t_{krit}$
Eastward wind [m/s]
East Antarctic – northward wind
anw,E)
Comparison Nino 3.4 index SST (ERSSTv5) with northward surface near wind Antarctica - East Antarctic Ice Sheet
Northward wind in East Antarctica - AIS [m/s]
Nino 3.4 index SST anomaly
Northward wind Antarctica - East Antarctic Ice Sheet

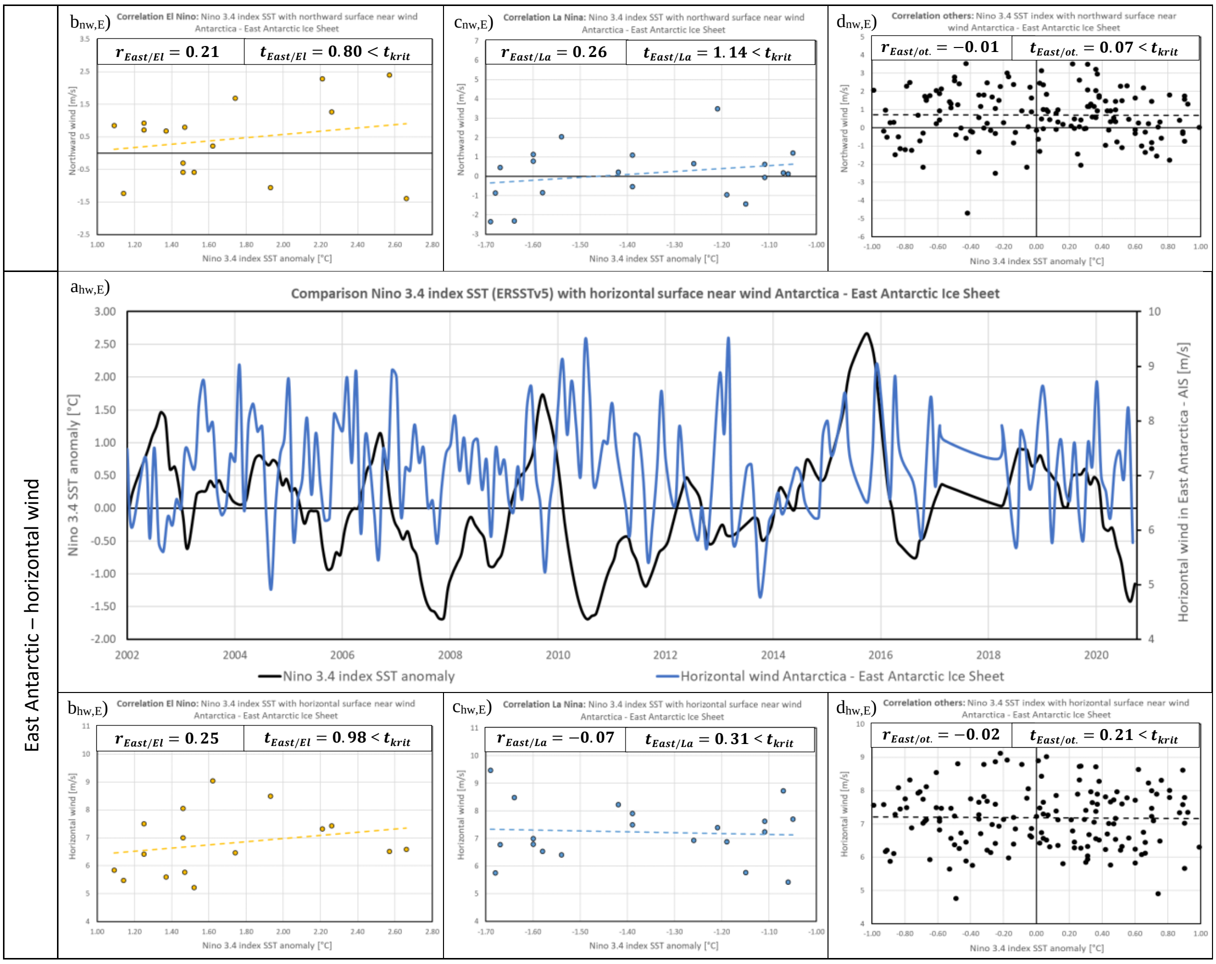

Figure 23: Main results of the correlation from the wind parameters of the supra-regional Antarctic Ice Sheets with the SST anomaly from the Niño 3.4 index [a) Wind field variable and Niño 3.4 index within the selected region between the years 2002 and 2020, b) Correlation of wind field variable with SST anomaly of Niño 3.4 index during Super El Niño events, c) Correlation of wind field variable with SST anomaly of Niño 3.4 index during Large La Niña events, d) Correlation of wind field variable with SST anomaly of Niño 3.4 index between Large La Niña and Super El Niño events]

7 Summary and discussion

Finally, to answer the stated hypotheses and research questions the revealed results will be summarized and discussed. The goal of this work was to find possible anomalies within the water cycle of the Antarctica connected to ENSO. Furthermore, the water cycle anomalies due to the intensification of ENSO events in future were discussed. Therefore, the recorded ENSO events and their regional impacts were stated. Additionally, the terrestrial water cycle of the Antarctica was investigated. As a result, the key variables of the water cycle were defined. By application of the Pearson correlation method, the Niño 3.4 index was correlated with the ice-mass change, the connected key variables of the water cycle, as well as three different parameters of the Antarctic wind fields. Within the correlation calculations, monthly averaged data from ECMWF for the water cycle and wind fields as well as GRACE for the ice-mass change, were correlated with monthly data from the Niño 3.4 index, which assumes that an existing relation takes place immediately. The investigation was conducted for the total Antarctica and supra-regional parts of the Antarctica. Furthermore, the sub-regions of the Antarctica were investigated for the ice-mass change. The investigated time period was between 2002 and 2020, which was limited to the available data period according to GRACE. Within this period, four Super El Niño events (2002/03, 2006/07, 2009/10, 2015/16) and three Large La Niña events were recorded (2007/08, 2010/11/12, 2020/21). Super El Niño events were defined by an SST anomaly of the Niño 3.4 index of > 1°C and Large La Niña events by an SST anomaly of < -1°C, which is an indicator of the strength of ENSO events. Therefore, the correlations were investigated for the data pairs, which are located within Super El Niño event periods, data pairs that are located within Large La Niña event periods and for crosschecking for all the other data pairs. In Table 3, the correlation results, which are explained in detail in chapter 6, are summarized. Therein, it can be seen, that the ice-mass change (i.m.c.), the evaporation (evap.), the total precipitation (precip.), the water balance, the eastward (eastw.), the northward (northw.) and horizontal (horiz.) surface near wind speed were correlated with the Niño 3.4 index. The results show that there is a correlation between the ice-mass change and the Niño 3.4 index during Super El Niño events. For the total Antarctica and the West Antarctic and Antarctic Peninsula, a high negative correlation between the ice-mass change and the Niño 3.4 index was observed. For the East Antarctica, a positive average correlation and for the Central Antarctica a positive high correlation could be determined during Super El Niño events. This means that with increasing SST anomaly the ice-mass is decreasing in the total Antarctica and West Antarctic and Antarctic Peninsula. Within the East and Central Antarctica, the ice-mass is increasing with rising SST anomaly. Furthermore, for the total Antarctica, a negative average correlation between the evaporation and the Niño 3.4 index as well as between the water balance and the Niño 3.4 index could be observed during Large La Niña events. Within the Central Antarctica, a negative average correlation between the water balance and the Niño 3.4 index could be determined during Super El Niño events. Finally, within the West Antarctic and Antarctic Peninsula, a positive average correlation could be recognized between the eastward surface near wind speed and the Niño 3.4 index during Super El Niño events. All the other correlation calculations resulted in low correlation coefficients ($|r| < 0.4$). The correlation results for the ice-mass change within the sub-regions of the Antarctica, which are not listed in Table 3, fit together with the correlation results of the supra-regional parts of the Antarctica and total Antarctica.

Table 3: Summarized correlation results of the total Antarctic Ice Sheet and supra-regional parts of the Antarctic Ice Sheet (i.m.c. …ice-mass change, evap. …evaporation, precip. …total precipitation, eastw. …eastward wind, northw. …northward wind, horiz. …horizontal wind)

correlation results		i.m.c.	**water cycle**			**wind fields**		
			evap.	precip.	water balance	eastw.	northw.	horiz.
Total Antarctica	El Niño	-0.77	-0.09	-0.06	-0.13	0.29	-0.38	0.35
	La Niña	-0.26	-0.49	-0.03	-0.41	0.24	0.05	0.29
	Others	-0.12	0.12	-0.11	0.00	-0.02	-0.08	0.00
West Antarctic and Antarctic Peninsula	El Niño	-0.76	-0.10	-0.16	-0.15	0.40	0.01	0.15
	La Niña	-0.31	0.10	0.04	0.14	-0.03	0.25	0.00
	Others	-0.09	0.03	-0.07	-0.04	0.10	-0.04	-0.12
East Antarctica	El Niño	0.62	-0.08	0.21	0.15	-0.02	0.21	0.25
	La Niña	0.36	-0.01	-0.03	-0.04	0.02	0.26	-0.07
	Others	0.02	0.01	-0.06	-0.05	0.21	-0.01	-0.02
Central Antarctica	El Niño	0.82	-0.34	-0.14	-0.41	-0.08	-0.07	0.09
	La Niña	-0.07	0.20	0.07	0.13	0.04	0.07	0.16
	Others	-0.09	0.02	-0.03	-0.03	-0.07	-0.05	0.00
(dark green)		positive high correlation						
(light green)		positive average correlation						
(white)		low or no correlation						
(light orange)		negative average correlation						
(dark orange)		negative high correlation						

As mentioned in chapter 4 and 5, the impacts of ENSO events on the Southern Hemisphere (SH) especially to the Antarctica are not that much studied (cf. DOMEISEN et al. 2019: 14). Summed up, ENSO events are influencing the global atmospheric and oceanic circulation (cf. DOMEISEN et al. 2019: 1). Further, the warm surface water and the colder nutrient-rich deep water become separated. Every ENSO event is different regarding location, magnitude and the upcoming impacts (cf. DOMEISEN et al. 2019: 8). El Niño events lead to an upward wave propagation in the SH and to anomalies within the stratospheric polar vortex. The stratosphere influences the surface weather and the global climate. Furthermore, strong eastward winds in the polar stratosphere are upcoming with El Niño events and sea level pressure. SST anomalies are the consequence, which are also evident in wind and rainfall anomalies (cf. DOMEISEN et al. 2019:1 ff).

The West Antarctic climate and water cycle, such as sea ice extent, temperature and precipitation, are strongly influenced by the Amundsen Sea Low. Changes in the water cycle within the West Antarctica are driven by ocean circulation changes, controlled by surface near wind-fields (cf. RAPHAEL et al. 2016:1). During El Niño events, surface near winds are more northwest to southeast, which results due to atmospheric circulation of warmer air from the ocean to the West Antarctica in more snow. Furthermore, the upwelling warmer depth water layer leads to melting of ice shelves. The effect of basal melting in the West Antarctica is much higher than the increasing snowfall (cf. PAOLO et al. 2018: 1). In case of La Niña events, the opposite anomalies could often be observed (cf. DOMEISEN et al. 2019: 1).

By comparison of the literature review with the correlation results, it could be concluded that the ice-mass change correlation results and the literature statements agree. The ice-mass within the West Antarctica and Antarctic Peninsula decreases by increasing SST of the Niño 3.4 index, which is an indicator for the magnitude of the El Niño event. Therefore, teleconnections could be verified. Furthermore, ENSO is a climate phenomenon in the Tropical Equatorial Pacific. Therefore, the large responses of the West Antarctic and Antarctic Peninsula could be explained by their geographical location, which is nearest to the Equatorial Pacific compared to the other supra-regional parts of the Antarctica.

Within the East and Central Antarctica, the opposite correlation was calculated. This could be explained by geological differences within the Antarctica. The East and Central Antarctica mostly consists of a stable shield of rocks (cf. LUIS 2013: 2) above sea level. Therefore, the basal melting is not the dominant driver within these regions. Low correlations within the West Antarctica and Antarctic Peninsula during El Niño events could be observed for the eastward winds, which agree with the literature review. The water cycle anomalies due to precipitation, runoff and evaporation and high correlations due to La Niña events could not be confirmed within the correlations in this thesis. Inaccuracies within the correlation calculations could be explained by the delay between upcoming ENSO events in the Niño 3.4 region and the impacts on the Antarctica. Within the correlations in this thesis, no time delays were assumed. Furthermore, the combined consideration of a number of ENSO events could be lead to inaccuracies, because every ENSO event is different in magnitude and location. The water cycle and wind field data are based on ECMWF. The supra-regions of the Antarctica are not exactly based on the same longitudes and latitudes within the ECMWF data compared to GRACE. Furthermore, the runoff data of ECMWF within the whole Antarctica are very low compared to the evaporation and precipitation, which could be explained by assuming no basal melting and floating ice shelves. Furthermore, the time period between 2002 and 2020 is very short for such correlation approaches, because ENSO events only appear every 2 to 7 years. Therefore, the stated hypotheses and research questions could be answered as followed:

H1: Anomalies in the water cycle of the Antarctica are connected to ENSO.

RQ1: Does ENSO have a crucial impact on the key variables of the Antarctic water cycle?

RQ2: Are there disparities of the anomalies in different regions in the Antarctica?

The correlation results showed that the El Niño events are correlating with the ice-mass change within the Antarctica. Within the West Antarctica and Antarctic Peninsula, there is a negative correlation between ice-mass change and SST of the Niño 3.4 index. Positive correlation results could be observed for the East and Central Antarctic region. Due to a literature review, it could also be concluded that ENSO have a crucial impact on the key variables of the water cycle. Therefore, for example more snowfall and more basal melting during El Niño events could be observed. Due to the missing consideration of basal melting within ECMWF data, no correlation within the calculations in this thesis could be concluded.

H2: Due to the intensification of ENSO- events owing to climate change, anomalies in the Antarctic water cycle occur more often.

RQ3: Which impacts on the Antarctic water cycle does the intensification of ENSO-events have?

RQ4: What does this mean for the average climate in the Antarctica?

The quantification of impacts on the Antarctic water cycle due to the intensification of ENSO events is very difficult. Mainly because ENSO is a complicated phenomenon, existing of various factors. All of them can be differently influenced by climate change. Therefore, a general statement about the future is just not possible.

Furthermore, there are also other climate phenomena besides ENSO, which have impacts on the global climate pattern. Therefore, a separation of ENSO teleconnections from other climate phenomena are crucial for the quantification due to the intensification of ENSO events. Nevertheless, within this thesis the recorded ENSO events between the years 1950 to 2020 were conducted. Therein, it could be observed that between the first half of this period (1950-1985) six El Niño events and in the second half of this period (1985-2020) nine El Niño events were observed. This means that between 1950 and 1985 in average every six years and between 1985 and 2020 every 4 years an El Niño event was notified. Therefore, an intensification of recorded El Niño events could be assessed. This assumption will be underlined by the study of CAI et al. 2018. For a correlation between the ice-mass change and the intensification of ENSO events, the used GRACE dataset (2002-2020) is too short for such statistical approaches. In case of the La Niña events, no intensification within the last 70 years could be recorded. Nevertheless, it could be concluded, that the intensification of El Niño events will be accelerated. Under the assumption that due to the higher concentration of greenhouse gas emissions in the future ENSO events intensifies, the ice-mass and water cycle anomalies within the Antarctica could possibly increase. An intense heating of the SST and the lower atmosphere lead to changes of the water deposit and lead to stronger precipitations. An assumption for the Antarctica could therefore be that more snowfall could fall. On the other hand, consequences could also include less precipitation. With the retreatment of glaciers and the decrease of ice-masses in some areas, the natural water deposits, such as the storage in ice and snow suffer (cf. KERRES et al. 2020: 25).

As the correlation showed, the Antarctic ice-mass requires a differentiated assessment. Different regions react different to climate patterns. The West Antarctic Ice Sheet will further decrease under global warming and intense ENSO events. Therein, the effect of basal melting is stronger than the snowfall. The consequence would be a further rise of the sea level. Within the East and Central Antarctica, the snowfall could be the crucial indicator for the water cycle anomaly. Therefore, the ice-mass within these regions will further increase.

8 Perspectives

As presented in this master thesis, ENSO events have various impacts on the regional and global climate and weather patterns, which also lead to different reactions of the Antarctic ice sheet.
An explicit investigation of these reactions should be done within future research. Therefore, the ECWMF datasets need to be extended by basal melting and data from floating ice shelfs, like the Ronne or Ross Ice Shelf. Additionally, the wind fields in the Antarctica are crucial for the investigation of the water cycle. Within these correlations only the most important surface near neutral wind speed parameters were considered. Future research work could focus on a detail investigation of the Antarctic wind fields and additionally possible anomalies due to ENSO events.
Future work should also implement the factor of a possible time delay of ENSO impacts on variables of the water cycle, as well as on the regional Antarctic Ice Sheets. Impacts from ENSO events on the ice sheet and variables within the water cycle, could occur delayed. No correlations could therefore be reduced to time delays. For this reason, it may be meaningful to consider time delays over months for each parameter and each event.
In addition to that, also the difference in magnitude and location of ENSO events could be investigated. Nonlinear and multicomponent correlation methods could help by the consideration of the difference between the ENSO events. For a better understanding of the global impacts of ENSO, teleconnections need to be separated from influences through other weather and climate anomalies.
A further major issue within the ENSO research, which should be considered in future, is the prediction of the future behavior of ENSO events. Therein, mainly the intensity and the duration should be studied. Though this field remains uncertain, it has high importance for human beings.

References

BANWELL A.F., MACAYEAL D.R., SERGIENKO O.V. (2013): Breakup of the Larsen B Ice Shelf triggered by chain reaction drainage of supraglacial lakes. – In: Geophysical Research Letter 40, 5872-5876.

BAYR T., DOMMENGET D., MARTIN T., POWER S.B. (2013): The eastward shift of the Walker Circulation in response to global warming and its relationship to ENSO variability. – In: Clima Dynamics, 2747-2763.

BALDENHOFER K.G (2017): Das ENSO Phänomen. Informationen zum ozeanisch-atmosphärischen Phänomen El Niño/ Southern Oscillation. – In: ErdWare: Friedrichshafen, 1-69.

BODART J. A. and BINGHAM R. J. (2019): The impact of the extreme 2015 2016 El Niño on the mass balance of the Antarctic ice sheet. – In: Geophysical Research Letters 46, 13862-13871.

BOM (2021): About ENSO Outlooks. Commonwealth of Australia; available online at: https://www.bom.gov.au/climate/ahead/about-ENSO-outlooks.shtml (04.04.2021).

BUNGE L., CLARKE A.J. (2009): A verified estimation of the El Niño Index Niño-3.4 since 1877. – In: Journal of Climate 22 (14), 3979-3992.

BJERKNESS J. (1966): A possible response of the atmospheric Hadley circulation to equatorial anomalies of ocean temperature. – In: Tellus 18, 820-829.

CAI W., MCPHADEN M.J., GRIMM A.M., RODRIGUES R.R., TASCHETTO A.S., GARREAUD R.D., DEWITTE B., POVEDA G., HAM Y.G., SANTOSO A., NG B., ANDERSON W., GUOJIAN W., GENG T., JO H.S., MARENGO J.A., ALVES L.M., OSMAN M., LI S., WU S., KARAMPERIDOU C., TAKAHASHI K., VERA C. (2020): Climate Impacts of the El Niño-Southern Oscillation on South America. – In: Nature Reviews Earth and Environment 1 (1), 215-231

CAI W., SANTOSO A., WANG G., YEH S.W., AN S.I., COBB K.M., COLLINS M., GUILYARDI E., JIN F.F., KUG J.S., LENGAIGNE M., MCPHADEN M.J., TAKAHASHI K., TIMMERMANN A., VECCHI G., WATANABE M., WU L. (2015): ENSO and greenhouse warming. – In: nature climate change 5, 849-859.

CAI W., WANG G., DEWITTE B., WU L. SANTOSO A., TAKAHASHI K., YANG C., CARRERIC A., MCPHADEN M. (2018): Increased variability of eastern Pacific El Niño under greenhouse warming. – In: Nature 564, 201-206.

CAPOTONDI A., WITTENBERG A., NEWMAN M., DI LORENZO E., YU J.Y., BRACONNOT P., COLE J., DEWITTE B., GIESE B., GUILYRDI E., JIN F.F., KARNAUSKAS K., KIRTMAN B., LEE T., SCHNEIDER N., XUE Y., and YEH S.W. (2015): Understanding ENSO Diversity. – In: Bulletin of the American Meteorological Society 96 (6), 921- 938.

COBB K. (2013): Systematic ENSO – driven nutrient variability recorded by central equatorial Pacific corals. – In: Research Letters 40, 3956-3961.

DAGBEGNON C., SOHOULANDE D., VIJAY P. (2015): Impact of climate change on the hydrologic cycle and implications for society. – In: Environment and Social Psychology 1 (1), 36-49.

DELNINNO C. and DOROSH P.A. (2001): Averting a food crisis: Private imports and public targeted distribution in Bangladesh after the 1998 flood. – In: Agricultural Economics 25 (2-3), 337-346.

DI LIBERTO T. (2018): Changes in ENSO impacts in a warming world. – In: climate- science and information for a climate- smart nation; available online at: https://www.climate.gov/news-features/blogs/enso/changes-enso-impacts-warming-world (25.06.2021).

DOMEISEN D.I., GARFINKEL C.I., BUTLER A.H. (2019): The teleconnection of El Niño Southern Oscillation to the Stratosphere. – In: Reviews of Geophysics 57 (1), 5-47.

ECMWF – European Centre for Medium- Range Weather Forecasts (2021a): Datasets; available online at: https://www.ecmwf.int/en/forecasts/datasets (15.04.2021).

ECMWF – European Centre for Medium- Range Weather Forecasts (2021b): Who we are; available online at: https://www.ecmwf.int/en/about/who-we-are (15.04.2021).

ECMWF – European Centre for Medium- Range Weather Forecasts (2021c): ERA5 monthly averaged data on single levels from 1979 to present; available online at: https://cds.climate.copernicus.eu/cdsapp#!/dataset/reanalysis-era5-single-levels-monthly-means?tab=overview (15.04.2021).

GLANTZ M.H., RAMIREZ I.J. (2020): Reviewing the Oceanic Niño Index (ONI) to enhance societal readiness for El Niño´s Impacts. – In: International Journal of Disaster Risk Science 11, 394-403.

GFZ – Geoforschungszentrum Potsdam (2021): Antarctic Ice- Mass Change/ Grace Data; available online at: gravis.gfz-potsdam.de/antarctica (16.04.2021)

HAESELER S., ZIESE M. (2016): El Niño 2015/16 und seine klimatischen Folgen im Vergleich zu 1982/83 und 1997/98. – In: DWD – Deutscher Wetterdienst, 1-13.

HAMEED S.N., JIN D., THILAKAN V. (2018): A model for super El Niños. – In: Nature Communications 9 (2528), 1-15.

HELLER K., ROSEMANN B. (1979): Planung und Auswertung empirischer Untersuchungen – Eine Einführung für Pädagogen, Psychologen und Soziologen. Ernst Klett Verlag Stuttgart: Stuttgart.

HONG L.C., HO L., JIN F.F (2014): A Southern Hemisphere booster of super El Niño. – In: Geophysical Research Letters 410, 2141–2149.

HOVE L., KAMBANJE C. (2019): Lessons from the El Niño – induced 2015/16 drought in the Southern Africa region. – In: Current Directions in Water Scarcity Research 2, 33-54.

KERRES M., SERVOS M., KRAMER A., HATTERMANN F., TÄNZLER D., PILZ T., MUELLER A. (2020): Stop Floating, Start Swimming - Water and climate change – interlinkages and prospects for future action. Deutsche Gesellschaft für Internationale Zusammenarbeit (GIZ) GmbH: Bonn.

KUNDZEWICZ Z.W. (2008): Climate change impacts on the hydrological cycle. – In: Ecohydrology and Hydrobiology 8(2), 195-203.

LATIF M, SEMENOV V.A., PARK W. (2015): Super El Niños in response to global warming in a climate model. – In: Climatic Change 132, 489-500.

LATIF M. (2018): Neue Erkenntnisse über El Niño und La Niña. – In: Warnsignal Klima Extremereignisse, 193-200.

LATIF M, SEMENOV V.A., PARK W. (2015): Super El Niños in response to global warming in a climate model. – In: Climatic Change 132: 489-500.

LIPPELT J. and SCHRICKER J. (2016): Kurz zum Klima: Alle Jahre wieder? Das Klimaphänomen El Niño und die Agrarmärkte. – In: IFO 18, 57-62.

L´ HEUREUX M., LEE S., (2013): Recent multidecadal strengthening of the Walker circulation across the Tropical Pacific. – In: Nature Climate Change 3 (6), 571-576.

LUIS A. J. (2013): Past, Present and Future Climate of Antarctica. – In: International Journal of Geosciences 4, 959-977.

MCPHADEN M.J., ZHANG X., HENDON H.H. and WHEELER M.C. (2006): Large scale dynamics and MJO forcing of ENSO variability. – In: Geophysical research letters 33, 1-5.

MCPHADEN M.J., ZEBIAK S.E., GLANTZ M.H. (2006): ENSO as an integrating concept in earth science. – In: Science 314 (5806), 1740-1745.

NASA- National Aeronautics and Space Administration (2010): The Water Cycle and Climate Change. – In: NASA Earth Observatory; available online at: https://earthobservatory.nasa.gov/features/Water/page3.php (02.06.2021)

NASA- National Aeronautics and Space Administration (2010): Unusually Intense Monsoon Rains. – In: NASA Earth Observatory; available online at: https://earthobservatory.nasa.gov/images/45177/unusually-intense-monsoon-rains (05.02.2021).

NASA- National Aeronautics and Space Administration (2017): El Niño. – In: NASA Earth Observatory; available online at: https://earthobservatory.nasa.gov/features/ElNino (01.06.2021).

NOAA – National Oceanic and Atmospheric Administration (2004): Kelvin Wave SSTs across Pacific Basin. – Maryland; available online at: https://www.ncdc.noaa.gov/sotc/enso/200408 (15.03.2021).

NOAA – National Oceanic and Atmospheric Administration (2012): ENSO Episodes in the Tropical Pacific. – Maryland; available online at: https://www.cpc.ncep.noaa.gov/products/analysis_monitoring/impacts/warm_impacts.shtml (12.04.2021).

NOAA – National Oceanic and Atmospheric Administration (2016): What are El Niño and La Niña. – Maryland; available online at: https://www.climate.gov/print/808421 (04.02.2021).

NOAA – National Oceanic and Atmospheric Administration (2019): The water cycle on Earth. – Maryland; available online at: https://www.noaa.gov/education/resource-collections/freshwater/water-cycle (23.05.2021).

NOAA – National Oceanic and Atmospheric Administration (2021a): Cold and Warm Episodes by Season. – Maryland; available online at: https://origin.cpc.ncep.noaa.gov/products/analysis_monitoring/ensostuff/ONI_v5.php (01.04.2021).

NOAA – National Oceanic and Atmospheric Administration (2021b): Monthly Atmospheric & SST Indices; available online at: https://www.cpc.ncep.noaa.gov/data/indices/ (15.04.2021).

NOBLE T. L., ROHLING E. J., MCCORMACK F. S. (2020): Antarctica in a changing climate – In: Eos, 101.

OLIVER J. E. (2004): Walker Circulation– In: Encyclopedia of World Climatology. Indiana State University, 798-805.

PAOLO F. S., PADMAN L., FRICKER H. A., ADUSUMILLI S., HOWARD S., SIEGFRIED M. R. (2018): Response of Pacific-sector Antarctic ice shelves to the El Niño/Southern Oscillation. – In: Nature Geoscience 11, 121-126.

RAHAMAN W., CHATTERJEE S., EJAZ T., THAMBAN M. (2019): Antarctic temperature since the Industrial Era. – In: Nature 9, 1- 12.

RAPHAEL M. N., MARSHALL G. J., TURNER J., FOGT R., SCHNEIDER D., DIXON D. A., HOSKING J. S., JONES J. M., HOBBS W. R. (2016): The Amundsen Sea Low. – In: American Meteorological Society.

RIAHI K., RAO S., KREY V., CHO C., CHIRKOV C. (2011): RCP 8.5- A scenario of comparatively high greenhouse gas emissions. – In: Climatic Change 109, 33-57.

RIGNOT E., MOUGINOT J., SCHEUCHL B., VAN DEN BROEKE M., VAN WESSEM M.J., MORLIGHEM M. (2019): Four decades of Antarctic Ice Sheet mass balance from 1979-2017. – In: PNAS 116 (4), 1095-1103.

RINTOUL S.R., CHOWN S.L., DECONTO R.M., ENGLAND M.H., FRICKER H.A., MASSON-DELMOTTE V., NAISH T.R., SIEGERT M.J., XAVIER J.C. (2018): Choosing the future of Antarctica. – In: Nature 558, 233- 241.

RUTH S. (2016): Paraguay: Feeling the brunt of El Niño– In: European Commission; available online at: https://ees.kuleuven.be/hydrant/hydrant.html (10.05.2021).

SANTOSO A., MCPHADEN M., CAI W. (2017): The Defining Characteristics of ENSO Extremes and the Strong 2015/2016 El Niño. – In: Reviews of Geophysics 55, 1079-1129.

SHEPARD A., GILBERT L., MUIR A.S., KONRAD H., MCMILLAN M., SLATER T., BRIGGS K.H, SUNDAL A.V, HOGG A.E, ENGDAHL M.E (2019): Trends in Antarctic Ice Sheet Elevation and Mass. – In: Geophysical Research Letter 46, 8174-8183.

TAPLEY B. D., WATKINS M. M., FLECHTNER F., REIGBER C., BETTADPUR S., RODELL M., SASGEN I., FAMIGLIETTI J. S., LANDERER F. W., CHAMBERS D. P., REAGER J. T., GARDNER A. S., SAVE H., IVINS E. R., SWENSON S. C., BOENING C., DAHLE C., WIESE D. N., DOBSLAW H., TAMISIEA M. E. and VELICOGNA I. (2019): Contributions of GRACE to understanding climate change – In: Nature Climate Change 9, 358-369.

TRENBERTH K.E. (1997): The definition of El Niño. – In: National Center of Atmospheric Research 78 (12), 2771-2778.

VAN DE BERG W.J., NOËL B., VAN WESSEM M., REIJMER C., KUIPERS MUNNEKE P., BRILS M., VAN TIGGELEN M., VAN MEJGAARD E. (2019): The contemporary and projected climate of Greenland and Antarctica, Abstract special project request, Utrecht University: Netherlands.

VAN DEN BROEKE M.R., NOËL B, VAN DE BERG W.J., VAN WESSEM M. (2018): Mass balance of the Antarctic Ice Sheet from 1992 to 2017, Nature 558, 219-222.

VAN LIPZIG (2016): Hydrant project: scientific goals. – In: KU Leuven. available online at: https://ees.kuleuven.be/hydrant/hydrant.html (01.07.2021).

VAN OLDENBORGH G.G., HENDON H., STOCKDALE T., L´HEUREUX M., DE PEREZ E.C., SINGH R., VAN AALST M. (2021): Defining El Niño indices in a warming climate. – In: Environmental Research Letters 16, 1-9.

VIKAS M. and DWARAKISH G.S. (2015): El Niño: A Review. – In: International Journal of Earth Sciences and Engineering 8 (2), 130-137.

YANG S. and LAU M.K (2002): Walker Circulation available online at: http://meteo.fisica.edu.uy/Materias/climatologia/teorico_climatologia_2013/LauWalkercirculation.pdf (25.05.2021).

YU J.Y., KAO H.Y., KIM S.T. (2009): Subsurface ocean temperature indices for Central-Pacific and Eastern-Pacific types of ENSO. – In: Geophysical Research Letters, 1-20.

Appendix

- **Further results of the correlation from the ice-mass change of the Antarctic sub-regions with the SST anomaly from the Niño 3.4 index**

  a) Ice-mass change and Niño 3.4 index within the selected region between the years 2002 and 2020,

  b) Correlation of ice-mass change with SST anomaly of Niño 3.4 index during Super El Niño events,

  c) Correlation of ice-mass change with SST anomaly of Niño 3.4 index during Large La Niña events,

  d) Correlation of ice-mass change with SST anomaly of Niño 3.4 index between Large La Niña and Super El Niño events.

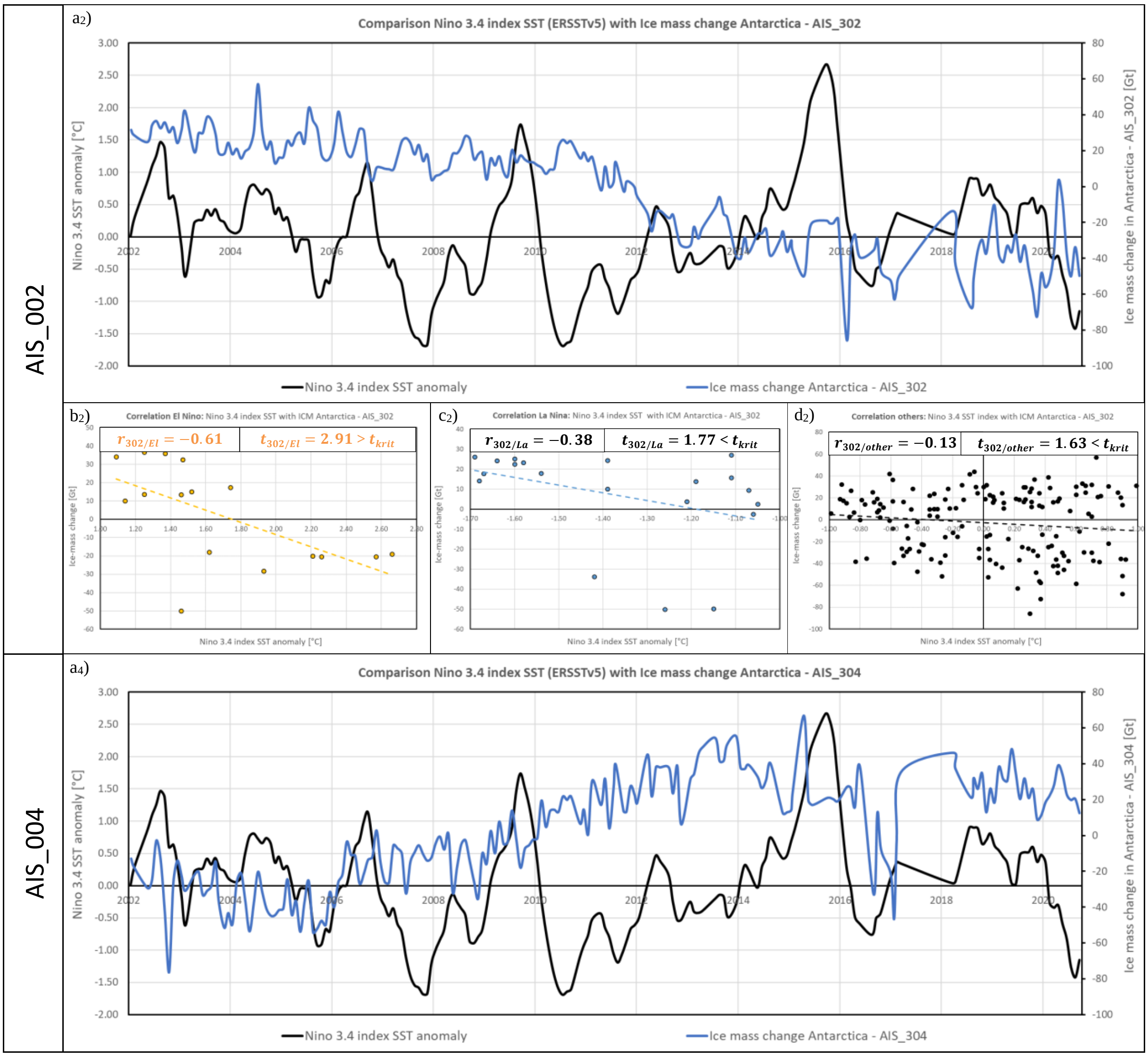

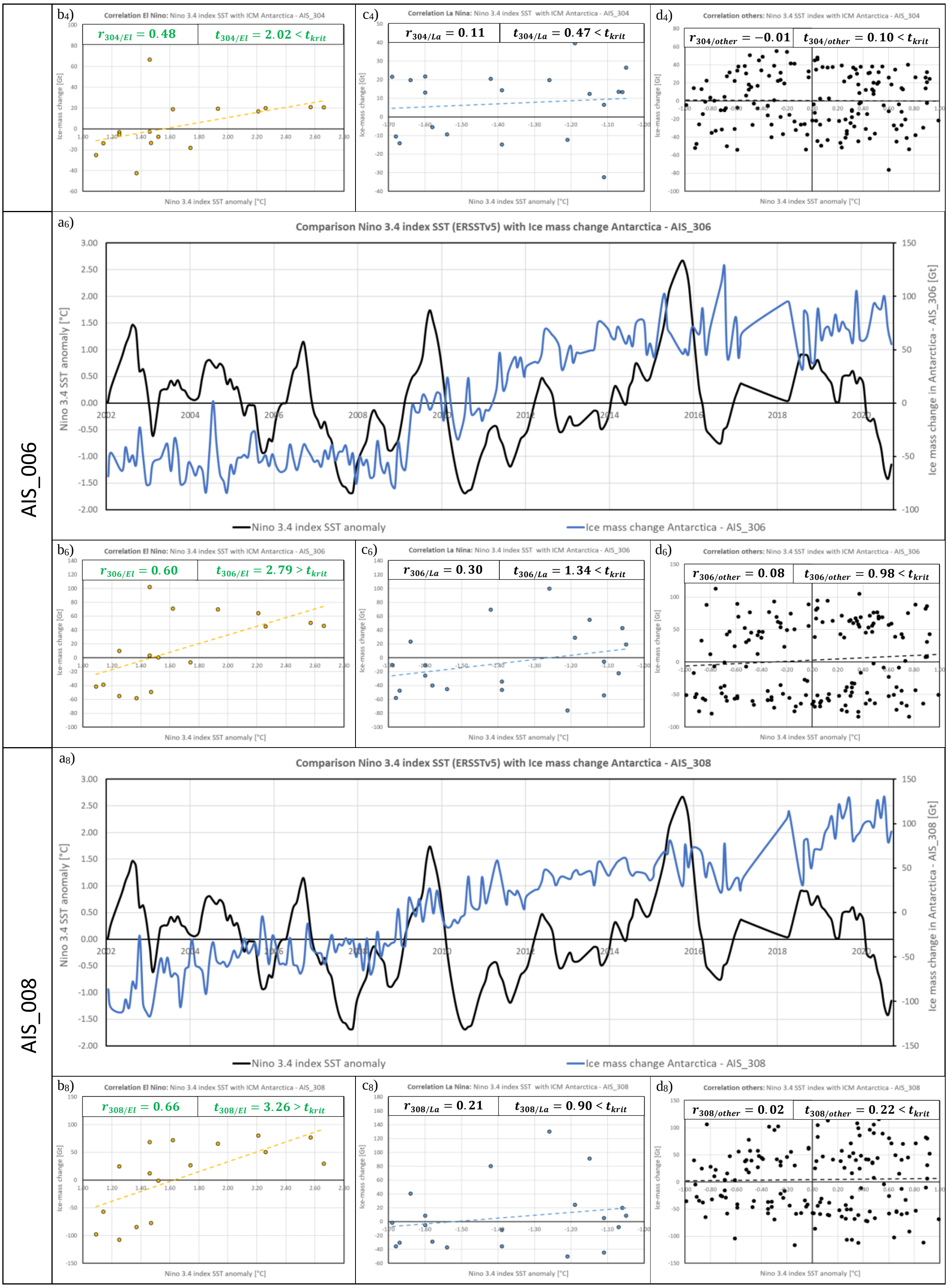

b4)
Correlation El Nino: Nino 3.4 index SST with ICM Antarctica - AIS_304
$r_{304/El} = 0.48$
$t_{304/El} = 2.02 < t_{krit}$
Ice-mass change [Gt]
Nino 3.4 index SST anomaly [°C]
c4)
Correlation La Nina: Nino 3.4 index SST with ICM Antarctica - AIS_304
$r_{304/La} = 0.11$
$t_{304/La} = 0.47 < t_{krit}$
Ice-mass change [Gt]
Nino 3.4 index SST anomaly [°C]
d4)
Correlation others: Nino 3.4 SST index with ICM Antarctica - AIS_304
$r_{304/other} = -0.01$
$t_{304/other} = 0.10 < t_{krit}$
Ice-mass change [Gt]
Nino 3.4 index SST anomaly [°C]
AIS_006
a6)
Comparison Nino 3.4 index SST (ERSSTv5) with Ice mass change Antarctica - AIS_306
Nino 3.4 SST anomaly [°C]
Ice mass change in Antarctica - AIS_306 [Gt]
Nino 3.4 index SST anomaly
Ice mass change Antarctica - AIS_306
b6)
Correlation El Nino: Nino 3.4 index SST with ICM Antarctica - AIS_306
$r_{306/El} = 0.60$
$t_{306/El} = 2.79 > t_{krit}$
Ice-mass change [Gt]
Nino 3.4 index SST anomaly [°C]
c6)
Correlation La Nina: Nino 3.4 index SST with ICM Antarctica - AIS_306
$r_{306/La} = 0.30$
$t_{306/La} = 1.34 < t_{krit}$
Ice-mass change [Gt]
Nino 3.4 index SST anomaly [°C]
d6)
Correlation others: Nino 3.4 SST index with ICM Antarctica - AIS_306
$r_{306/other} = 0.08$
$t_{306/other} = 0.98 < t_{krit}$
Ice-mass change [Gt]
Nino 3.4 index SST anomaly [°C]
AIS_008
a8)
Comparison Nino 3.4 index SST (ERSSTv5) with Ice mass change Antarctica - AIS_308
Nino 3.4 SST anomaly [°C]
Ice mass change in Antarctica - AIS_308 [Gt]
Nino 3.4 index SST anomaly
Ice mass change Antarctica - AIS_308
b8)
Correlation El Nino: Nino 3.4 index SST with ICM Antarctica - AIS_308
$r_{308/El} = 0.66$
$t_{308/El} = 3.26 > t_{krit}$
Ice-mass change [Gt]
Nino 3.4 index SST anomaly [°C]
c8)
Correlation La Nina: Nino 3.4 index SST with ICM Antarctica - AIS_308
$r_{308/La} = 0.21$
$t_{308/La} = 0.90 < t_{krit}$
Ice-mass change [Gt]
Nino 3.4 index SST anomaly [°C]
d8)
Correlation others: Nino 3.4 SST index with ICM Antarctica - AIS_308
$r_{308/other} = 0.02$
$t_{308/other} = 0.22 < t_{krit}$
Ice-mass change [Gt]
Nino 3.4 index SST anomaly [°C]

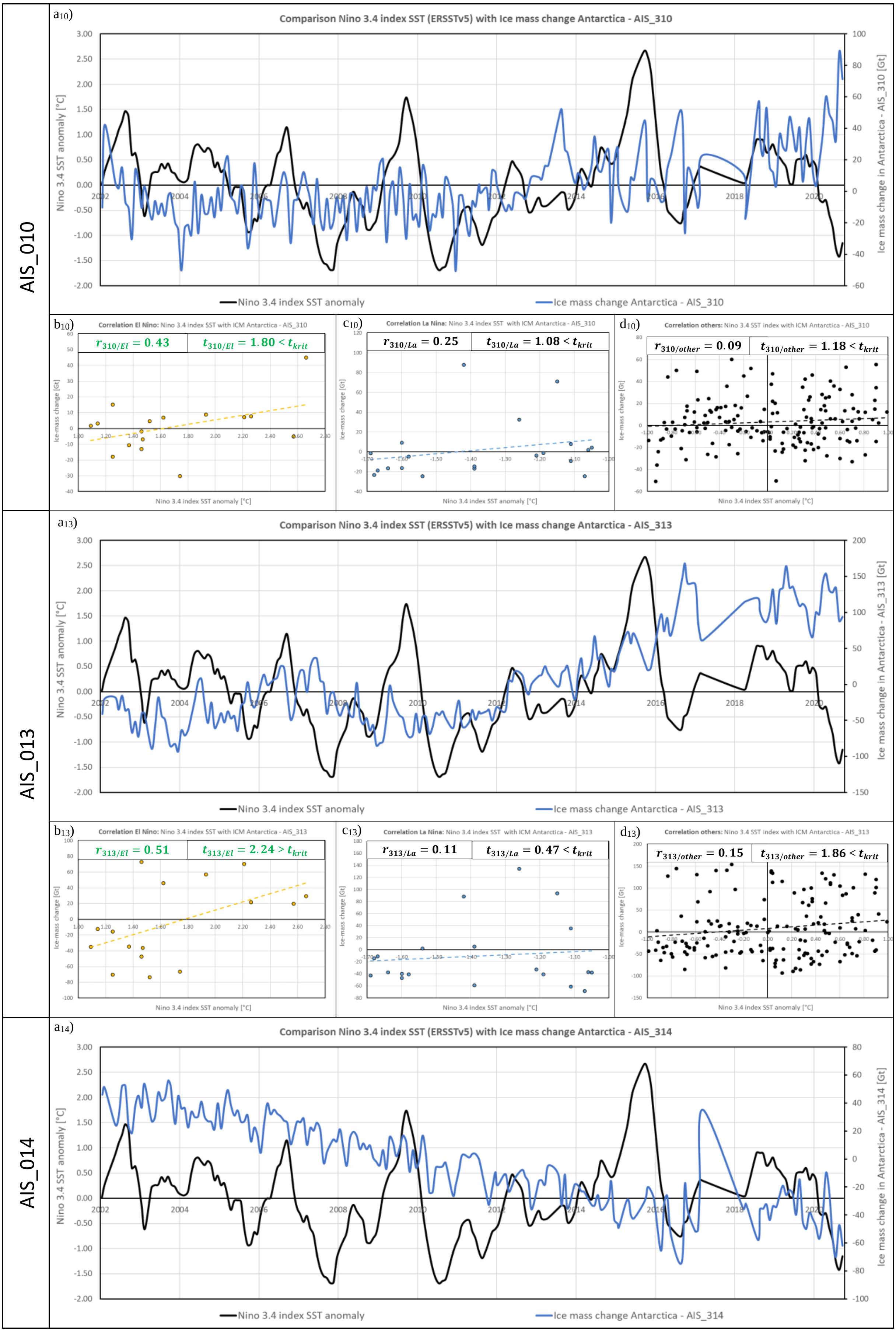
AIS_010
a10)
Comparison Nino 3.4 index SST (ERSSTv5) with Ice mass change Antarctica - AIS_310
Nino 3.4 SST anomaly [°C]
Ice mass change in Antarctica - AIS_310 [Gt]
Nino 3.4 index SST anomaly
Ice mass change Antarctica - AIS_310
b10)
Correlation El Nino: Nino 3.4 index SST with ICM Antarctica - AIS_310
$r_{310/El} = 0.43$
$t_{310/El} = 1.80 < t_{krit}$
c10)
Correlation La Nina: Nino 3.4 index SST with ICM Antarctica - AIS_310
$r_{310/La} = 0.25$
$t_{310/La} = 1.08 < t_{krit}$
d10)
Correlation others: Nino 3.4 SST index with ICM Antarctica - AIS_310
$r_{310/other} = 0.09$
$t_{310/other} = 1.18 < t_{krit}$
Ice-mass change [Gt]
Nino 3.4 index SST anomaly [°C]
AIS_013
a13)
Comparison Nino 3.4 index SST (ERSSTv5) with Ice mass change Antarctica - AIS_313
Nino 3.4 SST anomaly [°C]
Ice mass change in Antarctica - AIS_313 [Gt]
Nino 3.4 index SST anomaly
Ice mass change Antarctica - AIS_313
b13)
Correlation El Nino: Nino 3.4 index SST with ICM Antarctica - AIS_313
$r_{313/El} = 0.51$
$t_{313/El} = 2.24 > t_{krit}$
c13)
Correlation La Nina: Nino 3.4 index SST with ICM Antarctica - AIS_313
$r_{313/La} = 0.11$
$t_{313/La} = 0.47 < t_{krit}$
d13)
Correlation others: Nino 3.4 SST index with ICM Antarctica - AIS_313
$r_{313/other} = 0.15$
$t_{313/other} = 1.86 < t_{krit}$
Ice-mass change [Gt]
Nino 3.4 index SST anomaly [°C]
AIS_014
a14)
Comparison Nino 3.4 index SST (ERSSTv5) with Ice mass change Antarctica - AIS_314
Nino 3.4 SST anomaly [°C]
Ice mass change in Antarctica - AIS_314 [Gt]
Nino 3.4 index SST anomaly
Ice mass change Antarctica - AIS_314

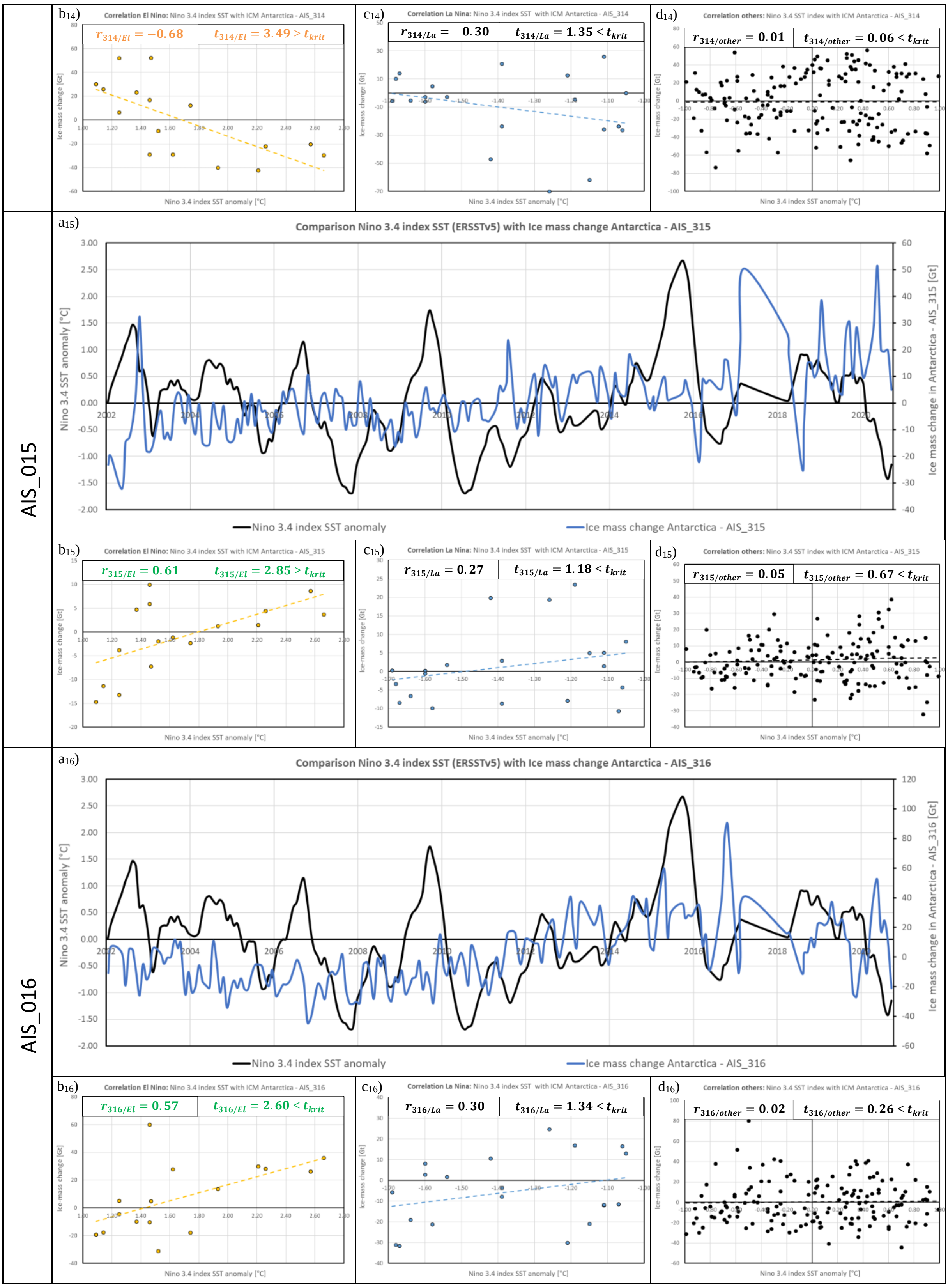
b14)
Correlation El Nino: Nino 3.4 index SST with ICM Antarctica - AIS_314
$r_{314/El} = -0.68$
$t_{314/El} = 3.49 > t_{krit}$
c14)
Correlation La Nina: Nino 3.4 index SST with ICM Antarctica - AIS_314
$r_{314/La} = -0.30$
$t_{314/La} = 1.35 < t_{krit}$
d14)
Correlation others: Nino 3.4 SST index with ICM Antarctica - AIS_314
$r_{314/other} = 0.01$
$t_{314/other} = 0.06 < t_{krit}$
Ice-mass change [Gt]
Nino 3.4 index SST anomaly [°C]
AIS_015
a15)
Comparison Nino 3.4 index SST (ERSSTv5) with Ice mass change Antarctica - AIS_315
Nino 3.4 SST anomaly [°C]
Ice mass change in Antarctica - AIS_315 [Gt]
Nino 3.4 index SST anomaly
Ice mass change Antarctica - AIS_315
b15)
Correlation El Nino: Nino 3.4 index SST with ICM Antarctica - AIS_315
$r_{315/El} = 0.61$
$t_{315/El} = 2.85 > t_{krit}$
c15)
Correlation La Nina: Nino 3.4 index SST with ICM Antarctica - AIS_315
$r_{315/La} = 0.27$
$t_{315/La} = 1.18 < t_{krit}$
d15)
Correlation others: Nino 3.4 SST index with ICM Antarctica - AIS_315
$r_{315/other} = 0.05$
$t_{315/other} = 0.67 < t_{krit}$
AIS_016
a16)
Comparison Nino 3.4 index SST (ERSSTv5) with Ice mass change Antarctica - AIS_316
Nino 3.4 SST anomaly [°C]
Ice mass change in Antarctica - AIS_316 [Gt]
Nino 3.4 index SST anomaly
Ice mass change Antarctica - AIS_316
b16)
Correlation El Nino: Nino 3.4 index SST with ICM Antarctica - AIS_316
$r_{316/El} = 0.57$
$t_{316/El} = 2.60 < t_{krit}$
c16)
Correlation La Nina: Nino 3.4 index SST with ICM Antarctica - AIS_316
$r_{316/La} = 0.30$
$t_{316/La} = 1.34 < t_{krit}$
d16)
Correlation others: Nino 3.4 SST index with ICM Antarctica - AIS_316
$r_{316/other} = 0.02$
$t_{316/other} = 0.26 < t_{krit}$

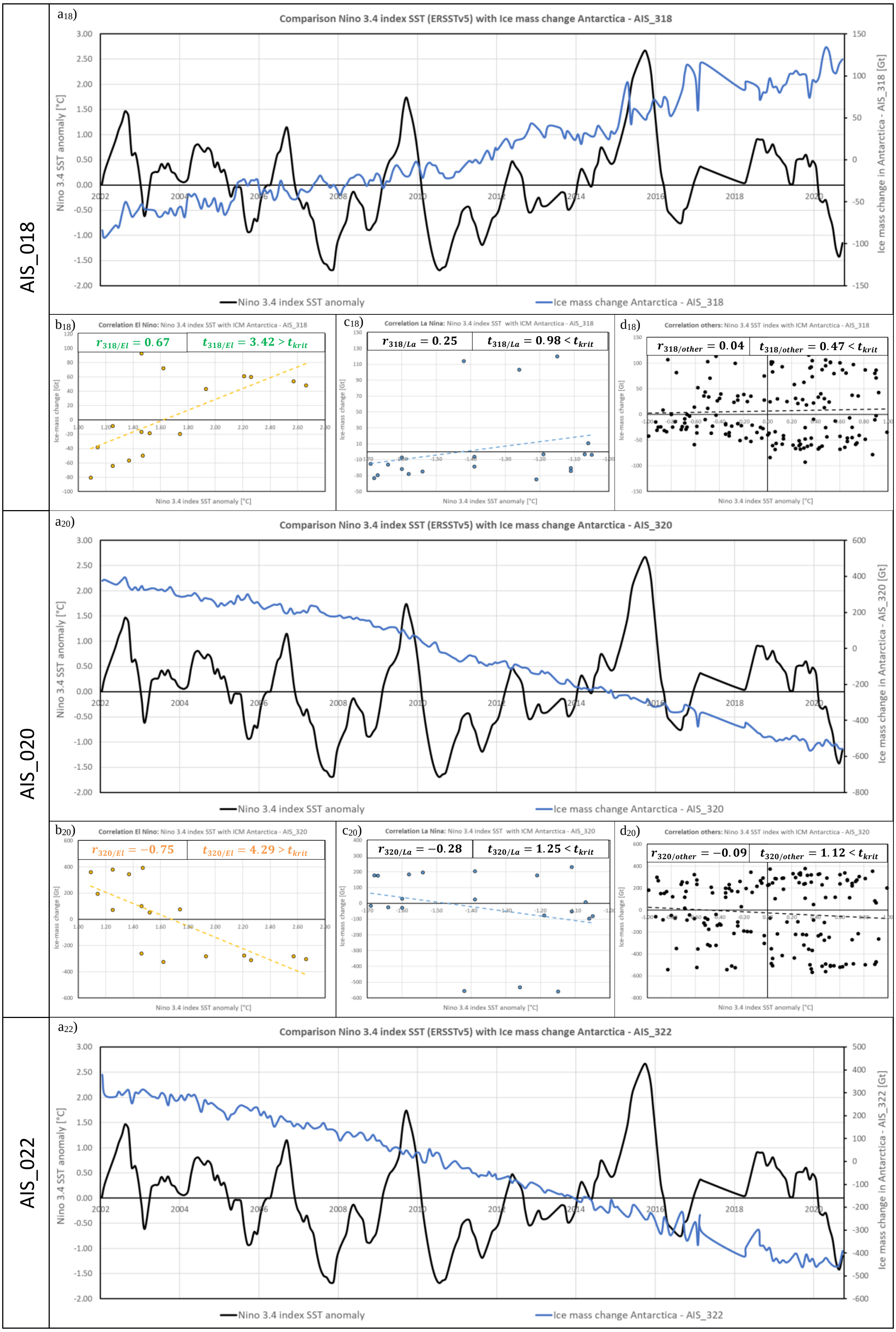
AIS_018
a18)
Comparison Nino 3.4 index SST (ERSSTv5) with Ice mass change Antarctica - AIS_318
Nino 3.4 SST anomaly [°C]
Ice mass change in Antarctica - AIS_318 [Gt]
Nino 3.4 index SST anomaly
Ice mass change Antarctica - AIS_318
b18)
Correlation El Nino: Nino 3.4 index SST with ICM Antarctica - AIS_318
$r_{318/El} = 0.67$
$t_{318/El} = 3.42 > t_{krit}$
c18)
Correlation La Nina: Nino 3.4 index SST with ICM Antarctica - AIS_318
$r_{318/La} = 0.25$
$t_{318/La} = 0.98 < t_{krit}$
d18)
Correlation others: Nino 3.4 SST index with ICM Antarctica - AIS_318
$r_{318/other} = 0.04$
$t_{318/other} = 0.47 < t_{krit}$
Nino 3.4 index SST anomaly [°C]
Ice-mass change [Gt]
AIS_020
a20)
Comparison Nino 3.4 index SST (ERSSTv5) with Ice mass change Antarctica - AIS_320
Nino 3.4 SST anomaly [°C]
Ice mass change in Antarctica - AIS_320 [Gt]
Nino 3.4 index SST anomaly
Ice mass change Antarctica - AIS_320
b20)
Correlation El Nino: Nino 3.4 index SST with ICM Antarctica - AIS_320
$r_{320/El} = -0.75$
$t_{320/El} = 4.29 > t_{krit}$
c20)
Correlation La Nina: Nino 3.4 index SST with ICM Antarctica - AIS_320
$r_{320/La} = -0.28$
$t_{320/La} = 1.25 < t_{krit}$
d20)
Correlation others: Nino 3.4 SST index with ICM Antarctica - AIS_320
$r_{320/other} = -0.09$
$t_{320/other} = 1.12 < t_{krit}$
Nino 3.4 index SST anomaly [°C]
Ice-mass change [Gt]
AIS_022
a22)
Comparison Nino 3.4 index SST (ERSSTv5) with Ice mass change Antarctica - AIS_322
Nino 3.4 SST anomaly [°C]
Ice mass change in Antarctica - AIS_322 [Gt]
Nino 3.4 index SST anomaly
Ice mass change Antarctica - AIS_322

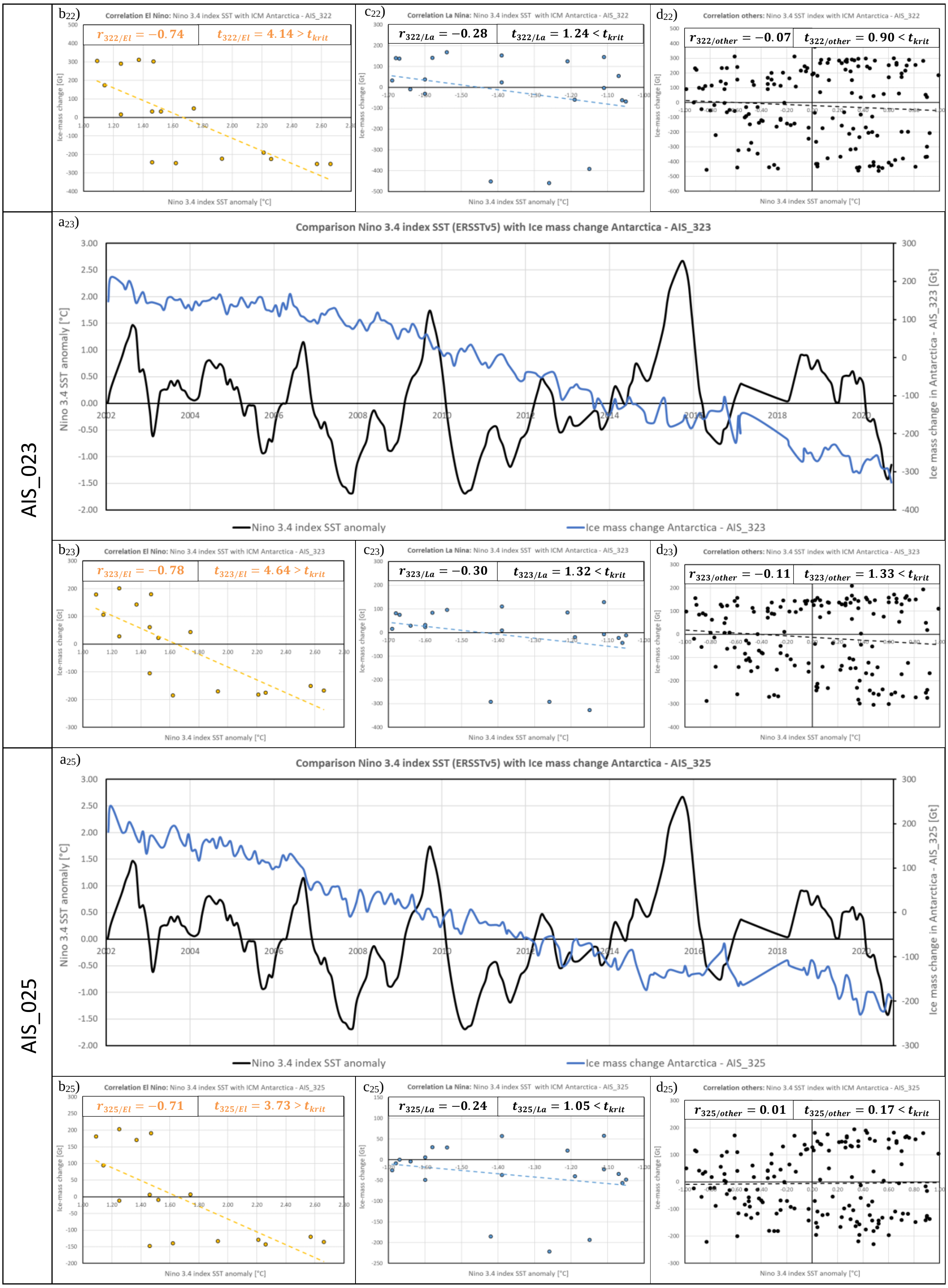

b22)
Correlation El Nino: Nino 3.4 index SST with ICM Antarctica - AIS_322
$r_{322/El} = -0.74$
$t_{322/El} = 4.14 > t_{krit}$
c22)
Correlation La Nina: Nino 3.4 index SST with ICM Antarctica - AIS_322
$r_{322/La} = -0.28$
$t_{322/La} = 1.24 < t_{krit}$
d22)
Correlation others: Nino 3.4 SST index with ICM Antarctica - AIS_322
$r_{322/other} = -0.07$
$t_{322/other} = 0.90 < t_{krit}$
Nino 3.4 index SST anomaly [°C]
Ice-mass change [Gt]
AIS_023
a23)
Comparison Nino 3.4 index SST (ERSSTv5) with Ice mass change Antarctica - AIS_323
Nino 3.4 SST anomaly [°C]
Ice mass change in Antarctica - AIS_323 [Gt]
Nino 3.4 index SST anomaly
Ice mass change Antarctica - AIS_323
b23)
Correlation El Nino: Nino 3.4 index SST with ICM Antarctica - AIS_323
$r_{323/El} = -0.78$
$t_{323/El} = 4.64 > t_{krit}$
c23)
Correlation La Nina: Nino 3.4 index SST with ICM Antarctica - AIS_323
$r_{323/La} = -0.30$
$t_{323/La} = 1.32 < t_{krit}$
d23)
Correlation others: Nino 3.4 SST index with ICM Antarctica - AIS_323
$r_{323/other} = -0.11$
$t_{323/other} = 1.33 < t_{krit}$
AIS_025
a25)
Comparison Nino 3.4 index SST (ERSSTv5) with Ice mass change Antarctica - AIS_325
Nino 3.4 SST anomaly [°C]
Ice mass change in Antarctica - AIS_325 [Gt]
Nino 3.4 index SST anomaly
Ice mass change Antarctica - AIS_325
b25)
Correlation El Nino: Nino 3.4 index SST with ICM Antarctica - AIS_325
$r_{325/El} = -0.71$
$t_{325/El} = 3.73 > t_{krit}$
c25)
Correlation La Nina: Nino 3.4 index SST with ICM Antarctica - AIS_325
$r_{325/La} = -0.24$
$t_{325/La} = 1.05 < t_{krit}$
d25)
Correlation others: Nino 3.4 SST index with ICM Antarctica - AIS_325
$r_{325/other} = 0.01$
$t_{325/other} = 0.17 < t_{krit}$

- **Further results of the correlation from the water cycle of the supra-regional Antarctic Ice Sheets with the SST anomaly from the Niño 3.4 index**

  a) Water cycle key variable and Niño 3.4 index within the selected region between the years 2002 and 2020,

  b) Correlation of water cycle key variable with SST anomaly of Niño 3.4 index during Super El Niño events,

  c) Correlation of water cycle key variable with SST anomaly of Niño 3.4 index during Large La Niña events,

  d) Correlation of water cycle key variable with SST anomaly of Niño 3.4 index between Large La Niña and Super El Niño events.

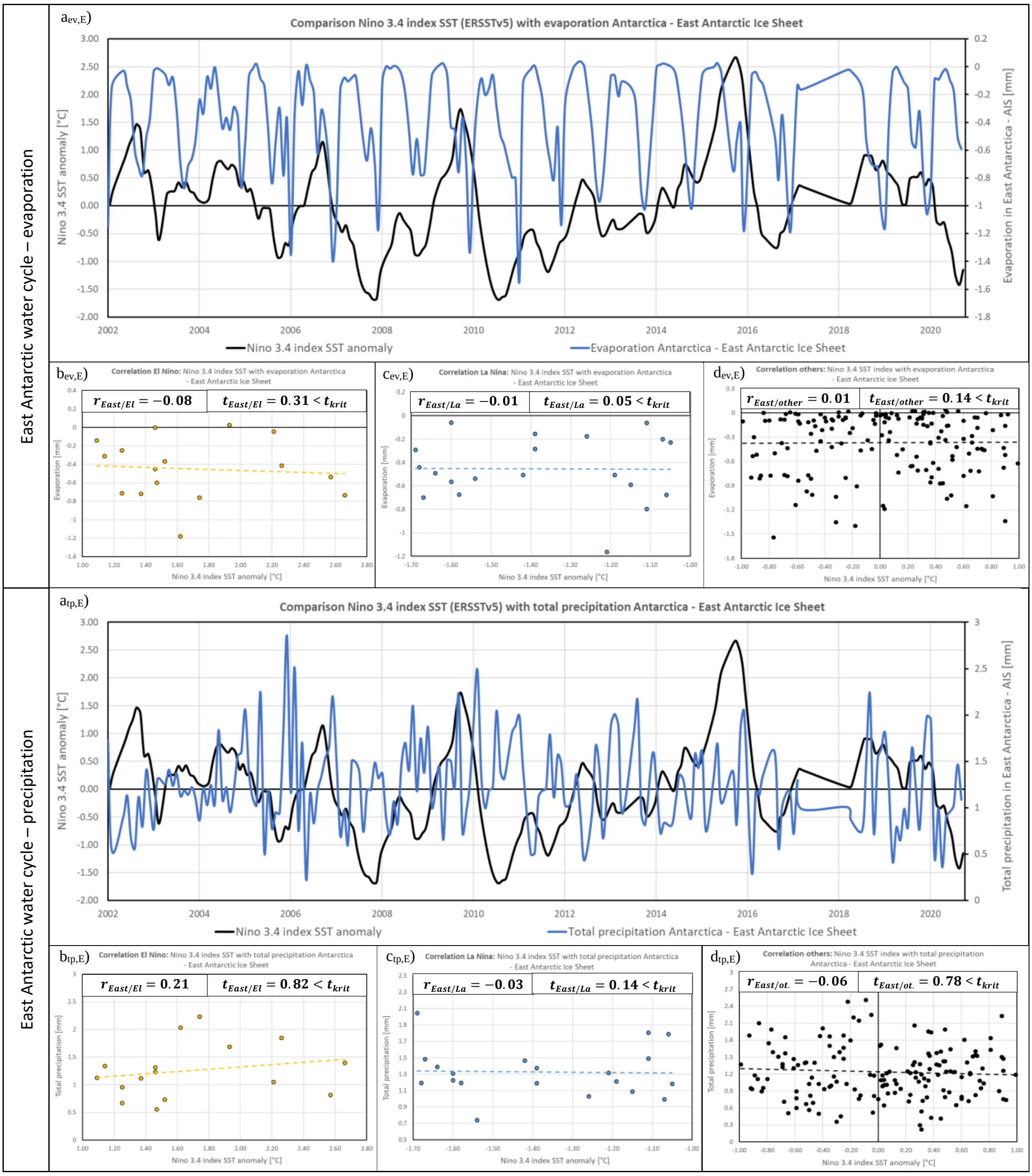

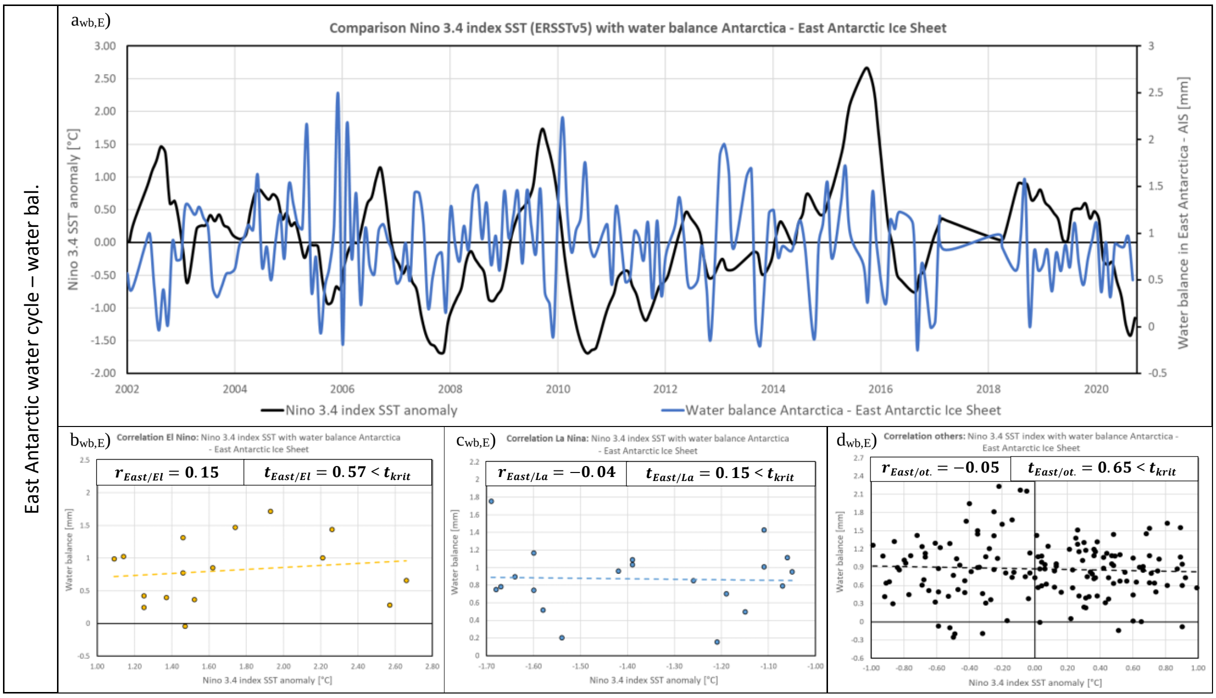
East Antarctic water cycle – water bal.
awb,E)
Comparison Nino 3.4 index SST (ERSSTv5) with water balance Antarctica - East Antarctic Ice Sheet
Nino 3.4 SST anomaly [°C]
Water balance in East Antarctica - AIS [mm]
Nino 3.4 index SST anomaly
Water balance Antarctica - East Antarctic Ice Sheet
bwb,E)
Correlation El Nino: Nino 3.4 index SST with water balance Antarctica - East Antarctic Ice Sheet
$r_{East/El} = 0.15$
$t_{East/El} = 0.57 < t_{krit}$
Water balance [mm]
Nino 3.4 index SST anomaly [°C]
cwb,E)
Correlation La Nina: Nino 3.4 index SST with water balance Antarctica - East Antarctic Ice Sheet
$r_{East/La} = -0.04$
$t_{East/La} = 0.15 < t_{krit}$
Water balance [mm]
Nino 3.4 index SST anomaly [°C]
dwb,E)
Correlation others: Nino 3.4 SST index with water balance Antarctica - East Antarctic Ice Sheet
$r_{East/ot.} = -0.05$
$t_{East/ot.} = 0.65 < t_{krit}$
Water balance [mm]
Nino 3.4 index SST anomaly [°C]

- **Further results of the correlation from the wind parameters of the supra-regional Antarctic Ice Sheets with the SST anomaly from the Niño 3.4 index**
  a) Wind field variable and Niño 3.4 index within the selected region between the years 2002 and 2020,
  b) Correlation of wind field variable with SST anomaly of Niño 3.4 index during Super El Niño events,
  c) Correlation of wind field variable with SST anomaly of Niño 3.4 index during Large La Niña events,
  d) Correlation of wind field variable with SST anomaly of Niño 3.4 index between Large La Niña and Super El Niño events.

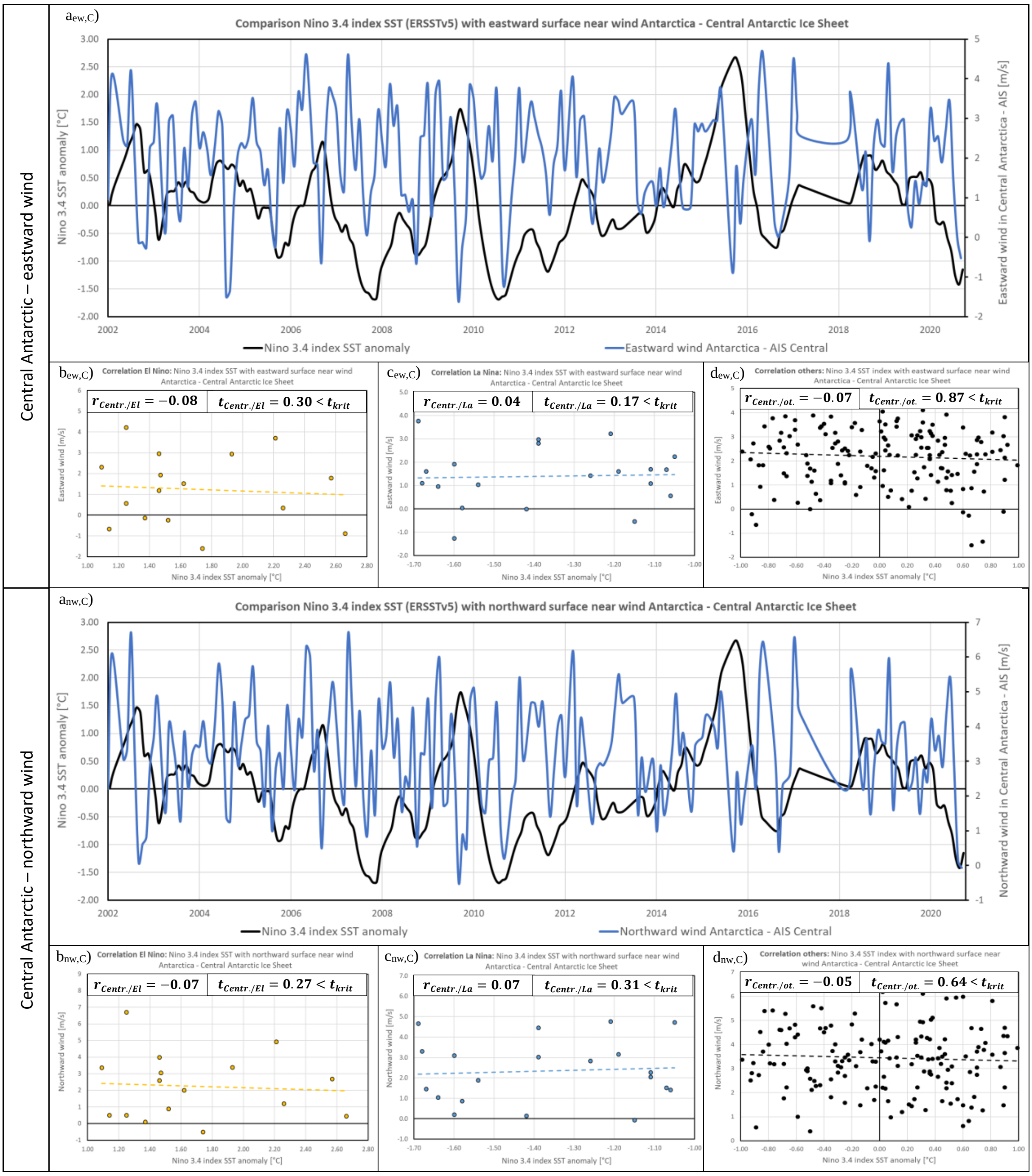

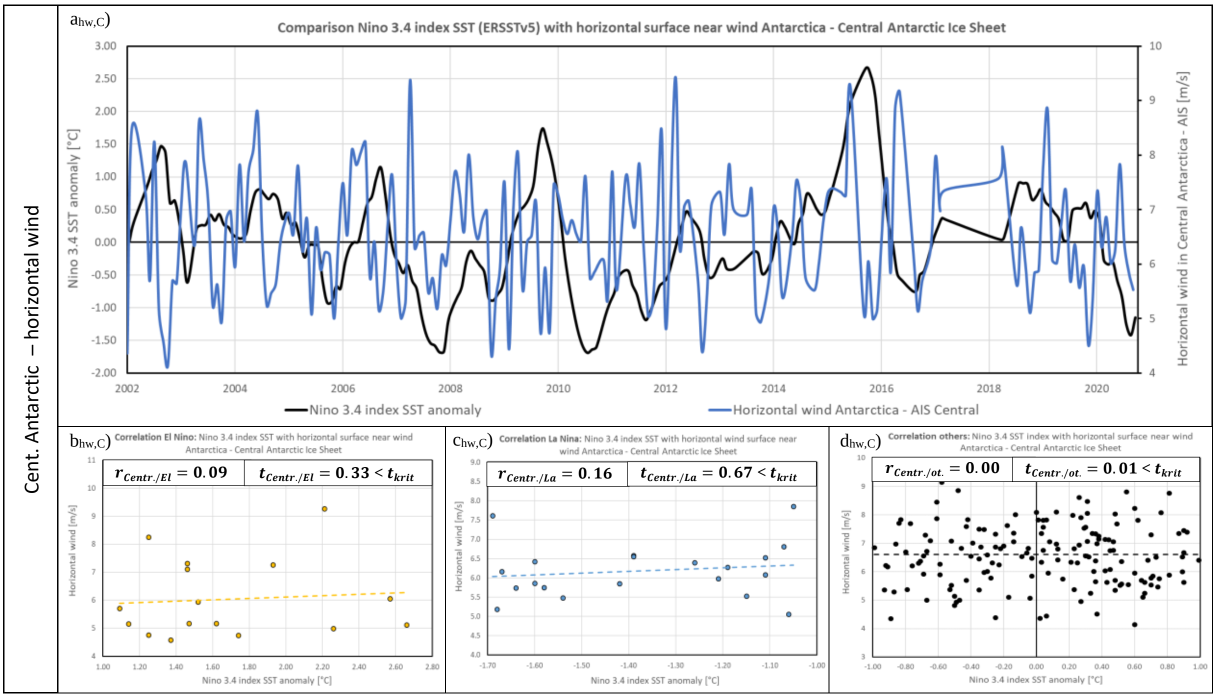

Cent. Antarctic – horizontal wind
a_hw,C)
Comparison Nino 3.4 index SST (ERSSTv5) with horizontal surface near wind Antarctica - Central Antarctic Ice Sheet
Nino 3.4 SST anomaly [°C]
Horizontal wind in Central Antarctica - AIS [m/s]
Nino 3.4 index SST anomaly
Horizontal wind Antarctica - AIS Central
b_hw,C)
Correlation El Nino: Nino 3.4 index SST with horizontal surface near wind Antarctica - Central Antarctic Ice Sheet
$r_{Centr./El} = 0.09$
$t_{Centr./El} = 0.33 < t_{krit}$
Horizontal wind [m/s]
Nino 3.4 index SST anomaly [°C]
c_hw,C)
Correlation La Nina: Nino 3.4 index SST with horizontal wind surface near wind Antarctica - Central Antarctic Ice Sheet
$r_{Centr./La} = 0.16$
$t_{Centr./La} = 0.67 < t_{krit}$
Horizontal wind [m/s]
Nino 3.4 index SST anomaly [°C]
d_hw,C)
Correlation others: Nino 3.4 SST index with horizontal surface near wind Antarctica - Central Antarctic Ice Sheet
$r_{Centr./ot.} = 0.00$
$t_{Centr./ot.} = 0.01 < t_{krit}$
Horizontal wind [m/s]
Nino 3.4 index SST anomaly [°C]